



LUND UNIVERSITY

Pericyte Dynamics in Glioblastoma and Ischemic Stroke

Buizza, Carolina

2025

Document Version:
Publisher's PDF, also known as Version of record

[Link to publication](#)

Citation for published version (APA):
Buizza, C. (2025). *Pericyte Dynamics in Glioblastoma and Ischemic Stroke*. [Doctoral Thesis (compilation), Department of Clinical Sciences, Lund]. Lund University, Faculty of Medicine.

Total number of authors:
1

General rights

Unless other specific re-use rights are stated the following general rights apply:
Copyright and moral rights for the publications made accessible in the public portal are retained by the authors and/or other copyright owners and it is a condition of accessing publications that users recognise and abide by the legal requirements associated with these rights.

- Users may download and print one copy of any publication from the public portal for the purpose of private study or research.
- You may not further distribute the material or use it for any profit-making activity or commercial gain
- You may freely distribute the URL identifying the publication in the public portal

Read more about Creative commons licenses: <https://creativecommons.org/licenses/>

Take down policy

If you believe that this document breaches copyright please contact us providing details, and we will remove access to the work immediately and investigate your claim.

LUND UNIVERSITY

PO Box 117
221 00 Lund
+46 46-222 00 00



Pericyte Dynamics in Glioblastoma and Ischemic Stroke

CAROLINA BUIZZA | DEPARTMENT OF CLINICAL SCIENCES, LUND
FACULTY OF MEDICINE | LUND UNIVERSITY





CAROLINA BUIZZA studied Pharmaceutical Chemistry and Technology at the University of Milano (Italy), completing her thesis in Neuroscience in collaboration with Radboud University (the Netherlands). Her growing passion for Neuroscience led her to pursue a PhD at Lund University, where she joined the Translational Neurology group under the supervision of Gesine Paul in 2021. Her doctoral research focused on investigating transcriptomic, morphological, and secretome changes in pericytes in the contexts of glioblastoma, ischemic stroke, and diabetes.



Pericyte Dynamics in Glioblastoma and Ischemic Stroke

Pericyte Dynamics in Glioblastoma and Ischemic Stroke

Carolina Buizza



LUND
UNIVERSITY

DOCTORAL DISSERTATION

Doctoral dissertation for the degree of Doctor of Philosophy (PhD) at the Faculty of Medicine at Lund University to be publicly defended on 14th of March 2025 at 08.00 in Segerfalksalen, Sölvegatan 17, Lund, Sweden

Faculty opponent
Annika Keller, PhD

Department of Neurosurgery, Zurich University Hospital & Zurich University

| | |
|--|---|
| Organization: LUND UNIVERSITY Faculty of Medicine Department of Clinical Sciences Translational Neurology Group | Document name: Doctoral Thesis |
| | Date of issue: March 14, 2025 |
| | Sponsoring organization: Lund University |
| Author: Carolina Buizza | |
| Title and subtitle: Pericyte Dynamics in Glioblastoma and Ischemic Stroke | |
| Abstract: <p>Glioblastoma (GBM) and ischemic stroke represent two challenging brain pathologies which still lack an optimal therapeutic strategy. Central to these diseases are pericytes, mural cells that regulate blood-brain barrier (BBB) integrity, vascular stability, and immune responses. However, the disease-specific alterations in pericytes that contribute to GBM progression and their influence on the post-stroke cascade are still not fully understood.</p> <p>For these reasons, this thesis delves into the dynamic roles of pericytes in these pathologies, exploring their responses at the transcriptome, morphological, and secretome levels. We firstly addressed pericyte heterogeneity and defined their transcriptomic changes depending on the proximity to the tumor in GBM (Paper I). This was followed by a temporal analysis of pericyte transcriptional responses during the acute phases of ischemic stroke (Paper II). Morphological studies in Papers III and IV provided insights into pericyte detachment, activation, and their role in BBB disruption and vascular remodeling following ischemic stroke. Lastly, Paper V investigated the changes in the pericyte secretome under hypoxic conditions in vitro.</p> <p>We found that in GBM, pericytes in the tumor vicinity showed increased gene expression and enhanced communication with immune cells. In ischemic stroke, we observed that pericytes responded rapidly within the first hour, and over time formed a distinct stroke-specific cluster, characterized by unique transcriptional changes. Additionally, under hypoxic conditions, pericytes altered their secretome, highlighting their dynamic response to the ischemic environment.</p> <p>By integrating findings across GBM and ischemic stroke, this thesis underscores the dynamic and plastic nature of pericytes, highlighting their critical role in extracellular matrix remodeling, vascular regulation, and immune modulation. The results position pericytes as promising therapeutic targets for improving outcomes in brain diseases. Future studies will benefit from further exploration of pericyte interactions within the broader cellular landscape of the brain.</p> | |
| Key words: pericytes, glioblastoma, stroke, transcriptome, signalling, secretome | |
| Supplementary bibliographical information: Lund University, Faculty of Medicine Doctoral Dissertation Series 2025:26 | |
| Classification system and/or index terms (if any): | Language: English |
| ISSN and key title: 1652-8220 | ISBN: 978-91-8021-679-1 |
| Number of pages: 99 | Price: |
| Recipient's notes: | Security classification: |

I, the undersigned, being the copyright owner of the abstract of the above-mentioned dissertation, hereby grant to all reference sources permission to publish and disseminate the abstract of the above-mentioned dissertation.

Signature

Date 2025-01-17

Pericyte Dynamics in Glioblastoma and Ischemic Stroke

Carolina Buizza



LUND
UNIVERSITY

2025

Thesis cover generated by Carolina Buizza using Adobe Firefly and later refined. The image portrays an abstract brain shaped like a tree, with wooden branches symbolizing blood vessels and surrounding flowers representing pericytes.

Copyright © Carolina Buizza

Paper 1 © by the Authors (Manuscript unpublished)

Paper 2 © Publisher

Paper 3 © Publisher

Paper 4 © Publisher

Paper 5 © Publisher

Faculty of Medicine

Department of Clinical Sciences, Lund

ISBN 978-91-8021-679-1

ISSN 1652-8220

Printed in Sweden by Media-Tryck, Lund University

Lund 2025



Media-Tryck is a Nordic Swan Ecolabel certified provider of printed material. Read more about our environmental work at www.mediatryck.lu.se

MADE IN SWEDEN 

To anyone in need of a little encouragement

Table of Contents

| | |
|---|-----------|
| LAY SUMMARY | 12 |
| SINTESI | 13 |
| PAPERS INCLUDED IN THIS THESIS | 15 |
| ABBREVIATIONS | 16 |
| INTRODUCTION | 19 |
| The brain and the blood vessels | 19 |
| Mural cells | 19 |
| Morphology | 20 |
| Gene and protein expression | 20 |
| Pericyte subtypes in mouse | 22 |
| Pericyte subtypes in human | 24 |
| Mural cell functions in health | 24 |
| Blood-brain barrier formation and maintenance | 25 |
| Angiogenesis and vascular support | 26 |
| Secretory ability | 28 |
| Pericyte role in immune modulation | 28 |

| | |
|--|-----------|
| Mural cell functions in disease | 29 |
| Pericyte pathology in GBM..... | 30 |
| Pericyte pathology in ischemic stroke | 32 |
| Pericyte pathology in type 2 diabetes | 34 |
| From the transcriptome to the secretome: state-of-the-art | 35 |
| AIMS | 37 |
| KEY METHODOLOGY | 39 |
| Animal models..... | 39 |
| Glioblastoma | 39 |
| Stroke..... | 40 |
| Diabetes..... | 40 |
| Cell culture..... | 40 |
| Virus production and stable cell line generation..... | 41 |
| Spheroid co-culture generation | 41 |
| Biotin treatment and hypoxia induction | 41 |
| Tissue processing..... | 41 |
| 10x genomics | 42 |
| FACS..... | 42 |
| Sequencing | 42 |
| Real-time quantitative PCR..... | 43 |
| Immunofluorescence | 43 |
| 3-3'-diaminobenzidine (DAB) staining..... | 43 |
| Sections on glass (snap-frozen tissue) | 43 |
| Free-floating sections..... | 44 |
| Immunocytochemistry | 44 |
| Image acquisition and processing..... | 44 |
| Assessment of vascularization and blood-brain barrier leakage..... | 44 |
| Bioinformatics analysis..... | 45 |
| scRNA-seq data from mouse samples..... | 45 |

| | |
|---|-----------|
| scRNA-seq data from human published dataset..... | 45 |
| Statistical analysis..... | 45 |
| SUMMARY OF KEY RESULTS..... | 47 |
| Paper I Pericytes Change Function Depending on Glioblastoma Vicinity: Emphasis on Immune Regulation | 47 |
| Mural cell subclusters redistribute depending on tumor proximity | 47 |
| Mural cells exhibit distinct transcriptional changes depending on tumor proximity | 49 |
| Tumor-residing mural cells markedly enhance communication strength and immune signaling | 51 |
| Paper II The Transcriptional Landscape of Pericytes in Acute Ischemic Stroke | 54 |
| Pericytes form a new subcluster in the acute phase post-stroke which is related to angiogenesis and inflammation..... | 54 |
| IL11 is specifically expressed by PDGFR β ⁺ cells from the ipsilateral hemisphere after stroke | 56 |
| Paper III Pericyte Response to Ischemic Stroke Precedes Endothelial Cell Death and Blood-Brain Barrier Breakdown | 57 |
| Pericyte response starts already 1 hour after stroke..... | 57 |
| Zo-1 loss, BBB breakdown and endothelial cells death follow the pericyte response | 59 |
| Paper IV The SGLT2 Inhibitor Empagliflozin Promotes Post-Stroke Functional Recovery in Diabetic Mice..... | 61 |
| Empagliflozin improves stroke recovery in T2D mice, potentially through the regulation of pericyte density | 61 |
| T2D and Empagliflozin do not affect BBB integrity, vascularization and pericyte activation | 62 |
| Paper V Pericyte-Specific Secretome Profiling in Hypoxia Using TurboID in a Multicellular in Vitro Spheroid-Model..... | 65 |
| TID specifically biotinylates pericyte proteins in mono- and spheroids- cultures | 65 |
| Pericyte alter their secretome depending on oxygen level and culture conditions | 66 |

| | |
|--|-----------|
| DISCUSSION AND FUTURE PERSPECTIVES..... | 71 |
| ACKNOWLEDGEMENTS..... | 77 |
| REFERENCES..... | 80 |
| APPENDIX (PAPERS I-V)..... | 99 |

Lay Summary

Illnesses like brain tumor and stroke are two of the most severe conditions that affect the brain, both resulting in significant damages to the body and mind of patients. These diseases share common characteristics, such as problems with blood vessels and low oxygen levels, which cause the brain cells to behave abnormally. This thesis focuses on understanding how a specific group of cells called pericytes respond to these conditions. Pericytes play a crucial role in the brain's blood vessels and can affect disease progression by changing their behavior in response to injury.

In this research, we look closely at how pericytes react to changes in their environment during brain tumor and stroke. We studied how their activity changes over time and in different areas of the brain, depending on the pathology. A key focus of our study was the signals that pericytes send to immune cells, which play a crucial role in fighting tumors and aiding in tissue repair. We also investigated how pericytes change their ability to produce proteins that help support or alter their surrounding environment, especially when oxygen levels are low. Our findings suggest that pericytes are highly adaptable and can influence the severity of these diseases by affecting blood vessel function and their surroundings.

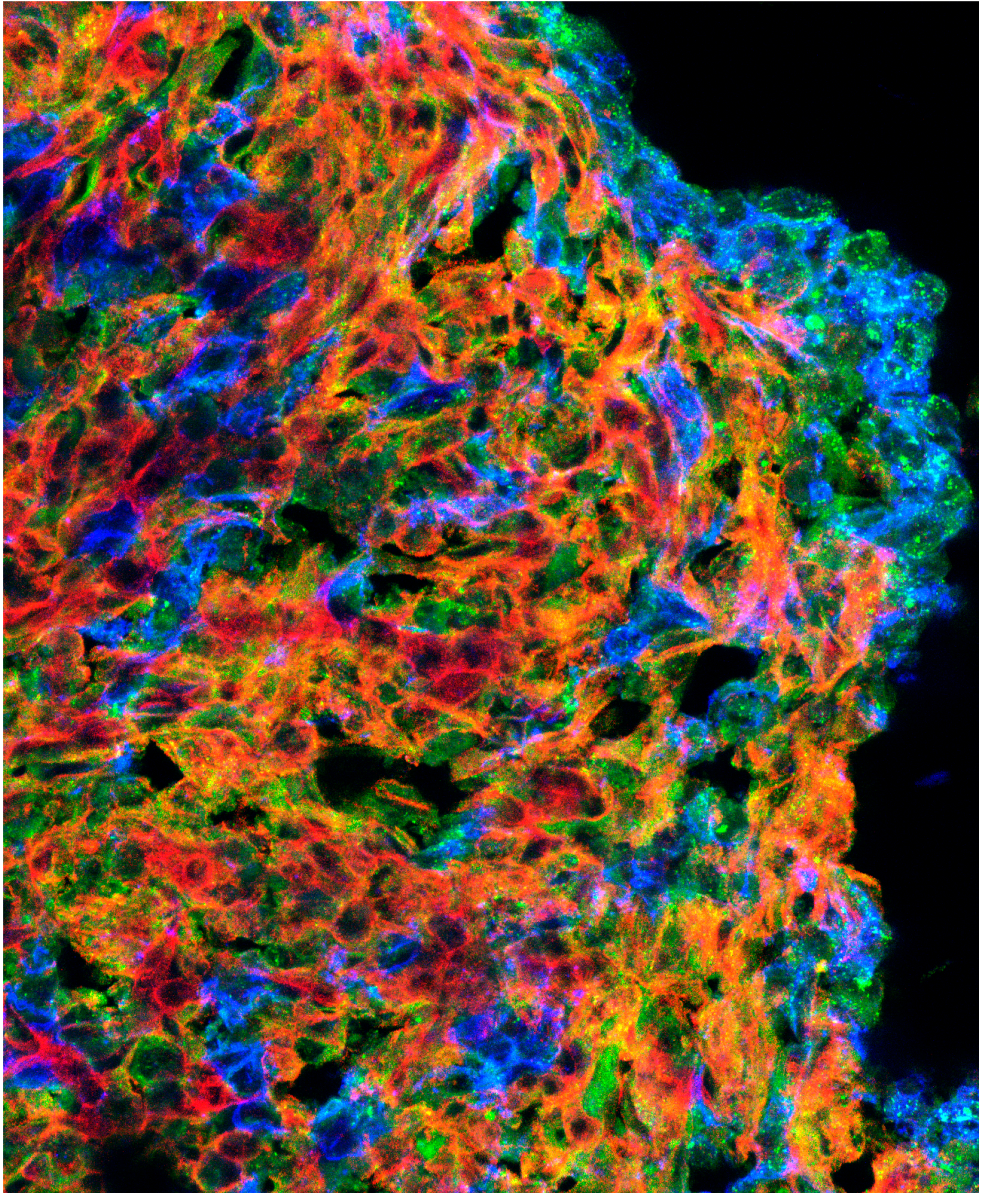
By better understanding the role of pericytes in these brain disorders, this work opens potential avenues for new treatments. Targeting pericytes could help improve outcomes by enhancing the action of immune cells, reducing damage to blood vessels and promoting recovery in conditions like glioblastoma and stroke.

Sintesi

Malattie come tumori e l'ictus sono tra le condizioni più gravi che colpiscono il cervello, causando danni significativi al corpo e alla mente dei pazienti. Queste patologie hanno delle caratteristiche in comune, come problemi ai vasi sanguigni e ridotti livelli di ossigeno nei tessuti, che fanno sì che le cellule cerebrali si comportino in modo anomalo. Questa tesi è focalizzata su come i periciti, un gruppo specifico di cellule, rispondono a queste malattie. I periciti svolgono un ruolo cruciale nei vasi sanguigni del cervello e, modificando il loro comportamento in risposta allo sviluppo delle patologie, ne possono modificare la progressione.

In questo studio, abbiamo esaminato da vicino come i periciti reagiscono ai cambiamenti nel loro ambiente durante il tumore cerebrale e l'ictus. Abbiamo studiato come la loro attività varia nel tempo e in diverse aree del cervello, a seconda della patologia. Un punto centrale della nostra indagine è stato il ruolo dei segnali che i periciti inviano alle cellule immunitarie, le quali svolgono funzioni essenziali nel combattere i tumori e nel favorire la riparazione dei tessuti. Inoltre, abbiamo analizzato come i periciti modificano la loro capacità di produrre proteine che supportano o alterano l'ambiente circostante, soprattutto in condizioni di carenza di ossigeno. I nostri risultati suggeriscono che i periciti siano cellule altamente adattabili e che possano influenzare la gravità di queste malattie agendo sulla funzione dei vasi sanguigni e sull'ambiente circostante.

Comprendendo meglio il ruolo dei periciti in questi disturbi cerebrali, questo lavoro apre potenziali strade per nuovi trattamenti. Intervenire sui periciti potrebbe contribuire a migliorare i risultati clinici, potenziando l'azione delle cellule immunitarie, riducendo i danni ai vasi sanguigni e favorendo il recupero in condizioni come il glioblastoma e l'ictus.



Tight Connection

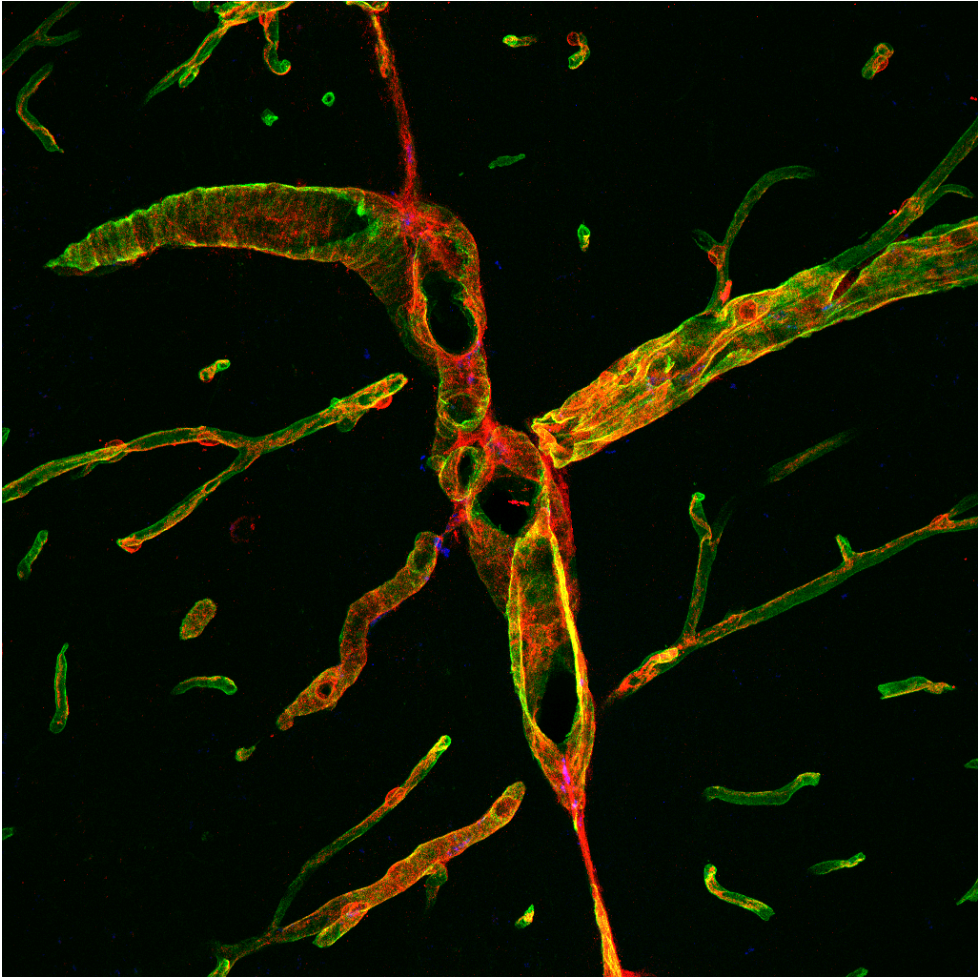
Papers Included in This Thesis

- I. **Buizza C.**, Carlsson R., Gamper C., Chitale G., Bengzon J., Paul G. Pericytes Change Function Depending on Glioblastoma Vicinity: Emphasis on Immune Regulation. *Manuscript submitted for publication.*
- II. **Buizza C.**, Enström A., Carlsson R. & Paul G. (2023) The Transcriptional Landscape of Pericytes in Acute Ischemic Stroke. *Translational Stroke Research*
- III. Roth M., Carlsson R., **Buizza C.**, Enström A., Paul G. (2024) Pericyte Response to Ischemic Stroke Precedes Endothelial Cell Death and Blood-Brain-Barrier Breakdown. *Journal of Cerebral Blood Flow and Metabolism*
- IV. Vercalsteren E., Karampatsi D., **Buizza C.**, Nyström T., Klein T., Paul G., Patrone C., Darsalia V. (2024) The SGLT2 Inhibitor Empagliflozin Promotes Post-Stroke Functional Recovery in Diabetic Mice. *Cardiovascular Diabetology*
- V. Enström A., Carlsson R., **Buizza C.**, Lewi M., Paul G. (2024) Pericyte-Specific Secretome Profiling in Hypoxia Using TurboID in a Multicellular In Vitro Spheroid-Model. *Molecular & Cellular Proteomics*

Abbreviations

| | |
|--------|------------------------------------|
| Acta2 | Smooth muscle actin alpha |
| BBB | Blood-brain barrier |
| CD13 | Aminopeptidase N |
| CNS | Central nervous system |
| Contra | Contralateral hemisphere |
| cPC | Classical pericytes |
| cSMC | Classical smooth muscle cells |
| DC | Dendritic cells |
| DEGs | Differentially expressed genes |
| ECM | Extracellular matrix |
| ecm-PC | Extracellular matrix PC |
| ER | Endoplasmic reticulum |
| FACS | Fluorescent activated cell sorting |
| FGSEA | Fast gene set enrichment analysis |
| GBM | Glioblastoma |
| GFP | Green fluorescent protein |
| GL261 | Glioma 261 |
| GO: BP | Gene ontology biological processes |
| HBVP | Human brain vascular pericytes |
| hsPC | Human scavenging PC |
| IHC | Immunohistochemistry |
| IL | Interleukin |
| Ipsi | Ipsilateral hemisphere |
| LR | Ligand-receptor |
| Mhc | Major histocompatibility complex |
| msPC | Mouse scavenging PC |
| ND | Non-diabetic |
| nPC | Normal pericytes |

| | |
|---------------|--|
| PC | Pericytes |
| PDGFR β | Platelet-derived growth factor receptor beta |
| PECAM1 | Platelet endothelial cell adhesion molecule |
| pMCAO | Permanent middle cerebral artery occlusion |
| RGS5 | Regulator of G protein signaling 5 |
| rSMC | Reactive smooth muscle cells |
| RT | Room temperature |
| scRNA-seq | Single-cell RNA sequencing |
| SMC | Smooth muscle cells |
| T2D | Type 2 diabetes |
| T2D-E | Type 2 diabetes + Empagliflozin |
| T2D-VH | Type 2 diabetes + vehicle |
| TAM | Tumor-associated macrophages |
| TID | Turbo ID |
| TJ | Tight Junction |
| tMCAO | Transient middle cerebral artery occlusion |
| TME | Tumor microenvironment |
| vPC | Vascular pericytes |
| WT | Wild type |



Travelling North

Introduction

The brain and the blood vessels

The brain is the central organ of the nervous system in all vertebrates, and it is responsible for controlling and coordinating most bodily functions, including thought, memory, emotion, sensory perception, and motor skills. Being the most specialized organ, a high supply of blood and oxygen is essential. The brain consumes about 20 % of the body's total oxygen supply, despite accounting for only about 2 % of the body's weight [1, 2]. The brain's blood vessels, including arteries, veins, and capillaries, collectively form an incredibly long network of about 640 kilometers [3]. The smallest and most numerous blood vessels, the capillaries, are particularly important because they facilitate the exchange of oxygen, nutrients, and waste products between the blood and the brain tissue.

In vertebrates, the larger vessels, arteries and veins, are composed of three layers: the tunica intima, tunica media, and tunica adventitia. The tunica intima, the innermost layer, consists of a single sheet of endothelial cells lining the vessel's lumen, in direct contact with the blood. Surrounding this layer is the tunica media, made up of several concentric layers of vascular smooth muscle cells (SMCs). The tunica adventitia, the outermost layer, is a fibrous structure rich in collagen, fibroblasts, immune cells, and progenitor cells. In smaller vessels, the capillaries, the single layer of endothelial cells is enclosed by a discontinuous layer of pericytes instead of SMCs.

Mural cells

Pericytes and SMCs are collectively referred to as mural cells. Mural cells originate from different embryonic layers, and their origin depends on the tissue and organ in which they are located. Mesoderm-derived pericytes and SMCs are the most common and include those found in most vascularized organs, including the brain, muscles, and lungs [4]. Ectoderm-derived pericytes are present in specific areas such as the neural crest, contributing to the vasculature of the face and forebrain [5].

The primary subject of investigation in this thesis is pericytes. In the past, pericytes have been overlooked and their contribution was often underestimated, but in recent

years they have gained increasing recognition for their critical roles in vascular biology and pathology. Studies have shown that during aging and in pathologies such as Alzheimer's disease [6], diabetic retinopathy [7], and arteriovenous malformations [8], pericyte degeneration can lead to BBB disruption, altered vascular architecture, and decreased cerebral blood flow. While in the body the ratio between pericytes and endothelial cells is 1:10, in the brain the ratio increases up to 1:1/1:3 with a coverage of the abluminal surface ranging from 10 % to 30 % [9-11]. The diversity positively correlates with the vessel wall properties, with the brain holding the highest pericyte density and the brain BBB being the tightest barrier. These observations are therefore consistent with pericytes having multiple roles in the body and influencing a plethora of pathological mechanisms.

Being able to distinguish between pericytes and SMCs is essential because the two cell types differ in location, as explained above, but also in morphology, gene expression and functions.

Morphology

In terms of morphology, vascular (v) SMCs on arterioles have a flattened, spindle-shaped body with minimal cytoplasmic processes, while those on precapillary arterioles display more protruding cell bodies and multiple processes. In contrast, vSMCs on venules exhibit a stellate-shaped cell body with numerous branching processes, which, unlike arteriolar vSMCs, do not form circular wraps around the endothelium [9]. Pericytes, on the other hand, have a rounded cell body from which a few primary processes emerge. These primary processes extend longitudinally along capillaries, making contact with multiple endothelial cells. Thin secondary processes branch perpendicularly from the primary processes and partially encircle the vessels, creating a distinctive morphology [9].

Gene and protein expression

Currently, no single molecule uniquely distinguishes pericytes from SMCs. Markers commonly used for identification exhibit variable expression depending on factors such as developmental stage, *in vitro* culture conditions, inflammation and diseases, and they are not exclusively expressed by pericytes or SMCs. As a result, identification typically relies on a combination of markers along with morphological and location analyses. The most commonly used markers for pericytes include Regulator of G protein signaling 5 (Rgs5), Platelet-derived growth factor receptor beta (Pdgfr β), Chondroitin sulfate proteoglycan 4 (Cspg4, also known as Ng2), and Alanyl aminopeptidase (Anpep, also known as Cd13) [12] (Table 1).

RGS5 is a cytoplasmic protein that enhances the GTPase activity of G-protein-coupled receptors (GPCRs), facilitating the conversion of GTP to GDP and thereby

terminating GPCR signaling [13]. In the brain, RGS5 is exclusively expressed by mural cells [14, 15]. In our work, we are particularly interested in RGS5 since previous research indicates that its expression is one of the earliest responses of pericytes to hypoxic conditions [16, 17]. This makes RGS5 a potential pericyte-specific target for modulating their response during stroke pathogenesis.

Recently, ATPase 13A5 (Atp13a5) has been proposed as a specific marker for pericytes in the mouse brain, spinal cord, and retina [18]. For SMCs, markers include Smooth muscle actin alpha (also known as α SMA), Myocardin (Myocd), Transgelin (Tgln) and others depending on the differentiation stage of the cells [19] (Table 1). Among the well-established mural cell markers, Rgs5, Pdgfr β and Neurogenic locus notch homolog protein 3 (Notch3) are shared between human and mouse, while Atp13a5, Cspg4 and Potassium inward rectifying channel, subfamily J, member 8 (Kcnj8) are specific for mouse but almost absent in human [20].

The complexity in mural cells classification is increased due to the fact that various pericyte subpopulations have been identified, among which it is possible to distinguish different phenotypes and functions. Additionally, these subpopulations might also differ depending on whether the context is human or mouse [20, 21].

Table 1. Mural cell markers

| Marker | Gene symbol | Cell type | References |
|--|-----------------------|------------------|--------------|
| Regulator of G-protein 5 | Rgs5 | PC, lower in SMC | [14, 15, 22] |
| Cation-transporting ATPase 13A5 | Atp13a5 | PC | [18] |
| Platelet derived growth factor β | Pdgfr β | PC, SMC | [23-25] |
| Chondroitin sulfate proteoglycan 4 | Cspg4 (Ng2) | PC, SMC | [22, 26, 27] |
| Desmin | Des | PC, SMC | [28] |
| Alanyl aminopeptidase | Anpep (Cd13) | PC, SMC | [29] |
| ATP-binding cassette, subfamily 9 | Abcc9 | PC, SMC | [14, 22] |
| Potassium inward rectifying channel, subfamily J, member 8 | Kcnj8 | PC, SMC | [14, 22] |
| Neurogenic locus notch homolog protein 3 | Notch3 | PC, SMC | [30, 31] |
| α -smooth muscle actin | Acta2 (α SMA) | SMC, lower in PC | [32, 33] |
| Transgelin | Tagln | SMC | [33, 34] |
| Myocardin | Myocd | SMC | [35] |
| Calponin | Cnn1 | SMC | [36] |
| Myosin heavy chain 1 | Myh1 | SMC | [37] |
| Myosin heavy chain 2 | Myh2 | SMC | [37] |

Pericyte subtypes in mouse

In mice, several classifications of pericytes have been proposed, with marker expression and function or the anatomical location of pericytes within the vasculature tree used as criteria (Table 2).

For example, based on Nestin (Nes) expression, pericytes have been divided into type-1 (Nes⁻) and type-2 (Nes⁺) subtypes in organs such as the lung, kidney, heart, spinal cord, and brain [38]. Those subtypes were reflected in functional differences: Type-2 pericytes were capable of generating neural cells [39] and participated in muscle regeneration, while type-1 pericytes contributed to adipose and fibrous tissue accumulation in skeletal muscle and injured sites in the lung, kidney, and heart [39, 40]. Type-1 pericytes also produced collagen-I during pulmonary fibrosis and contributed to scar formation after central nervous system (CNS) injury [38].

Another classification, based on Desmin (Des) and/or Acta2 expression, was introduced in studies of spinal cord injury. This classification distinguished type-A pericytes (Des⁻/Acta2⁻), which constituted ~10 % of pericytes in the adult spinal cord, from type-B pericytes (Des⁺/Acta2⁺) [41]. Following spinal cord injury, type-A pericytes proliferated at the lesion core, detached from blood vessels, invaded surrounding tissue, and deposited abundant extracellular matrix (ECM). These cells were thus identified as a source of scar-forming cells in the adult spinal cord [41].

Another study identified two distinct but unnamed pericyte subsets, one which was CD90⁺ with limited expression of ACTA2, and one was CD90⁻, with higher expression of ACTA2 and PDGFRB [42].

Another study found that Vascular cell adhesion protein 1 (VCAM1, or CD106) and Programmed death-ligand 1 (PD-L1, or CD274), expressed by the PC1, could distinguish them from the Delta Like Non-Canonical Notch Ligand 1 (DLK1⁺) PC2 [4]. The use of this marker combination was also confirmed by another group in rhesus macaques [43]. PC1 was the main subpopulation in the brain of young uninfected adults, while PC2 were more frequent in older adults and were associated with virus infection [43]. The same group recently found that PC2 increased expression of genes associated with phagocytosis and peripheral immune cell infiltration [44], while PC1 displayed increased expression of genes involved in hedgehog signaling, known to promote tight junction formation at the BBB. The authors suggested that PC2 originate from PC1 in response to pathological conditions [44].

In the mouse brain, pericytes have been further categorized into ensheathing and capillary pericytes based on their microvascular zonation and morphology, rather than marker expression. Morphologically, capillary pericytes aligned with the classical pericyte phenotype, while ensheathing pericytes exhibited intermediate features between SMCs and capillary pericytes [45]. Ensheathing pericytes were contractile *in vivo* and expressed ACTA2 together with a mixed pericyte-SMC

morphology. Ensheathing pericytes have also been referred to as “pre-capillary smooth muscle cells” [46], adding complexity to the nomenclature.

One year after the previous classification was proposed, Vanlandewijck et al. (2018) [47] were the first who used single-cell RNA sequencing (scRNA-seq) to describe how vascular zonation in the mouse brain is reflected upon gene expression. Their analysis did not reveal the existence of distinct pericytes subtypes but identified two distinct transcriptional profiles associated with different locations along the vascular tree. The first profile encompassed pericytes and venous SMCs, while the second included arteriolar and arterial SMCs [47].

Table 2. Subtypes of pericytes

| Classification | Markers/ Location | Species | Functions | References |
|-------------------|--|-----------------------------|---|------------|
| Type I | Nes- | Mouse | Produce collagen I; contribute to adipose and fibrous tissue accumulation and scar formation. | [38-40] |
| Type II | Nes+ | | Generate neural cells; participate in muscle regeneration | |
| Type A | Des ⁻ Acta2 ⁻ | Mouse Human | Scar-forming cells after injury, ~10 % of the pericytes | [41, 48] |
| Type B | Des ⁺ Acta2 ⁺ | | ~90 % of the pericytes | |
| Ensheathing | Pre-capillary venules | Mouse | Contractile, mixed PC-SMC morphology | [45] |
| Capillary | Capillaries | | Canonical pericytes | |
| CD90 ⁺ | CD90 ⁺ Acta2 ⁻ | Human (<i>in vitro</i>) | Higher proliferation | [42] |
| CD90 ⁻ | CD90 ⁻ Acta2 ⁺ | | ECM production, pro-inflammatory | |
| PC 1 | VCAM ⁺ CD274 ⁺ Capillary | Human (<i>in vitro</i>) | Pro-inflammatory | [4] |
| PC 2 | DLK1 ⁺ Arteriolar | | Contractile | |
| PC 1 | PDGFRB ⁺ aSMA ⁻ MYH11 ⁻ | Mouse, Rhesus macaque | Associated with young healthy brains and BBB homeostasis, can transition into PC 2; expression of genes involved in hedgehog signaling. | [43, 44] |
| PC 2 | PDGFRB ⁺ SMA ⁺ MYH11 ⁻ | | Associated with aging, CNS infection, increased gene expression related to phagocytosis and immune cells infiltration | |
| Transport | SLC20A2 SLC6A1 SLC12A7 | Human | Canonical PC functions | [49] |
| Matrix | Collagen Laminin ADAMTS1 | | ECM production | |

Pericyte subtypes in human

In humans, a single-nucleus transcriptomics study of the hippocampus and cortex in Alzheimer's disease identified two pericyte subtypes: T-pericytes (transport-related) and M-pericytes (ECM-related), marked by distinct gene expression profiles [49] (Table 2). These subtypes were not segmented by vascular location, suggesting that, in human, gene expression and function, rather than anatomical position, may drive pericyte identity.

A recent *in silico* analysis of GBM patients identified multiple pericyte “signatures” that were overexpressed in patients: vascular, immunological, and macrophage-related signatures, all associated with poor patient survival [50]. It remains unclear whether these signatures represented distinct pericyte subtypes or different functional states within the tumor microenvironment (TME). Additionally, by harmonizing 26 datasets produced on GBM, gathering 240 patients and spanning over 1.1 millions of cells, Ruiz-Moreno et al. (2022) identified one canonical cluster of pericytes and one cluster of “scavenging” pericytes related to the tumor [51].

Whether these various classifications overlap remains unaddressed, underscoring the need for further studies to unify our understanding of pericyte diversity across species and conditions. In the attempt to contextualize our findings with the existing literature, in **Paper I** and partly in **Paper II**, we assessed the correspondence of pericytes to the subtypes previously described.

Mural cell functions in health

Vascular SMC mainly provide structural support and regulate blood pressure and flow through their contractile function in larger vessels. They are primarily responsible for vasoconstriction and vasodilation. On the other hand, pericyte functions include the regulation of the blood flow at the capillary level and support of endothelial cell survival (Fig. 1). Pericytes are involved in angiogenesis and vascular remodeling and are an essential component of the BBB. Both cell types have immune functions such as phagocytosis and leukocyte recruitment and activation. The following sections will focus on the specific functions of SMC and pericytes that are pertinent to the current thesis, emphasizing their involvement in the progression of brain diseases.

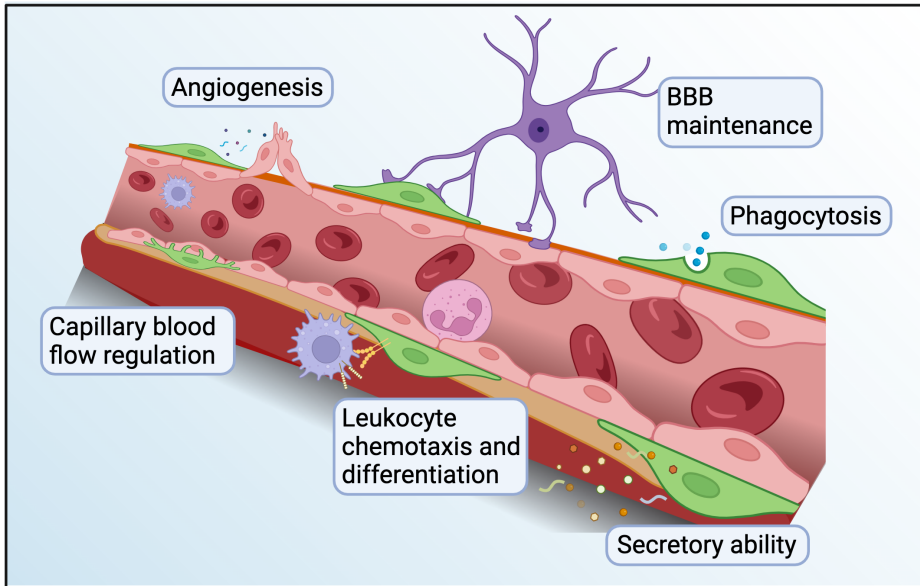


Figure 1. Pericyte functions. Pericytes have multiple roles in the brain, including angiogenesis, BBB maintenance, blood flow regulation, immune functions such as phagocytosis and leukocyte chemotaxis and differentiation, as well as a large secretory capacity. Image created in Biorender.

Blood-brain barrier formation and maintenance

The BBB is a tightly regulated barrier between the blood and the brain parenchyma, which is composed of endothelial cells and their linking tight junctions (TJs), astrocytic end feet, the basal lamina, and pericytes [52-54]. Due to their unique location at the interface between the blood and the brain parenchyma, pericytes are a crucial part of the BBB. They are recruited at the nascent vessels during embryonic development where they play an essential role in the formation of the BBB by regulating the formation of endothelial TJs and trans-endothelial trafficking [55]. *Pdgfr β ^{-/-}* mice, lacking 80-90 % of the pericytes, are perinatally lethal due to pericyte-loss-induced microaneurysms [23, 55]. During adulthood, pericytes maintain BBB tightness and integrity by regulating TJs expression and localization and transcytosis across the barrier [56, 57]. Previous studies have established a close correlation between pericyte density and permeability across the BBB [56].

Dysfunction of the BBB has emerged as an important factor and modifier of brain diseases [58], with its breakdown enabling toxic molecules, cells and pathogens to enter the brain and leading to inflammatory and immune responses, worsening the progression of several brain diseases [59]. As long as pericytes and endothelial cells are tightly connected and have a balanced cross talk, the endothelium and BBB are

safeguarded, while the detachment of the pericytes from the vessel walls in pathologies e.g. in ischemic stroke, can lead to endothelial damage, and as a result, to vessel leakage. It has been hypothesized that pathological pericyte activation and subsequent detachment are the first steps leading to BBB breakdown [60]. In **Papers II** and **III** we have studied the timeline of pericyte responses after stroke, in terms of changes in gene expression (**Paper II**) and impact of pericyte activation on BBB leakage and endothelial cell survival (**Paper III**). **Paper IV** also evaluated vascular changes after ischemic stroke in diabetic conditions, assessing angiogenesis and BBB leakage.

Angiogenesis and vascular support

The formation of blood vessels starts during embryonic development, where two distinct mechanisms, vasculogenesis and angiogenesis, give rise to the vascular network in the embryo [61]. Vasculogenesis is the process of blood vessel formation occurring by a de novo production of endothelial cells, while angiogenesis is the process of forming new blood vessels from pre-existing ones (Fig. 2) [61]. Vasculogenesis gives rise to the heart and the first primitive vascular plexus inside the embryo and in its surrounding membranes. Angiogenesis is responsible for the remodeling and expansion of this network [61]. Two types of angiogenesis are distinguished: sprouting angiogenesis, the formation of new vessels through endothelial cell sprouting [62], and intussusceptive angiogenesis, when existing vessels split to form new ones (Fig. 2) [63]. In this type of angiogenesis, instead of sprouting outward, endothelial cells move into the lumen of the vessels and form intravascular tissue folds and pillars, which lead to the growth of new capillary branches [63]. Pericytes participate in vessel development, stabilization, maturation, and regression in sprouting angiogenesis [9] and in the formation of the pillar core in intussusceptive angiogenesis [64]. Angiogenesis requires complex signaling pathways and a high degree of spatial and temporal coordination between endothelial cells and pericytes and is facilitated by bilateral cell signaling. Angiogenic factors secreted by pericytes include Vascular endothelial growth factor (VEGF)-A and VEGF-B, Transforming growth factor (TGF)- β , Angiopoietin (Ang)-1 [65].

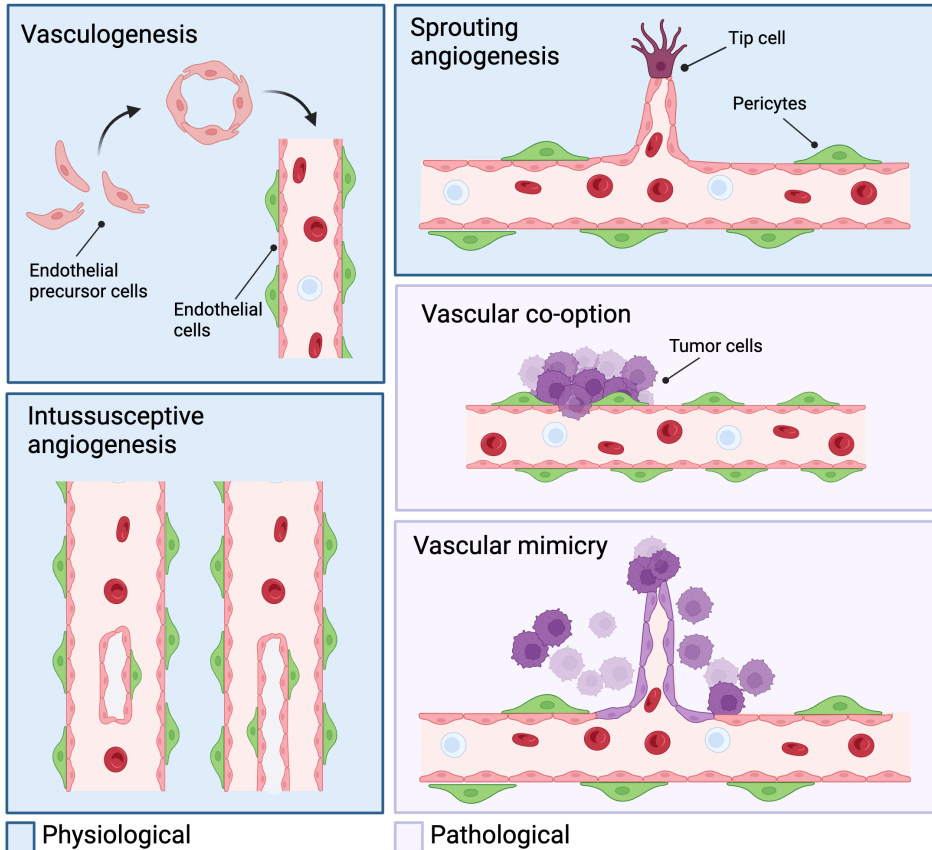


Figure 2. Physiological and pathological formation mechanisms of new blood vessels. Physiological blood vessel formation is represented with blue background. Vasculogenesis is the mechanism through which blood vessels are firstly generated during development, and it is followed by sprouting and intussusceptive angiogenesis, which continue during the entire lifetime. Pathological blood vessel formation is represented with pink background. Examples include vascular co-option and vascular mimicry, mechanisms through which GBM gains access to oxygen and nutrients. Image created with Biorender.

Angiogenesis continues throughout life in both health and disease, even though physiological angiogenesis in adults is quite rare and mainly happens during the menstrual cycle and wound healing [12]. On the other hand, pathological angiogenesis takes place in cancer, diabetic retinopathy and many other diseases. Pathological features include abnormal vascular permeability and defective vascular remodeling and maturation, promoting leakage, hemorrhaging and inflammation, processes that can determine the progression and detrimental effects of the diseases [12]. In GBM, the tumor can also grow without inducing angiogenesis through vessel co-option

and vasculogenic mimicry (Fig. 2). A more detailed explanation of the vessel pathology in GBM is found in the following paragraphs.

Secretory ability

In response to microenvironmental cues, pericytes secrete a plethora of growth factors, cytokines, chemokines, and ECM components [65, 66]. This allows them to communicate with neighboring cells, adapting their secretome in a tissue- and stimulus-specific manner to meet various physiological and pathological demands, reflecting their versatility and potential role in disease progression [54, 56, 65, 67, 68]. The factors secreted by pericytes influence tissue regeneration, immune responses, and vascular health, and include pro- and anti-inflammatory cytokines, growth factors, ECM components, microvesicles and exosomes. Under physiological conditions, pericytes release cytokines and adhesion molecules such as interleukin (IL)-1 α , IL-1 β , IL-6, IL-10, macrophage migration inhibitory factor (MIF) and express major histocompatibility complex (MHC)-I, E-selectin, VCAM-1, and intercellular adhesion molecule (ICAM)-1. Additionally, they secrete neurotrophic factors, including nerve growth factor, brain-derived neurotrophic factor, glial cell-derived neurotrophic factor, and hepatocyte growth factor [66]. The pericyte secretome is not only essential for brain homeostasis but, if dysregulated, likely contributes to the progression of diseases [65].

Pericyte role in immune modulation

Pericytes regulate both innate and adaptive immunity [69, 70] either through their ability to phagocytose and clear toxic cellular debris [71] or by influencing myeloid cell and lymphocyte chemotaxis and activation through the secretion of immunomodulatory molecules [72-77]. The secreted molecules can favor both inflammation and its resolution (reviewed in [66]). Pericytes have also been proposed to express macrophage-like markers, such as CD45, Fc receptors, scavenger receptors, CD11b (alpha chain of the integrin Mac-1/CR3), the pan-macrophage marker CD68 and the M2-polarized-specific marker CD163 [78-81]. Pericytes treated with interferon (IFN)- γ express MHC-II molecules and acquire the capacity to present antigen to primed syngeneic T cells [72, 82-84].

Leukocyte trafficking is facilitated by adhesion molecules and chemokines, which stabilize the dynamic interactions between immune cells and vessel walls. After that, in order to exit the vessels walls, the infiltrating cell must breach the basement membrane and cross the pericyte layer to enter the perivascular space, where a special milieu determines the behavior and fate of the infiltrated immune cells [85]. Pericytes, for example, instruct extravasating neutrophils and monocytes with migratory cues [73], and regulate the transmigration of mature T cell from the thymus into circulation [86]. Pericytes also express high levels of PD-L1 and PD-

L2, ligands for the inhibitory PD-1 receptor on activated T-cells [74, 87]. It has been reported that, despite MHC-II expression, human placental pericytes do not stimulate resting allogeneic CD4 T-cell proliferation or cytokine production. Instead, coculture with pericytes rendered T cells anergic [88]. In **Paper I**, we focused on pericytes immune functions in the context of GBM.

Mural cell functions in disease

Pericytes are known to alter their secretome in response to pathological conditions. For instance, under hypoxic conditions, they increase the production of angiogenic molecules and their corresponding receptors while suppressing growth factor production [65, 66, 89, 90]. In response to hypoxia, pericytes also modify their morphology, changing from a flat cell soma with longitudinal and thin processes [91] to a more bulging cell soma with shorter processes [91, 92].

Pericytes are one of the first responders to hypoxia (Fig. 3) [60, 93] and previous findings suggest that those responses might at least in part be determined by expression of RGS5 [94]. In the brain, RGS5 is exclusively expressed by pericytes. Increasing evidence supports the fact that under hypoxic conditions RGS5 protein is stabilized due to post-translational mechanisms, leading to rapid accumulation of intracellular RGS5 [95-97]. RGS5 expression determines pericyte detachment from the vessel, causing capillary leakage and subsequent oedema [16], effects that we have been able to reverse upon targeting RGS5 [98, 99].

Hypoxia is particularly relevant in the context of this thesis, as it is a hallmark of both GBM and ischemic stroke. In cerebral ischemia, low oxygen levels in affected regions result in hypoxia, whereas in GBM hypoxia occurs due to the presence of abnormal and leaky blood vessels. Throughout the papers included in the thesis, we study the altered functions of pericytes in GBM and ischemic stroke. In **Papers I and II**, we investigated the transcriptomic changes in pericytes associated with their proximity to the tumor in GBM and the temporal dynamics following ischemic stroke, respectively. In **Paper III** we continued studying the temporal dynamics of pericytes after ischemic stroke, from a more morphological perspective, while in **Paper IV** we investigated the responses of pericytes in a diabetes-stroke model treated with an antidiabetic drug. Finally, in **Paper V**, we explored the alterations in the pericyte secretome under hypoxic conditions, utilizing both co-culture and monoculture systems. This study employed a specialized method to exclusively examine the pericyte secretome, providing deeper insights into their functional adaptations to hypoxia.

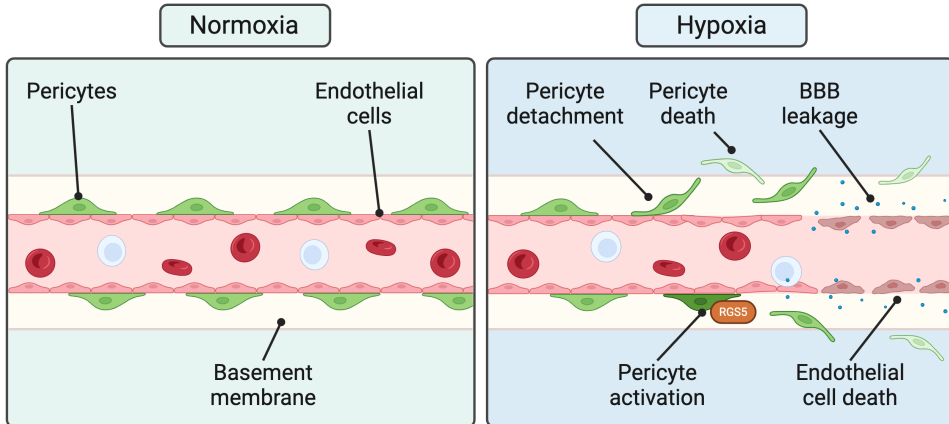


Figure 3. Normoxia and hypoxia. When hypoxia occurs, pericytes are one of the first responders, changing their morphology and their proteome. RGS5 is stabilized in hypoxia and favors pericytes activation and hence detachment from the blood vessels, which, in turns, leads to BBB opening and endothelial cell death. Image created with Biorender.

Pericyte pathology in GBM

GBM is a stage IV glioma and the most common and malignant primary brain tumor in adults [100]. Despite GBM accounts for 14.3 % of all primary brain and CNS tumors and 49.1 % of primary malignant brain tumors, current treatment options are limited and ineffective [101]. Typical treatment includes surgical resection followed by a combination of chemotherapy, radiotherapy, and temozolomide administration [101]. More recently, tumor-treating fields, which use electrical fields to disrupt the division of tumor cells, have received Food and Drug Administration approval as an additional treatment modality [102]. Although these approaches have extended the survival period, there remains no curative treatment for GBM. The median overall survival rate for patients is approximately 16 months, and this slightly increases to 20.9 months with incorporation of the latest therapies [100, 101, 103]. Reasons why treating GBM is particularly challenging include its vascular abnormalities and highly infiltrative growth patterns.

The vasculature in GBM is disorganized, dysfunctional, and highly permeable, often exhibiting abnormal pericyte coverage that compromises the integrity of the BBB. GBM cells exploit multiple mechanisms to promote the formation and development of new blood vessels. While classical angiogenesis plays a central role, GBM tumors can also proliferate without the formation of new blood vessels through processes such as vessel or vascular co-option and vascular mimicry [104, 105].

Vascular mimicry is the process through which tumor cells form vessel-like networks [106, 107]. In this condition, tumor cells reverse to an embryonic-like phenotype and acquire endothelial cell features. Vasculogenic mimicry is associated with tumor metastasis, poor prognosis, worse survival, and high risk of recurrence [108].

Vascular co-option is the process in which tumor cells interact with and exploit pre-existing blood vessels, rather than forming new ones [104]. The principal target cell of GBM during vascular co-option is the pericyte [71, 109]. GBM cells possess cytoplasmic extensions known as flectopodia, which are believed to assist in vessel co-option by interacting with the pericytes in the perivascular niche [71]. Following the co-option, the direct contact between GBM cells and pericytes triggers a cascade of pro-tumorigenic signaling events within pericytes, promoting tumor progression. Beyond supplying nutrients and oxygen via blood vessels, vascular co-option aids the tumor cells in their infiltration. The perivascular space becomes a highway for GBM cells, facilitating tissue invasion and driving the tumor's highly aggressive and invasive nature [104]. To navigate the ECM in the perivascular space, GBM cells secrete proteases like matrix metalloproteinases (MMPs) and disintegrin metalloproteinases (ADAMs), which degrade and exploit ECM components and facilitate invasion [110, 111].

In addition to the key role that pericytes play in tumor progression through the vascular co-option, their investment to the tumor blood vessels is aberrant [112, 113]. Pericytes also display an altered morphology within the tumor, adopting a large cell body with prominent projections, indicating an activated stage [114].

In a previous study, using the RGS5 knock-out/knock-in (*RGS5^{GFP/GFP}*) transgenic mouse strain, where green fluorescent protein (GFP) is expressed under the promoter of RGS5, we showed that pericytes become activated in both the ipsilateral and contralateral hemispheres and migrated into the orthotopically implanted GBM from distal regions [114]. Whether pericytes outside the tumor border communicate with tumor cells and “prepare” the perivascular infiltration of tumor cells is not known, but it is possible that pericyte dysfunction may alter the perivascular microenvironment facilitating the colonization and growth of these invasive cells [9]. In 2014, Caspani *et al.* [71] demonstrated that GBM malignancy proceeds via GBM-pericytes-specific interactions, resulting in enhanced cancer infiltration and tumor survival. Other studies report that vascular invasion of GBM is facilitated by a reduced pericyte coverage and that pericyte's complete depletion in PDGFβ knockout mice was connected to increased vascular permeability in GBM [9, 59, 115]. In addition, Huang *et al.* [26], showed that the ablation of NG2 from pericytes resulted in impaired vessel maturation and stabilization that in turn led to decreased tumor progression; in other words, NG2 expression by pericytes is a key factor in the development of a functional vasculature that can support the aggressive expansion of brain tumors. NG2 ablation was also reported to cause reduced collagen IV deposition [26].

In cancer, tumor-associated pericytes and their secretome have been gaining increasing attention for their potential role in the immune evasion within the TME. Pericytes from normal human brain and human malignant glioma have been shown to secrete various factors with immunosuppressive properties, such as Nitric oxide, Prostaglandin E2, and TGF- β [116]. Upregulated genes organizing into specific signatures from GBM-residing pericytes were correlated with worse overall survival in later stage glioma patients when compared to normal pericyte signatures [50]. These signatures were connected to vascular, immunosuppressive, and macrophage-communication functions. Considering this, targeting pericytes might be important in the context of successful cancer immunotherapy [117].

Pericyte pathology in ischemic stroke

According to the 1970 definition proposed by the World Health Organization, “*A stroke is a clinically defined syndrome of rapidly developing symptoms or signs of focal loss of cerebral function with no apparent cause other than that of vascular origin*” [118]. In 2021, stroke was the third most common cause of death after ischemic heart disease and COVID-19, and the fourth most common cause of disability worldwide [119]. The most recent stroke burden project has estimated that disability, deaths, and cost due to stroke will almost double from 2020 to 2050 [120]. Stroke can be classified as ischemic or hemorrhagic. Ischemic stroke is caused by the interruption of the blood supply to an area of the brain resulting in sudden loss of function, while hemorrhagic stroke is caused by the rupture of a blood vessel [121]. Ischemic stroke is the most prevalent type, accounting for about 80 % of stroke cases [121].

In ischemic stroke, the interruption of blood flow results in a rapid depletion of oxygen and nutrients in the affected brain regions, triggering a cascade of molecular and cellular events that begins within seconds to minutes and can persist for days to weeks. Stroke pathology progresses through distinct phases: hyperacute, acute, and chronic [122]. The hyperacute phase, spanning the initial hours after the event, is characterized by widespread cell death and BBB breakdown [123, 124]. This is followed by the acute phase, lasting up to several days, which involves the activation of microglia and astrocytes, enhanced BBB permeability, increased leakage, and inflammation [125]. Afterward, the chronic phase begins, lasting for several weeks and involving reparative processes such as vascular remodeling, neural plasticity, and scar formation [126, 127].

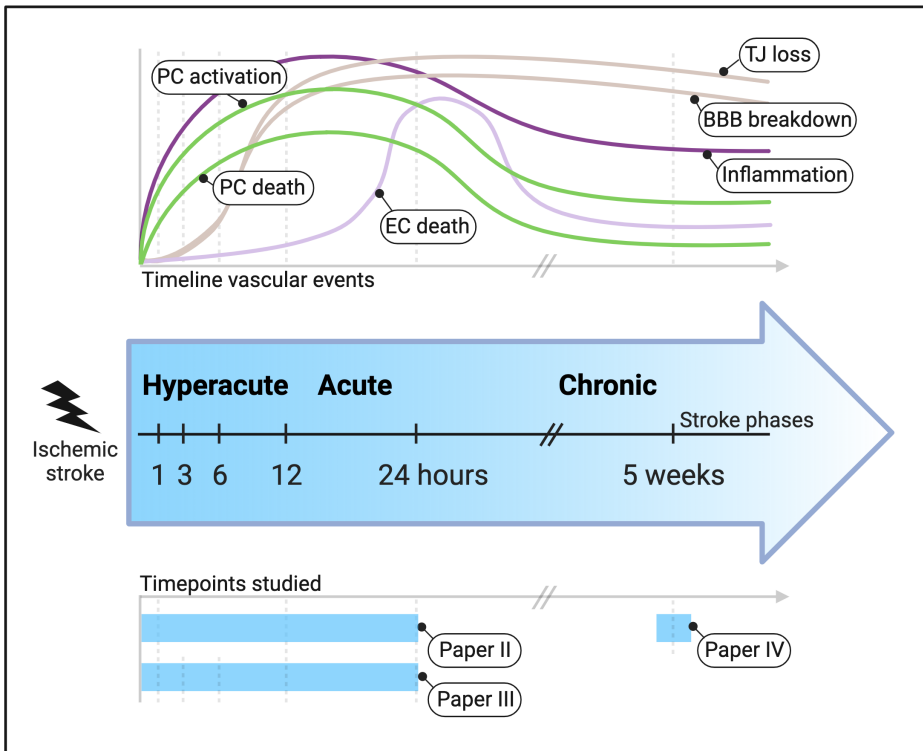


Figure 4. Overview of the experimental setup and timepoints assessed by Papers II-IV. By pMCAO we induced a cortical stroke with an infarct core demarcated by a peri-infarct area. Papers I and II analyzed timepoints in the acute phase after stroke, while Papers III and IV investigated timepoints in the chronic phase. Image created with Biorender.

Currently, the main treatments for acute ischemic stroke include intravenous thrombolysis, using clot-dissolving drugs like alteplase (tPA), and the more invasive mechanical thrombectomy. The choice of treatment depends on numerous factors, including the type of stroke, time since onset, severity of the stroke, and the patient's overall health condition [128]. A major challenge in stroke treatment is the time constraint, with better outcomes associated with faster treatment, and the limited time windows, typically up to 4.5 hours after symptom onset for tPA and 24 hours for thrombectomy in carefully selected patients and only in specialized centers [129]. Therefore, the development of therapeutic interventions that could target stroke pathogenesis beyond the limited time-window must be a worldwide health priority.

In ischemic stroke, the interruption of blood flow in the brain gives rise to a cascade of events, including capillary constriction and ischemic damage to the BBB, leading

to influx of immune cells, ion imbalance, vascular oedema and neuronal death, all of which have been related to a poorer prognosis. Pericytes are major contributors to capillary constriction [130] and BBB breakdown [131], processes that worsen stroke outcome. On the other hand, pericytes also regulate angiogenesis, stabilize newly formed vessels [59], and contribute to the fibrotic scar in stroke [132, 133], therefore playing an essential role in repair after ischemic stroke. Pericytes are one of the first cell types that respond to hypoxia (Fig. 4) [60, 133], possibly through RGS5 expression [16, 17, 94]. As introduced in the previous sections, pericytes expressing RGS5 dissociate from the capillaries causing leakage and subsequent oedema [16], effects that we have been able to reverse upon targeting RGS5 [98, 99].

The pathological BBB breakdown has emerged as an important factor in the cascade following ischemic stroke, and for this reason, preserving its integrity could represent a successful strategy to alleviate the progression of the ischemic injury. Despite this, studies describing the exact timeline of events leading to BBB disruption are still sparse, and often they do not focus on pericytes. In **Papers II** and **III** we assessed the temporal dynamics of the pericyte responses and other vascular events during the acute phase after the ischemic insult in a mouse model (Fig. 4).

Pericyte pathology in type 2 diabetes

Type 2 diabetes mellitus (T2D) is a chronic metabolic disease [134] characterized by hyperglycemia, insulin resistance and chronic inflammation [135]. T2D is associated with multiple microvascular complications, involving several organs including the brain.

Pericytes are affected by the metabolic state of the body, and contribute to the microvascular changes associated with diabetes in different tissues and organs, such as retina, kidney, skeletal muscle, and pancreas [105]. Pericyte degeneration is the earliest clinical manifestation of diabetic retinopathy [136]. In the brain, T2D leads to increased BBB leakage and angiogenesis, and to reduced pericyte coverage of the capillaries [137]. Interestingly, the anti-diabetic drugs Linagliptin and Glimepiride recover BBB integrity and restore the pericyte coverage [137]. Additionally, the drug Exendin-4 normalized pericyte density and coverage of the capillaries and restored fibrotic scar formation in T2D mice subjected to stroke [138] suggesting a potential role of anti-diabetic drugs to restore microvascular alterations. Stroke recovery is significantly worsened by the comorbidity of T2D. The class of anti-diabetic drugs sodium-glucose cotransporter-2 inhibitors (SGLT2i) such as Empagliflozin is known to have advantages beyond glycemic control, including weight reduction, reduced inflammation and improved endothelial dysfunction [139-143]. In **Paper IV**, we investigated the impact of Empagliflozin on pericyte density, pericyte coverage of blood vessels and BBB function as part of the stroke recovery in diabetic mice.

From the transcriptome to the secretome: state-of-the-art

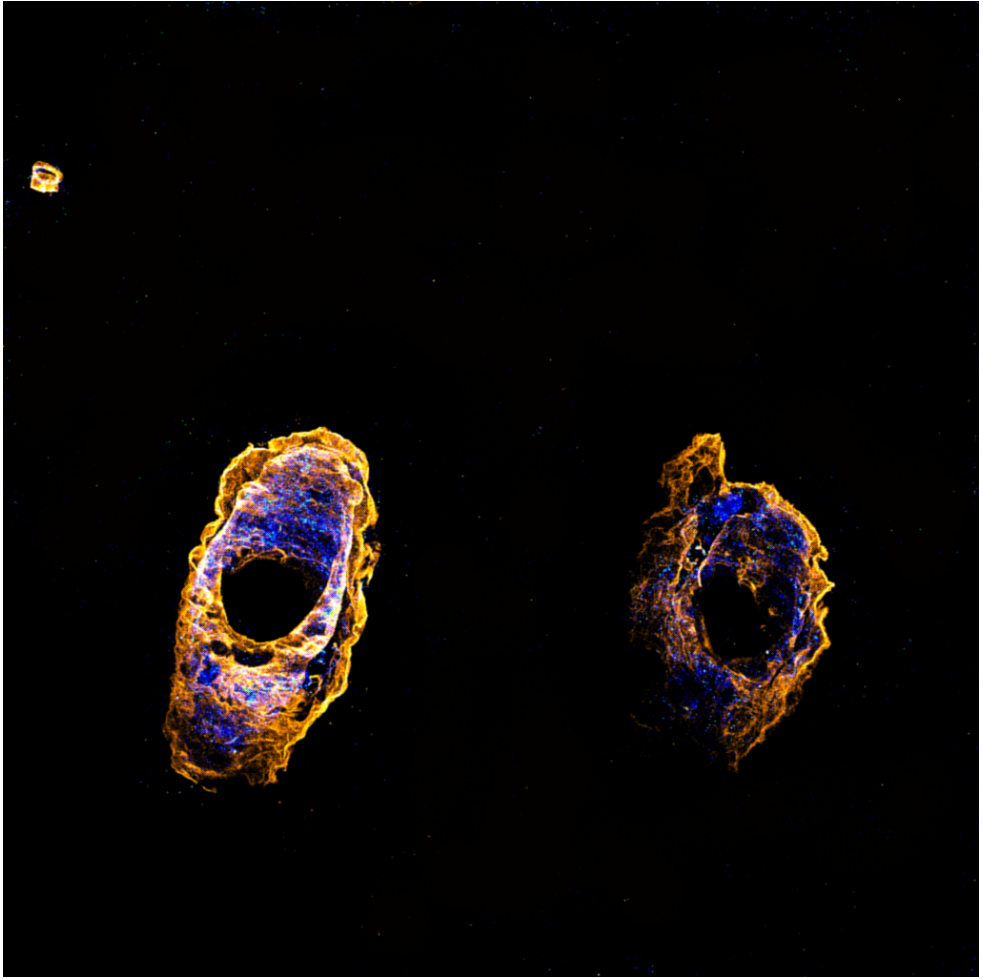
Recent advancements in transcriptomics have significantly enhanced our understanding of pericyte biology, heterogeneity, and potential therapeutic targets for various pathological conditions. For example, transcriptomic analysis enabled the discovery of novel pericyte markers and pericyte subtypes in the microvasculature of the brain [47, 144] and different organs [47].

Other studies focused on pericyte transcriptomic changes between health and disease. Yuan *et al.* (2018) investigated pericytes' role in hypertension, revealing several differentially expressed genes (DEGs) and altered signaling pathways between hypertensive rats and healthy controls [145]. Moreover, transcriptome analysis of pericytes from retinas of diabetic animals revealed novel genes and molecular pathways relevant to BBB alterations in diabetic retinopathy [146] and Alzheimer's disease (reviewed in [147]), but, overall, their role in diseases remains poorly evaluated.

Despite the advancements in sequencing technology, the correlation between transcript expression levels and their corresponding protein products is generally low [148, 149]. The relationship between mRNA and protein levels can be influenced by various factors, including post-transcriptional modifications, translation efficiency, and protein degradation rates. Since proteins are the active molecules performing cellular functions, understanding their levels and activities is essential for elucidating disease mechanisms. Therefore, studies on the proteome and secretome may offer greater utility in studying diseases, as they provide direct insights into protein levels, post-translational modifications, and functional changes that might not be evident from gene expression alone, making them particularly valuable for identifying potential biomarkers and drug targets.

Although there is growing interest in pericyte biology, the analysis of their proteome has undergone limited investigation compared to other cell types, such as endothelial cells [150]. A recent study examined the proteomic changes in aged pericytes, revealing metabolic alterations [151]. One challenge in studying the secretome remains the identification of the cell type that secretes the molecules of interest, so that most current research has been confined to monoculture systems. Despite being useful to control for specific conditions, these systems have limited resemblance with the *in vivo* conditions.

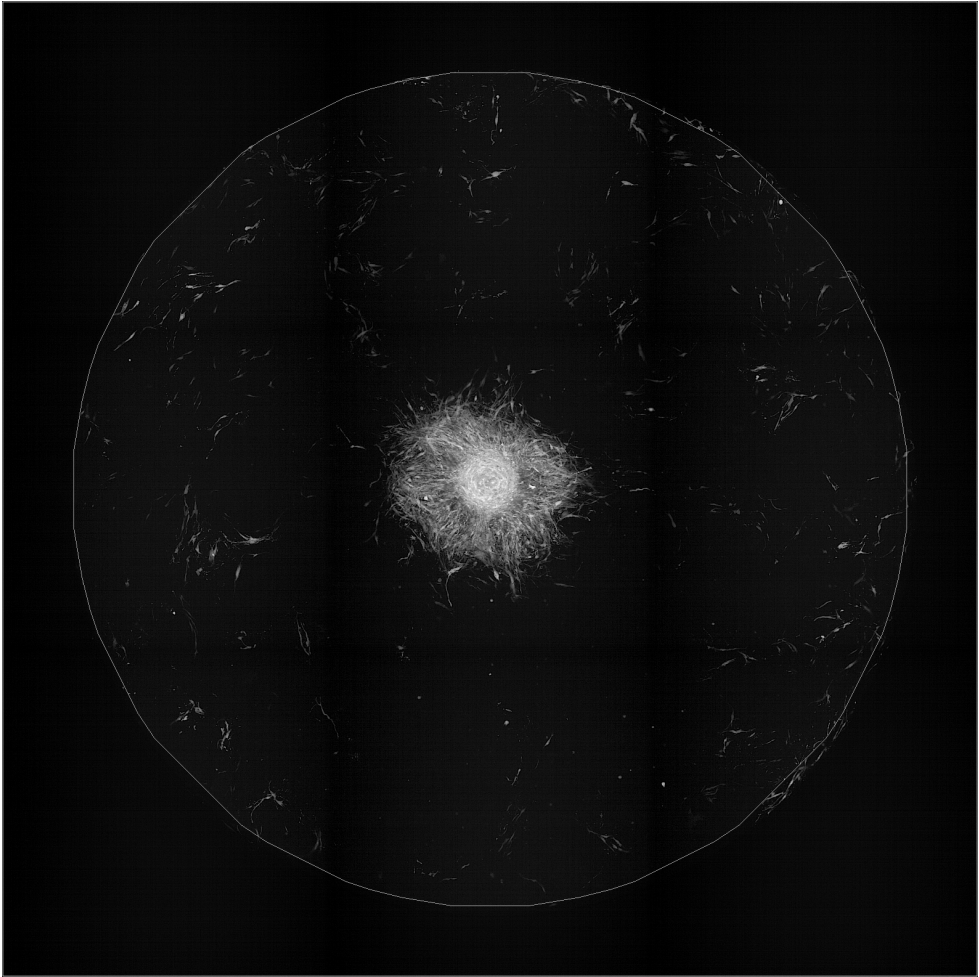
In **Paper V**, we employ Turbo ID, a biotin ligase, to selectively label and isolate proteins secreted by pericytes, introducing a novel approach to profiling the pericyte secretome within a co-culture model, which more accurately mimics *in vivo* tissue complexity compared to monocultures.



Black Holes

Aims

- I. In **Paper I** our aim was to investigate pericyte changes in transcriptional profiles and signaling to immune cells depending on their vicinity to GBM using single-cell RNA sequencing of different brain regions in a GBM mouse model and by analyzing a published human dataset.
- II. In **Paper II** we examined potential differences in the transcriptional profiles of pericytes across different timepoints in the acute phase after ischemic stroke, that might be of interest for the pathological progression of the stroke cascade.
- III. In **Paper III** we established a detailed timeline of microvascular events in the acute phase after ischemic stroke, including pericyte activation, blood-brain barrier leakage, and endothelial cell death.
- IV. In **Paper IV** we investigated whether a post-stroke intervention with the anti-diabetic drug Empagliflozin could improve stroke recovery in diabetic mice.
- V. In **Paper V** we aimed at characterizing the alterations in the pericytes secretome following hypoxia in co-culture or monoculture conditions by adopting a method to study specifically the pericyte secretome.



Spoilt Symmetries

Key Methodology

The following section provides an overview of the principal methods used in this thesis. For in-depth description, protocols, and supplementary files, please refer to the attached papers.

Animal models

All animal experiments were approved by the ethical committee of Lund University or the regional ethical committee of the Karolinska Institute, and the procedures were carried out in accordance with the relevant guidelines and regulations. Animals were housed under standard conditions with a 12 hour light/dark cycle and had access to food and water *ad libitum*. Every effort was made to keep animal numbers minimal according to the 3 R guidelines and principles of the Swedish Research Council.

In **Paper I, II and III**, we utilized male C57bl/6 wild-type (WT) mice and RGS5^{GFP/+} mice from a knock-out/knock-in reporter mouse strain that expresses GFP under the promoter of RGS5 in a C57bl/6 background [152]. In this model, one allele of RGS5 is replaced by GFP, making it possible to track pericytes by GFP expression under the activated RGS5 promoter. In **Paper IV**, we used C57BL/6JRj mice (Janvier Labs, France).

Glioblastoma

The mouse glioma 261 (GL261) cell line (RRID:CVCL_Y003), when intracranially injected into a C57BL/6 syngeneic mouse, recapitulates the characteristics of human GBM [153,154]. An advantage of this model is that the mice are immunologically competent. GL261 cells were transduced with mCherry to facilitate visualization when selecting the brain region for dissection. 100'000 mCherry-GL261 cells were injected over 3 minutes into the caudate nucleus of the mice using a 10 µl Hamilton syringe (Hamilton Bonaduz AG, Bonaduz, Switzerland) in the striatum. After injection, the needle was left in the brain for 5 minutes before it was slowly retracted. On day 21 after tumor inoculation, animals were sacrificed.

Stroke

In **Paper II and III** we used a permanent occlusion of the middle cerebral artery (pMCAO) model in order to obtain a localized and reproducible stroke lesion. The distal part of the left MCA was occluded using electrocoagulation to induce focal ischemia as previously described [155]. In **Paper IV**, stroke was induced by temporal occlusion of the MCA (tMCAO) using the intraluminal filament technique as described previously [156]. Shortly, left carotid arteries were exposed, and a silicone-coated monofilament was inserted until the origin of the MCA was blocked. The occluding filament was removed after 30 minutes. Sham operations were conducted in the same way, but without occluding the MCA.

Diabetes

For **Paper IV**, starting at 4 weeks of age, mice were kept on either standard laboratory chow diet (SD) or high fat diet (HFD; 60 % energy from saturated fat) for 8 months. After tMCAO or sham surgery, all mice were switched to SD to reflect the clinical situation of a balanced post-stroke diet. The diabetic mice were randomized into two experimental groups and treated daily orally with vehicle (0.5 % methylcellulose solution) or the SGLT2i Empagliflozin (Boehringer-Ingelheim, Germany) (10 mg/kg of body weight). At 5 weeks after stroke, mice were sacrificed to collect brains for further analyses.

Cell culture

Human brain vascular pericytes (HBVP, Sciencell) were cultured in pericyte medium supplemented with 2 % FBS, 100 µg/ml penicillin/streptomycin (P/S) and growth supplement supplied by the manufacturer. Human brain microvascular endothelial cells (HBMEC, Sciencell) were cultured in endothelial cell medium MV2 with 5 % FBS (PromoCell). HBVP and HBMEC plates were previously coated with 0.1 % gelatine. Primary human hippocampal astrocytes, obtained from the ventral mesencephalon from a 7-week-old embryo (HAsc, NGC-407), were cultured on fibronectin-coated plates (1 µg/ml) and the astrocyte medium composition contained Advanced Dulbecco's Modified Eagle Medium (DMEM F12, Gibco) supplemented with 10 % FBS and (100 µg/ml) P/S. The GL261 mouse glioma cell line (DSMZ, Germany) was cultured in DMEM supplemented with Glutamax (Gibco), 10 % FBS and 2 % P/S. All the cells were cultured at 37°C and 5 % CO₂.

Virus production and stable cell line generation

For lentivirus production we followed a previously described protocol [157]. Both lentiviruses TurboID (TID)-V5 pLX304 (Addgene #107175) and pLV-mCherry (Addgene #36084) were assembled with the viral envelope plasmid pMD2.G and packaging plasmid pBR8.91 in Optimem medium (Gibco). GL261 cells were transduced with the pLV-mCherry lentivirus for 24 hours and sorted in Fluorescent activated cell sorting (FACS) Aria 10 days after transduction. Dead cells were excluded as DAPI⁺. The mCherry⁺ sorted GL261 cells were confirmed to have low but detectable expression of mCherry, and were cryopreserved at -150 °C. For TurboID transduction, HBVP were incubated for 24 hours and selected by 4 µg/ml blasticidin for 14 days, replacing the medium every 3 days.

Spheroid co-culture generation

Spheroids for **Paper IV** were generated by mixing HBVP, HBMEC and HAsc in a 1:1:1 ratio with 10,000 cells of each cell type. The spheroids were cultured in 96-well plates coated with 1 % agarose in phosphate buffer saline (PBS) and cultured in spheroid medium generated from mixing the corresponding cell media in a 1:1:1 ratio.

Biotin treatment and hypoxia induction

500 µM [158] of exogenous biotin in DMSO was added to the cell-culture medium for both mono- and spheroid-cultures as a final concentration unless stated otherwise. For hypoxia treatment, cells were transferred to a humidified gas-tight hypoxia chamber (Electrotek) with a gas composition of 85 % N₂, 10 % H₂, and 5 % CO₂ generating an oxygen supply between ~ 0.5 – 1 %. An anaerobic indicator solution (Electrotek) was used for monitoring oxygen levels under 1 %, containing 2 % w/v C₆H₁₂O₆, 9 % w/v NaHCO₃ and 1 % w/v methylene blue solution in water.

Tissue processing

At the respective time point, mice were anesthetized using an i.p. injection with an overdose of sodium pentobarbital and then either transcidentally perfused with 0.9 % NaCl followed by 4 % paraformaldehyde (PFA) solutions or only perfused with 0.9 % NaCl solution. Brains from PFA-perfused animals were removed and postfixed in 4 % PFA at 4 °C overnight before being transferred to 30 % sucrose solution. Brains from saline-perfused animals were snap-frozen and stored at -80 °C until further use. Brains were then sectioned in 30 µm thick coronal sections with a Leica SM200 R sliding microtome and stored at -20 °C in anti-freeze solution or sectioned

in 20 or 30 μm thick coronal sections with a cryostat and kept at $-20\text{ }^{\circ}\text{C}$ until further analysis. Brains for FACS and single-cell sequencing were kept on ice and processed as described below.

10x genomics

Cells for sequencing were isolated according to Chang *et al.* [159]. After saline perfusion, the brains were mechanically minced and dissociated with enzymatic digestion using a mix of collagenase IV, dispase I and DNase I in PBS with CaCl_2 and MgCl_2 . The solution was incubated at $37\text{ }^{\circ}\text{C}$ for 1 hour with mechanical trituration every 10 min. After disaggregation, FBS was added to the solution to stop the enzymatic reaction, filtered, and centrifuged at $4\text{ }^{\circ}\text{C}$. The cells were washed with ice-cold PBS before being centrifuged again and resuspended in ice-cold 20 % BSA in 1x PBS and centrifuged for removal of myelin and neurons. The cells were then resuspended in 0.5 % BSA in PBS and kept on ice for subsequent FACS staining.

FACS

A similar protocol was applied for all FACS sorting experiments performed in this thesis. Please refer to the specific section in the respective papers for a more detailed description. Single cell suspensions were incubated with Fc-block for 15 min, followed by incubation with specific antibodies or corresponding isotype-matched control antibodies at a concentration of $1\text{ }\mu\text{g}/\mu\text{L}$ at $4\text{ }^{\circ}\text{C}$ for 30 minutes in darkness in FACS buffer. Then, the cell suspensions were washed twice with PBS. Cells were sorted on a FACS-ARIA II. After sorting, a fraction of the cells was re-stained and re-analyzed in the flow cytometer to check for the survival of pericytes and endothelial cells.

Sequencing

For **Paper II**, 10x reactions were prepared with the v3.1 3' x10 kit. cDNA and libraries were amplified according to 10x Genomics instructions and sequenced using Illumina NGS sequencing. The data was demultiplexed and genes were counted with the Cell ranger software (v.5). For **Paper II**, aggregation was run to normalize for sequencing depth between experiments.

Real-time quantitative PCR

Total mRNA was isolated with RLTPlus lysis buffer (Quiagen), and cDNA was retrotranscribed using Thermo Scientific Maxima First Strand cDNA Synthesis Kit for quantitative polymerase chain reaction (RT-qPCR). Samples were then prepared for qPCR using PowerUp™ SYBR® Green Master Mix (Thermo Fisher). Forward and reverse primers (TAG Copenhagen) of interest were added at a concentration of 0.05 µM/well. We then added 1 µl of cDNA from each sample and UltraPure water (Invitrogen) to reach the final volume of 10 µl/well. The analyses were run on a Bio-Rad CFX96 RT-qPCR system. Samples with a normal *β2m* amplification curve but an amplification of the target gene above 36 qPCR cycles were considered undetected and imputed with the R package nondetects [160].

Immunofluorescence

A similar protocol was applied for all the immunostainings performed in this thesis. Please refer to the specific section in the corresponding paper for a more detailed description.

3-3'-diaminobenzidine (DAB) staining

For visualization with DAB, in **Papers II** and **III** quenching of endogenous peroxidases was performed by a 20 minutes incubation at room temperature (RT) in PBS containing 3 % H₂O₂ and 10 % methanol. The sections were then incubated ON at 4 °C in PBS containing the primary antibody, 3-5 % normal donkey serum (NDS) and 0.25 % Tx-PBS. Incubation with biotinylated secondary antibody was followed by incubation with avidin-biotin complex according to manufacturer's instructions (Vectastain Elite ABC kit, Vector Laboratories), followed by visualization using DAB.

Sections on glass (snap-frozen tissue)

The sections were first rehydrated for 5 minutes with PBS and fixed in a solution of 4 % PFA in PBS. The sections were then permeabilized with a Triton-X 100 (Tx) 0.25 % or 1 % solution in PBS and incubated with a blocking solution (5 % or 10 % NDS or normal goat serum, 1 % Tx-PBS) for at least 1 hour at room temperature (RT), followed by incubation overnight at 4 °C with primary antibodies diluted in blocking solution. The sections were then incubated with the corresponding secondary antibodies diluted in PBS for 1 or 2 hours at RT and with DAPI (1:500)

for 5 min. Sections were washed in PBS, rinsed in deionized water and mounted using PVA-DABCO.

Free-floating sections

The sections were washed in PBS to remove anti-freeze solution and then blocked with 5 % NDS with 0.25 % triton-X100-PBS for 1 hours at RT. Following this, the sections were incubated ON at 4 °C with primary antibodies diluted in blocking solution. The day after, sections were washed and incubated 2 hours at RT with secondary antibody, 3-10 % NDS and 0.25 % Triton-X-100. Incubation with secondary antibody was followed by a 5 minutes incubation with PBS containing DAPI.

Immunocytochemistry

Both monocultures and spheroids were fixed with 2 % PFA for 20-30 minutes and then washed 3 x 5 minutes with PBS. Spheroids were then frozen on dry ice, cryo-sectioned at 20 µm and mounted on glass slides. For the staining, both cells and spheroids were blocked for 3h with NDS 5 % in PBS supplemented with 0.3 % Tx-PBS at RT. Primary antibodies were suspended in blocking solution and incubated ON at 4 °C. After washing, secondary antibodies were added to the cells and incubated for 1 hour at RT. DAPI was incubated for 5 minutes at RT before washing. Finally, the coverslips were mounted on glass slides using PVA-DABCO.

Image acquisition and processing

All the immunofluorescence images were acquired on a Leica DMI8 confocal microscope with an objective between 20-63x. The depth of z-stacks was changed according to the study and analysis. Images were analyzed and assembled using v.1.53v to 2.14.0/1.54f Fiji open-source image analysis software [161]. 2D images were produced from the z-stacks using Max Intensity function, followed by Split Channels function. For specific thresholds and cut-off, please refer to the relative sections in the attached papers.

Assessment of vascularization and blood-brain barrier leakage

To calculate area density, we expressed the percentage of the area of the specific marker to the total image area. For vessel length and branch counts, maximum projected images were binarized by automatic thresholding and skeletonized. Skeletons were analyzed using AnalyzeSkeleton plugin [162] as previously described [163]. To evaluate BBB leakage, we quantified extravascular fibrinogen

and albumin. Vessels were outlined to exclude intravascular proteins. Then, by applying an automatic threshold, the area covered by extravascular fibrinogen and albumin was quantified and expressed as percentage of total image area using the area fraction measurement tool. Image analysis was scripted and automated using the programming language ImageJ Macro minimizing potential for human error.

Bioinformatics analysis

scRNA-seq data from mouse samples

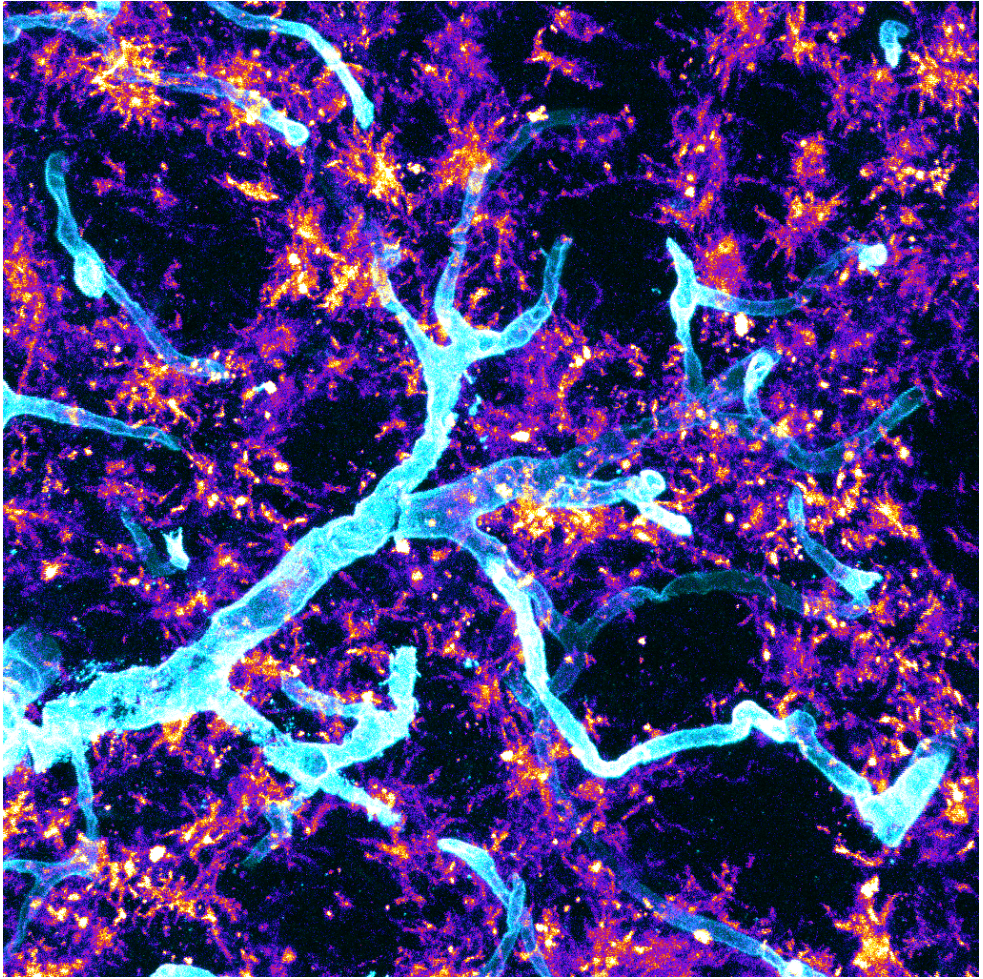
Cellranger (v. 5.0.1) was used to process the fastq files after the sequencing. For **Paper I**, background removal and doublets filtering were performed as indicated in the relative section of the manuscript. For **Paper II**, an additional aggregation step was performed for batch correction. Data were then processed in R using the Seurat package. Filtering was applied for cells with a number of features >200 and a mitochondrial content <10 %. The data was then log normalized, scaled and further processed to define cellular clusters. To define cluster identities, we compared the expression of cell type specific transcripts reported in the literature [47, 164-170]. To further study pericytes we used the Seurat function Subset. DEGs were identified with the findallmarker- functions in Seurat. Fast gene set enrichment analysis (FGSEA) was performed on the DEGs to define Hallmark (**Paper II**) or Gene Ontology Biological Processes (GO: BP) gene set enrichments (**Paper I**) within the data. Interacting ligand/receptor (LR) pairs were studied with CellChat [171].

scRNA-seq data from human published dataset

Raw scRNA-seq count data were downloaded from the NCBI Gene Expression Omnibus under accession number GSE12631 and processed as stated in the previous paragraph and according to the original publication [172]. Doublets were removed and data were processed similarly to the mouse samples as indicated in **Paper I**. Pericytes clusters were isolated for further analysis with the Subset function in Seurat. Cellchat was used to assess LR interaction pairs.

Statistical analysis

Different statistical analyses were applied to the specific studies according to the experimental setup. Please refer to the corresponding section in the paper for a more detailed description.



Night Fires

Summary of Key Results

This section summarizes the key results from the corresponding papers and manuscripts included in the thesis. For more details, see attached papers at the end of this thesis.

Paper I | Pericytes Change Function Depending on Glioblastoma Vicinity: Emphasis on Immune Regulation

To investigate whether pericytes in different brain regions interact differently with the immune system to influence GBM growth and invasion, we used scRNA-seq to examine mural cell transcriptomes across tumor-core, border and contralateral regions in both a GBM mouse model and human GBM datasets.

Mural cell subclusters redistribute depending on tumor proximity

In both mouse and human datasets, we identified multiple subclusters of pericytes and smooth muscle cells with region-specific dynamics.

In the mouse dataset, one pericyte subcluster exhibited a classic phenotype enriched in vascular and transport function pathways, while another subcluster showed an increase in RNA splicing and cell cycle pathways, suggesting a more active phenotype (Fig. 5A-D). These were respectively designated as “mouse transport” pericytes and “mouse signaling” pericytes. Similarly, of the two SMC subclusters, one had a classical phenotype while the other was involved in hematopoiesis, lymphocyte activation, and cell adhesion pathways. We named these “classical” SMC and “reactive” SMC, respectively. One subcluster expressed markers of both pericytes and SMCs and was enriched in immune response and phagocytosis pathways, and we therefore named it “mouse immune” pericytes (Fig. 5A-D).

In the human dataset, a subcluster related to immune functions was also found, which we designated as “human immune” pericytes (Fig. 5E-H). Another pericyte subcluster was enriched in pathways related to ion homeostasis, lipid biosynthesis, chemotaxis. We defined these cells as “human transport” pericytes. The last subcluster was enriched for ECM components, with pathway enrichment in collagen

each mural cell subcluster within each region in the mouse dataset colored according to the subcluster. E UMAP visualization of mural cells from the human dataset, separated into distinct subclusters. F UMAP visualization categorizing mural cells by region (tumor vs. non-malignant) colored by mural cell subcluster. G Dot plot showing the expression of pericyte and smooth muscle cell markers across subclusters in the human dataset. H Relative distribution of mural cell subclusters in normal or tumor region in the human dataset, colored by subcluster. mtPC = mouse transport PC; msPC = mouse signalling PC; miPC = mouse immune PC; cSMC = classical SMC; rSMC = reactive SMC; htPC = human transport PC; hiPC = human immune PC; ecm-PC = extracellular matrix PC.

Mural cells exhibit distinct transcriptional changes depending on tumor proximity

Mural cells exhibited changes in gene expression and associated pathways depending on the region of origin.

In the mouse contralateral region, mural cells expressed genes associated with biosynthesis, metabolism, and developmental processes (Fig. 6A, C), while human mural cells exhibited pathways linked to cellular component biogenesis and transport (Fig. 6G-H). At the tumor border, mouse mural cells displayed downregulation of reparative and supportive pathways, including autophagy and wound healing (Fig. 6B, E). Conversely, tumor-resident mural cells showed robust transcriptional activation, with significant upregulation of genes involved in vesicle trafficking, endocytosis, and protein secretion in mice (Fig. 6A, D), and genes linked to collagen synthesis and ECM remodeling in humans (Fig. 6H, F).

To identify conserved transcriptional responses, we compared the DEGs between tumor and non-tumor mural cells across species (Fig. 6I). From 767 mouse DEGs and 1,781 human DEGs, we identified 228 shared upregulated genes. Functional enrichment (FGSEA) revealed associations with RNA splicing, actin filament organization, and suppression of catabolic processes, suggesting conserved mechanisms by which mural cells contribute to the TME (Fig. 6J-K). Notably, while immune-related pathways [173-180], chaperone-mediated autophagy (CMA) [181-185], and ECM remodeling were not highlighted in the top FGSEA pathways, multiple shared genes implicated in these processes underscore their functional relevance.

In summary, tumor- and border- resident mural cells exhibited transcriptional changes indicative of functional adaptations in both mouse and human datasets. Border-residing mural cells reflected a transitional phenotype. Conversely, tumor-residing mural cells exhibited transcriptional changes indicating high protein secretion and signaling.

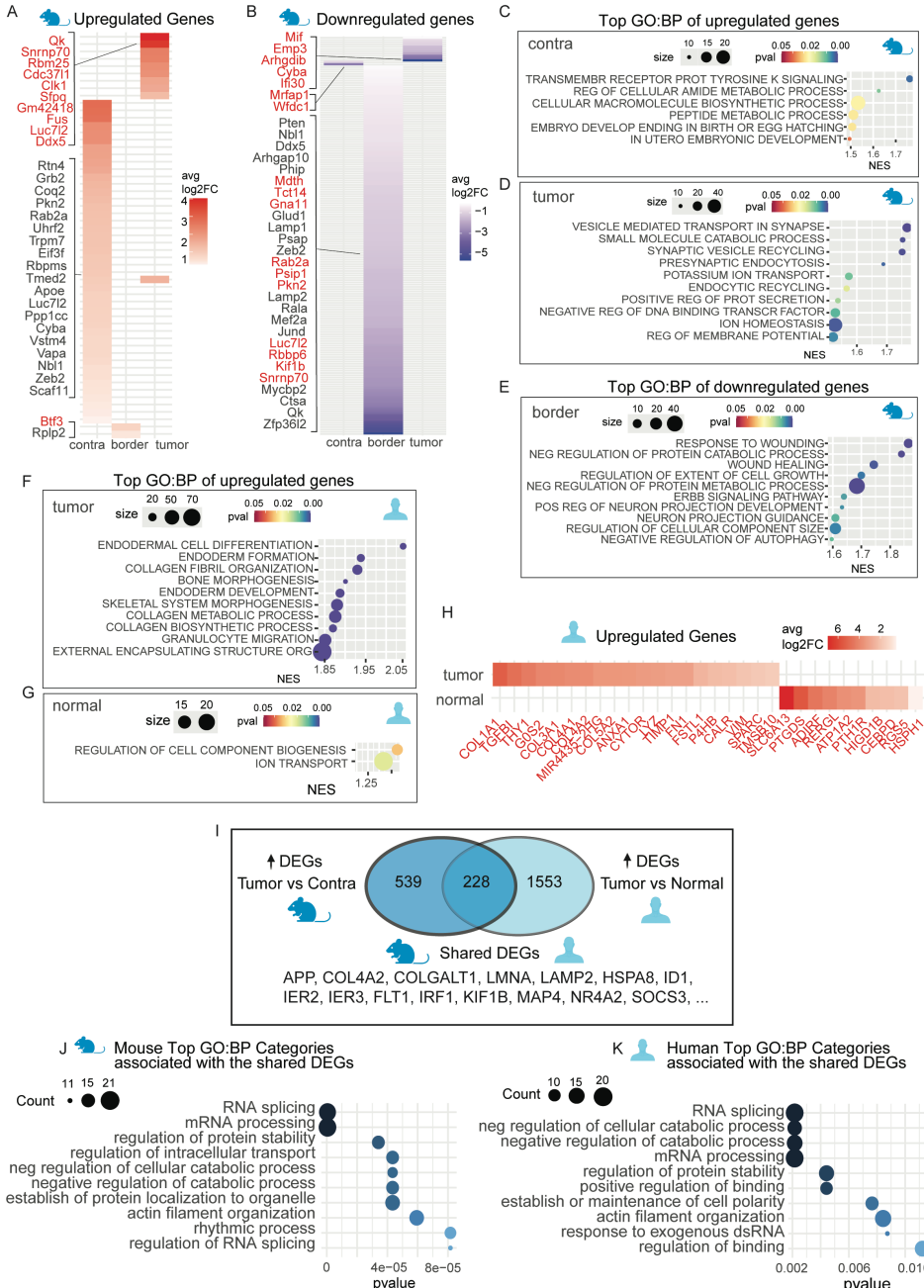


Figure 6. Differential gene expression and pathway analysis of mural cells across regions in mouse and human. A-B Heatmaps displaying the top upregulated (A) and downregulated (B) DEGs in mural cells, categorized by region, in mouse. Genes highlighted in red have a p-val <0.05. C-D-E GO terms associated with DEGs from each regional mural cell population. F-G GO terms associated with DEGs from the human tumor and non-malignant areas. H Heatmap of top upregulated DEGs for human mural cells, categorized by region. Genes highlighted in red have a p-val <0.05. I Schematic view of shared genes selection process: DEGs in mouse tumor mural cells were compared to contralateral cells and cross-referenced with DEGs in human tumor mural cells vs non-malignant tissue. Venn diagram shows the 228 shared DEGs, listed in Suppl. Tables. J-K Dot plots display enriched GO processes for the 228 shared genes, with J using mouse p-values and fold changes and the mouse GO database, and K using human p-values and fold changes and the human GO database. mtPC = mouse transport PC; msPC = mouse signalling PC; miPC = mouse immune PC; cSMC = classical SMC; rSMC = reactive SMC; htPC = human transport PC; hiPC = human immune PC; ecm-PC = extracellular matrix PC.

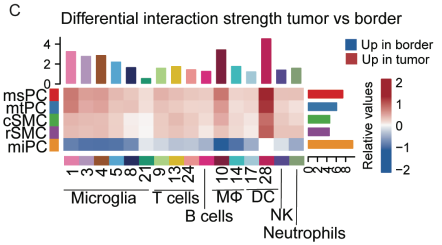
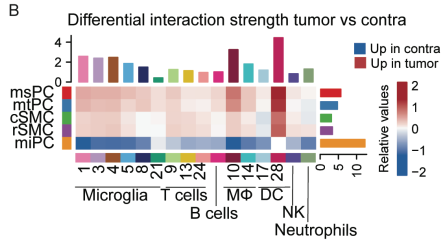
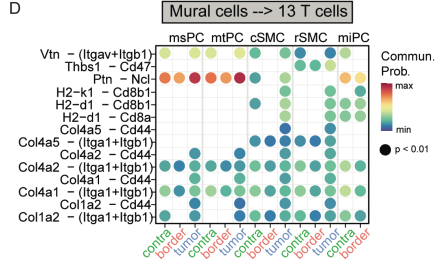
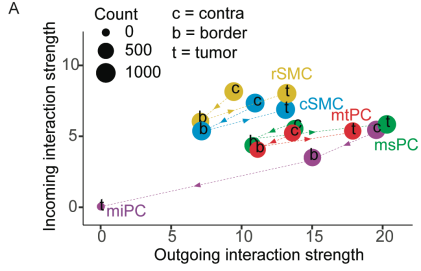
Tumor-residing mural cells markedly enhance communication strength and immune signaling

To further investigate mural cell interactions with immune cells across tumor, border, and contralateral regions, we performed ligand-receptor (L-R) communication modelling using CellChat. We highlighted region-specific and subcluster-specific communication patterns. In the mouse tumor core, “signaling” pericytes were the most active signaling hubs out of the mural cell subclusters, while “immune” pericytes played a negligible role (Fig. 7A-C). However, in the border and contralateral regions, “immune” pericytes were the dominant communicators (Fig. 7A-C). In human tissues, “matrix-associated” pericytes exhibited the highest activity across all regions (Fig. 7D-F).

At a global level, mural cells residing in tumor regions showed a markedly enhanced communication probability compared to those in non-malignant tissues in both species (Fig. 7C, F). In tumor areas, mural cells engaged in particularly strong signaling interactions with macrophages, followed by dendritic cells (in mice) (Fig. 7B-C) or monocytes (in humans) (Fig. 7E-F). In the mouse model, key interactions included Vitronectin-uPAR, Vitronectin-integrins, Pleiotrophin-Syndecan4, Nucleolin-CD74, and Amyloid Precursor Protein-CD74. In humans, tumor-associated pericytes exhibited increased ECM interactions, particularly with collagens and laminins, alongside immune-related signals such as annexin 1-formyl peptide receptor 1 and IL1B-CCR1. Notably, mural cells in both species demonstrated a functional shift in their interactions with T cells, characterized by suppression of MHC-I antigen presentation and a concurrent increase in adhesion and ECM-related signaling pathways (Fig. 7D, G). This suggests a loss of antigen-presenting capacity and a shift toward ECM-driven immune modulation.

In summary, our analysis indicated that tumor-residing mural cells enhanced signaling activity towards immune cells, in particular macrophages, monocytes and DC, with distinct region- and subtype-specific signaling patterns influencing immune modulation. A general switch in signaling towards adhesion and ECM interactions was observed, accompanied by a lower antigen presentation to T cells.

Mouse



Human

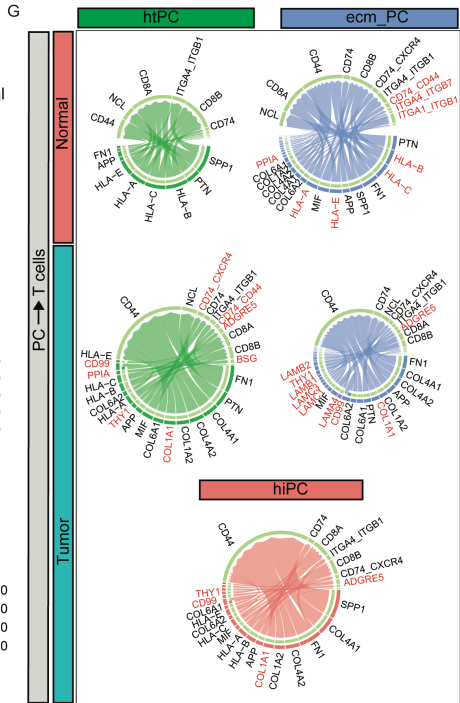
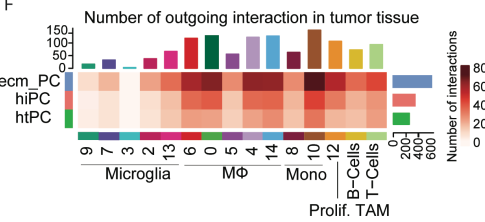
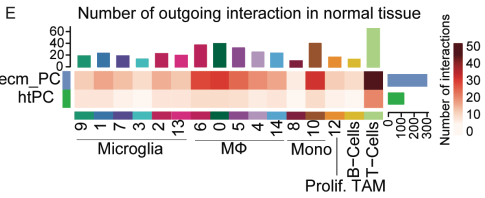
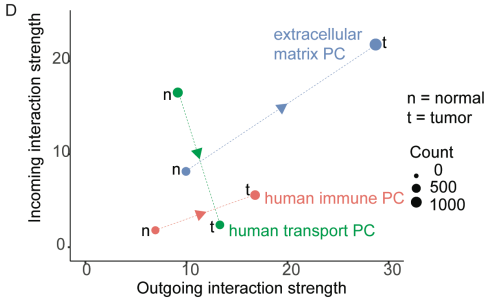


Figure 7. Cell–cell communication analysis of mouse and human mural cells using CellChat. A Scatterplot illustrating the total outgoing and incoming interaction strength for each mural cell subcluster across the contralateral (c), border (b), and tumor (t) regions in the mouse dataset. The x-axis represents the total outgoing communication probability, while the y-axis represents the total incoming communication probability for each cell group. Dot sizes correspond to the number of inferred connections (outgoing and incoming), and colors denote mural cell subclusters. Arrows on the dashed lines indicate the changes in communication as mural cells transition from the contralateral region to the border and into the tumor. B-C Heatmaps comparing differential interaction strength among cell populations across the three regions. The top-colored bar plot above each heatmap shows the sum of absolute values in each column, representing the total incoming signaling strength, while the right-colored bar plot shows the sum of absolute values in each row, representing the total outgoing signaling strength. Bar heights indicate the magnitude of changes in the number or strength of interactions. In each heatmap, red denotes increased signaling, and blue indicates decreased signaling between regions. Specifically, B highlights differences between the tumor and the contralateral region and C shows differences between the tumor and the border region. D Bubble plot showing outgoing signaling from mural cell subclusters to T cells (cluster 13) in each region. Rows display selected ligand–receptor pairs, while columns correspond to the contralateral, border, and tumor regions for each mural cell subcluster. Colors in the dots represent the communication probability, and dot sizes indicate the statistical significance (p-value). E Scatterplot illustrating the total outgoing and incoming interaction strength for each mural cell subcluster across the normal (n) and tumor (t) regions in the human dataset. F-G Heatmaps displaying differential interaction strength among cell populations across the two regions. The intensity of the red color denotes the number of interactions in the (E) non-malignant tissue and (F) tumor tissue. H Chord diagrams illustrating the significantly upregulated signaling ligand- receptor pairs from a specific pericyte subcluster towards a specific immune cell cluster either in the non-malignant or in the tumor region. htPC (green), ecm-PC (blue) and hiPC (orange) signals towards T cells are displayed. Genes that are specific for a region within the considered mural cell cluster are denoted in red. mtPC = mouse transport PC; msPC = mouse signalling PC; miPC = mouse immune PC; cSMC = classical SMC; rSMC = reactive SMC; htPC = human transport PC; hiPC = human immune PC; ecm-PC = extracellular matrix PC.

Paper II | The Transcriptional Landscape of Pericytes in Acute Ischemic Stroke

Moving from GBM to ischemic stroke, **Paper II** examines the pericyte response during the acute phase following stroke. As early responders to hypoxia and key regulators of BBB integrity, pericytes play complex, dual roles in stroke pathology and subsequent repair. To gain deeper insights into these dynamics, we characterized their transcriptomic responses at 1, 12, and 24 hours after pMCAO.

Pericytes form a new subcluster in the acute phase post-stroke which is related to angiogenesis and inflammation

After single-cell isolation and sequencing from either the ipsilateral (ipsi, i) or the healthy contralateral (contra, c) hemispheres at 1, 12, or 24 hours post stroke, we focused on the mural cells (*Pdgfrβ*⁺, *Rgs5*⁺) for further analysis.

By subclustering the mural cells, we obtained 8-10 subclusters, depending on timepoint and hemisphere (Fig. 8A). We found that, at 1 hour after stroke, ipsilateral residing pericytes had already changed their gene expression compared to the contralateral ones. DEG analysis showed that in the ipsilateral hemisphere compared to the contralateral one, the most active subcluster of pericytes upregulated genes such as Jun Proto-Oncogene (*Jun*), *Jund*, Fos Proto-Oncogene (*Fos*), ADAM metallopeptidase with thrombospondin type 1 motif 1 (*Adamts1*), *Ubc* and others (Fig. 8B).

Interestingly, one cluster of pericytes was present only at 12 and 24 hours after stroke in the ipsilateral hemisphere, suggesting a stroke-specific pericyte subpopulation (Fig. 8A). To characterize this subcluster, we assessed the DEGs of this subcluster compared to the other mural cell subclusters. The majority of the DEGs were conserved and significantly different at both 12 and 24 hours after stroke (Fig. 8C-D). The top 10 most upregulated genes in the pericytes stroke-specific subcluster were shared between 12 and 24 hours after stroke and included *Il11*, *Il6*, Retinol dehydrogenase 10 (*Rdh10*), Endothelin receptor B (*Ednrb*), C-C motif chemokine ligand 2 (*Ccl2*), Metallothionein-2 (*Mt2*), stanniocalcin 1 (*Stc1*), *Adamts4*, Drebrin 1 (*Dbn1*), and Follistatin like 1 (*Fstl1*) (Fig. 8C-D).

To gain insights into the functions associated with the pericyte stroke-specific subcluster, we performed the gene set expression analysis on the stroke-specific DEGs vs the rest of the mural cells subclusters. 24 hours after stroke, cells from the stroke-specific subcluster upregulated pathways related to downstream Myc targets, tumor necrosis factor (Tnf α) via nuclear factor kappa-light-chain-enhancer of activated B cells (NF- κ B), Il2/signal transducer and activator of transcription 5 (Stat5), mammalian target of rapamycin complex 1 (Mtorc1), hypoxia, apoptosis,

unfolded protein response, glycolysis, and pathways related to inflammation. At 12 hours, differentially expressed pathways were similar to the ones at 24 hours.

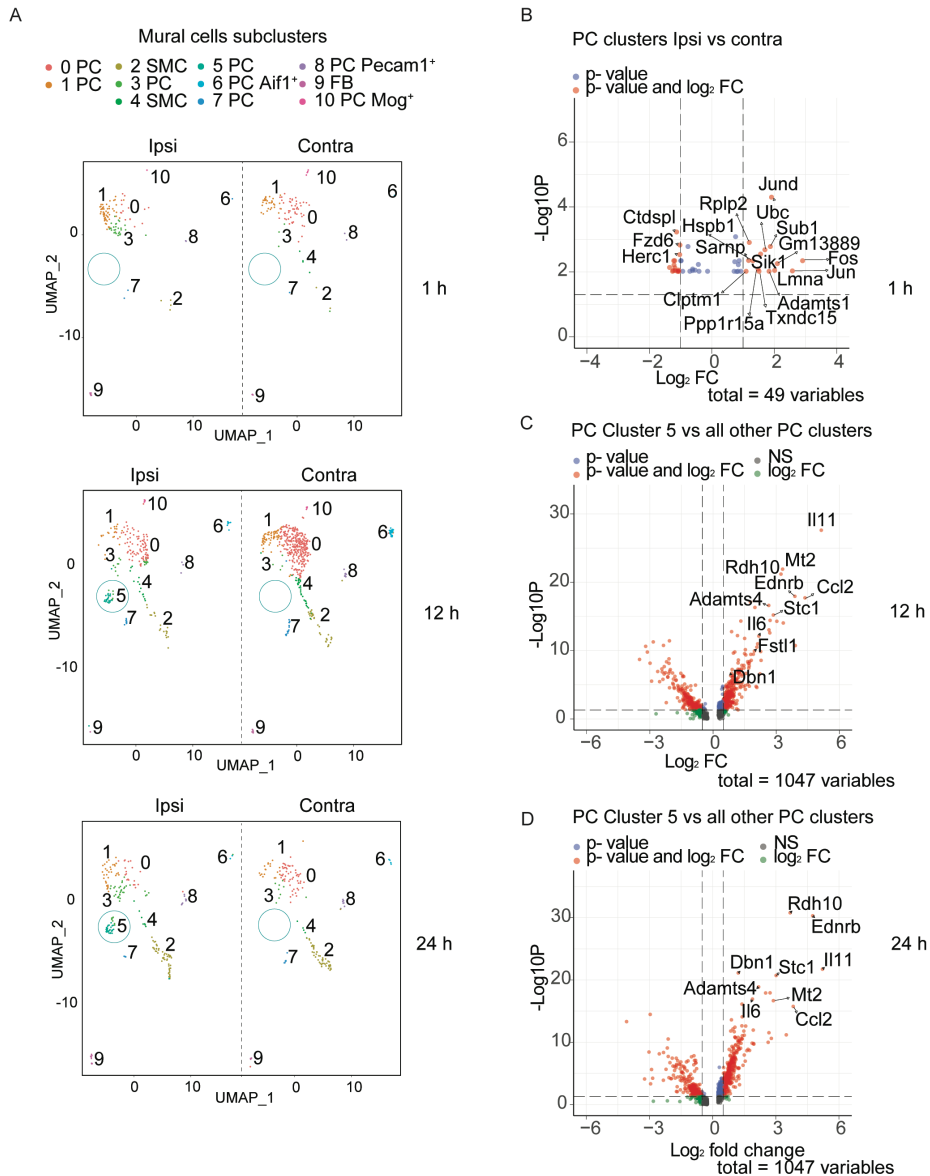


Figure 8. Pericytes are heterogeneous after stroke. A Pericytes subcluster analysis resulted in 8-10 different pericyte subclusters depending on the time point and hemisphere. Pericyte subcluster 5, which

is stroke-specific, is indicated by the green circle. B Volcano plots displaying the DEGs in the ipsi compared to the contra pericytes at 1 hour after stroke. C-D Volcano plots showing the DEGs in the stroke specific cluster compared to the remaining pericyte clusters at 12 and at 24 hours after stroke.

IL11 is specifically expressed by PDGFR β ⁺ cells from the ipsilateral hemisphere after stroke

Both transcriptomic and subsequent qPCRs analyses showed that *Il11* was among the top enriched genes specific to the stroke-associated subcluster of pericytes at 12 and 24 hours. IL11 is a cytokine mainly produced by stromal fibroblasts within the gastrointestinal tract [49], heart [50], liver [51], and lungs [52]. Since transcriptome changes do not always translate to differences in protein levels, we confirmed our findings by immunohistochemical analysis, showing the exclusive expression of IL11 in PDGFR β -expressing cells ipsilateral to the stroke (Fig. 9A-D).

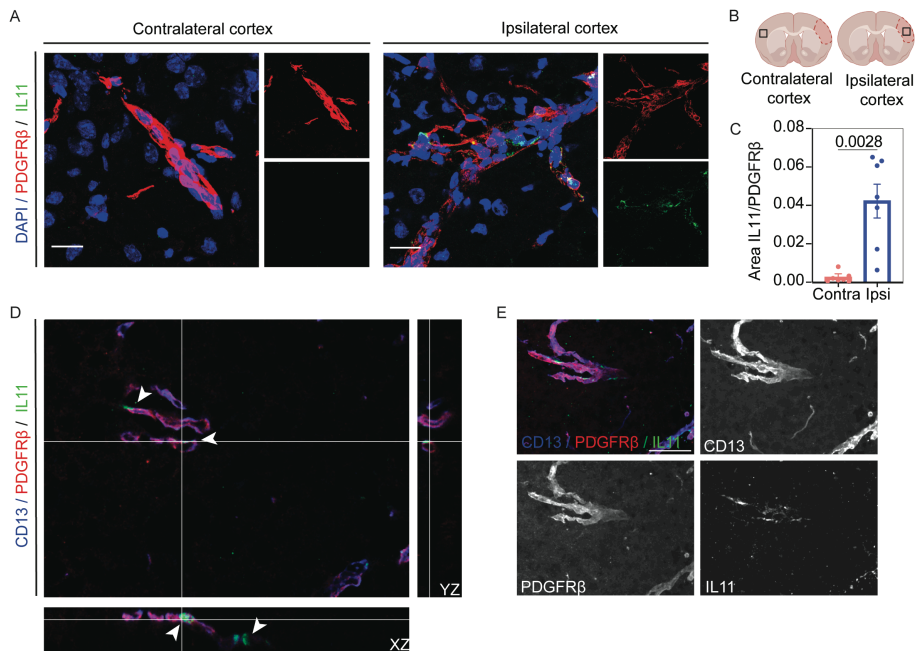


Figure 9. IL11 expression is increased in the ipsilateral hemisphere. A IL11 is only detected in the ipsi hemisphere after stroke in the proximity of pericytes. B Location of the selected images in the brain. The infarct core is outlined in red. C Area fraction occupied by IL11 and PDGFR β . Data are presented as mean \pm SEM. P-val = 0.028, paired t-test 95 % confidence level (confidence intervals 0.01985 to 0.05979). Scale bar = 20 μ m. D Orthogonal views showing IL11 expression in PDGFR β and CD13 expressing cells in the ipsilateral cortex and E 2D maximum projection of the merged channels. z stack = 24 μ m; scale bar = 25 μ m. Arrow points at IL11 signal.

Paper III | Pericyte Response to Ischemic Stroke Precedes Endothelial Cell Death and Blood-Brain Barrier Breakdown

As transcriptome changes do not always correspond with changes in protein expression, we complemented our transcriptomic analyses done in **Paper II** with morphological assessments of the vascular events characterizing the acute phase post-stroke. In this study, we examined the temporal dynamics of BBB disruption at 1, 3-, 6-, 12-, and 24-hours post-stroke using the pMCAO model in mice leveraging IHC and WB. This integrative approach allowed us to characterize the sequential breakdown of the BBB and its associated cellular changes, shedding new light on the vascular response during the early stages of ischemic injury.

Pericyte response starts already 1 hour after stroke

First, we assessed morphological changes in pericytes at the different timepoints after ischemic stroke. 1 hour after stroke, pericytes' morphology was comparable to the controls (Fig. 10A). From 3 hours after stroke, PDGFR β ⁺ pericytes displayed irregular cell bodies, and CD13⁺ pericytes detached from the vessels or extended their processes alongside the vessels, resulting in a higher pericyte coverage (Fig. 10A). 1 hour after stroke, GFP⁺ cells increased in number in RGS5^{+/GFP} mice. In addition, 1 hour after stroke, TUNEL⁺, NG2⁺ and pericytes were detected, while none were present under control conditions (Fig. 10B-C). NG2 and TUNEL pericytes did not co-label at any time point, suggesting that activated pericytes are not undergoing apoptosis. In summary, we observed that within the first hour after stroke pericytes exhibit two distinct behaviors: some undergo apoptosis, while others become activated expressing NG2 and RGS5, evading apoptotic processes.

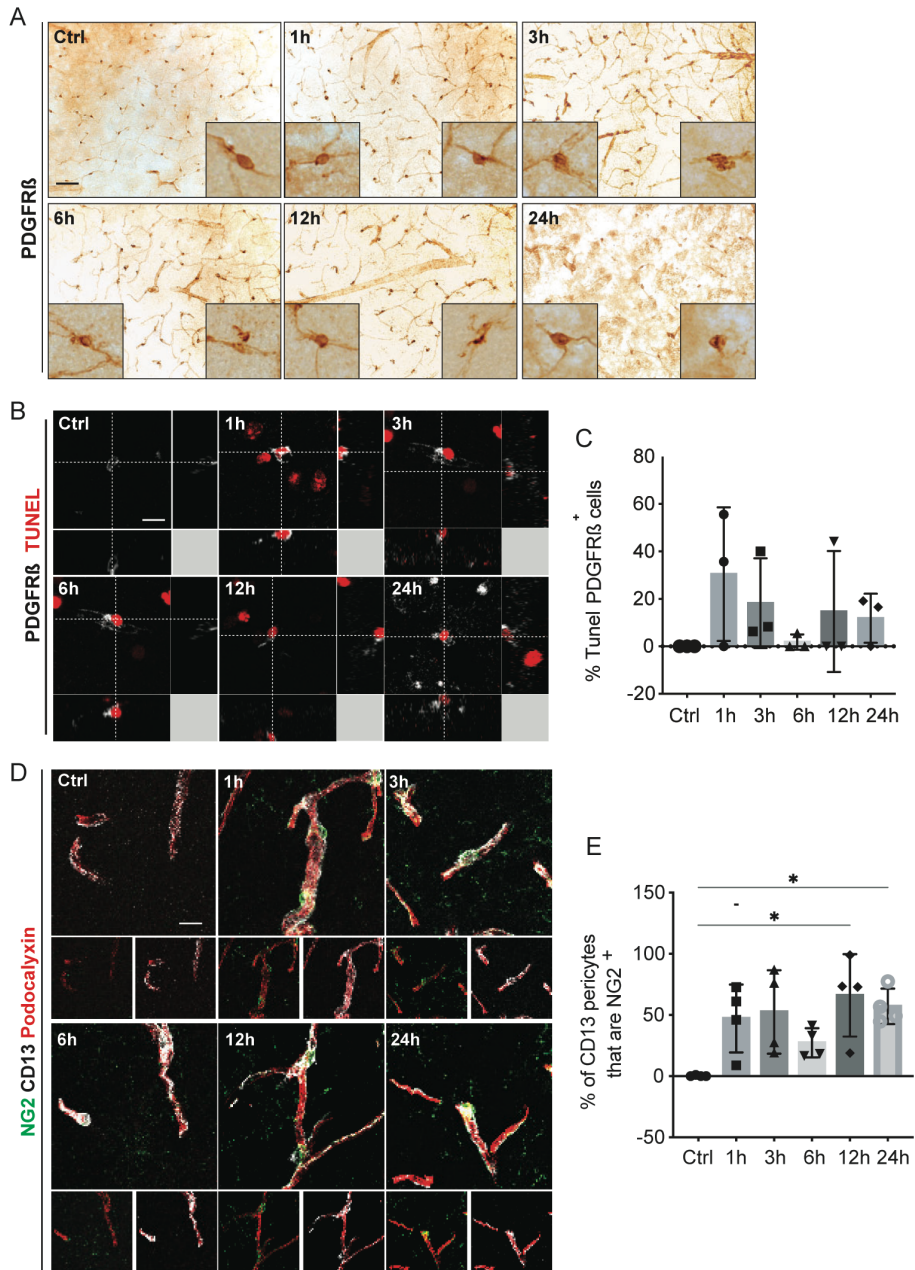


Figure 10: Pericyte responses start already 1 h after stroke. A Representative images of PDGFR β cells located in the infarct core after stroke. The boxes in the left lower corner show the usual morphology of PDGFR β cells at higher magnification; while the boxes in the right lower corner display higher

magnification of a morphologically abnormal PDGFR β cell. B Orthogonal views of PDGFR β pericytes (grey) that are positive for the apoptosis marker TUNEL (red). C Quantification of the percentage of PDGFR β pericytes that are positive for TUNEL. D Representative images showing the pericyte activation marker NG2 cells (green), the classic pericyte marker CD13 (grey), and the vasculature (Podocalyxin, red). E Quantification of the percentage of CD13 pericytes that co-label with NG2. n.3-4. *p<0.05. One-way ANOVA with Tukey's multiple comparisons. Scale bar 20 μ m and 10 μ m.

Zo-1 loss, BBB breakdown and endothelial cells death follow the pericyte response

Previous studies showed that also endothelial cells and their TJs are affected early after stroke [55, 186-188]. Therefore, we next investigated the levels of the TJ proteins ZO-1 and Occludin across the acute phase after stroke. We observed that Zonilla (ZO)-1 protein levels were reduced more than 50 % at 12 and 24 hours and that Occludin protein levels were reduced at 12 hours in the ipsilateral compared to the contralateral hemispheres following stroke (Fig. 11A-C). Endothelial cell death was first detectable only after 12 hours, with CD31/TUNEL⁺ cells significantly increased in number at 24 hours compared to controls (Fig. 11D-E). Assessment of the blood vessels total length also revealed that the total vessel length decreased significantly at 24 hours after stroke. In terms of BBB leakage, we observed that extravascular fibrinogen was significantly increased 12 and 24 hours after ischemic stroke, and that extravascular dextran was only observed after 12 hours (Fig. 11F-G).

Overall, our results reinforce the findings that pericytes respond rapidly after stroke, adopting diverse mechanisms. This positions pericytes as key players at the forefront of the pathological stroke cascade, highlighting their potential as a critical target for preventing BBB breakdown and endothelial cell death.

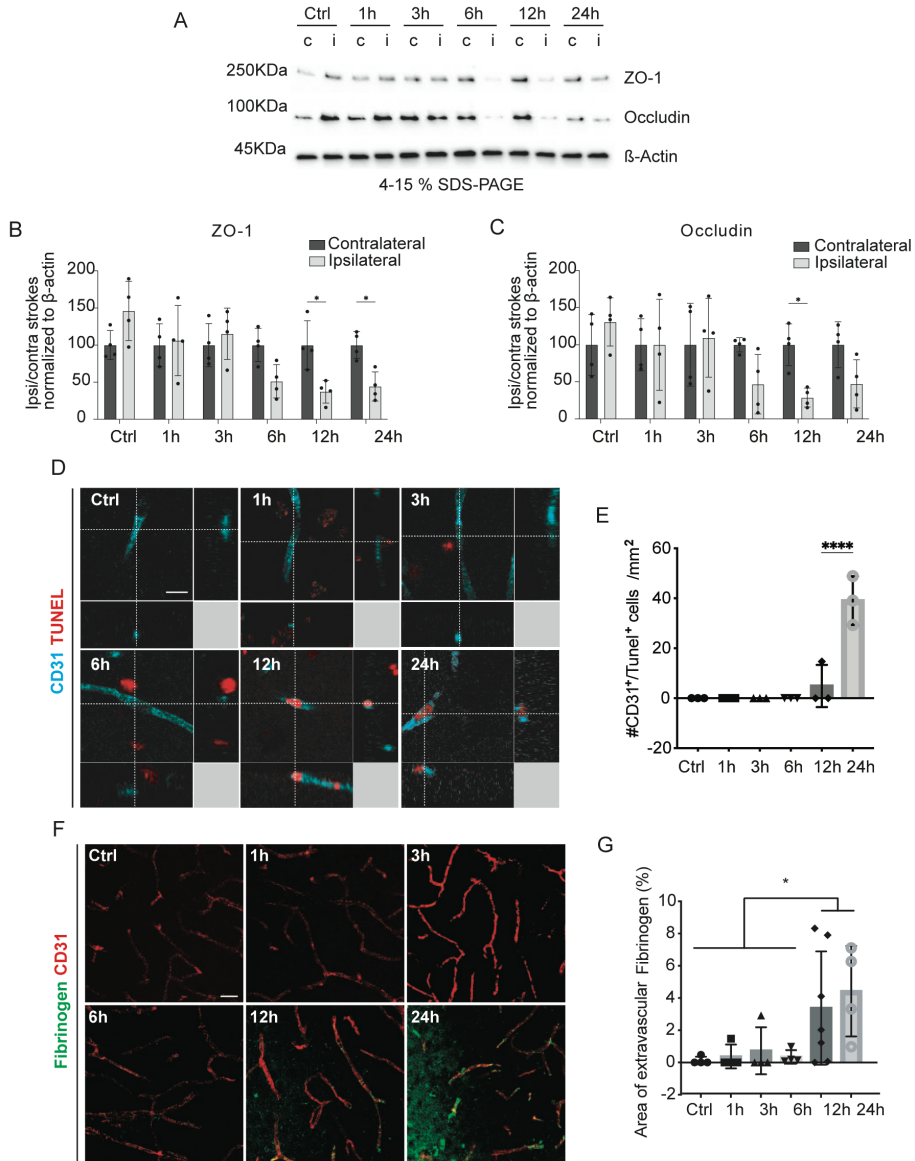


Figure 11: Endothelium responses begin 12 hours after stroke. A WB of protein lysates from mice ipsi or contra hemispheres after stroke or sham surgery. Representative blots of the TJ proteins ZO-1, Occludin or β -Actin. B-C Quantification of ZO-1 (B) or Occludin (C) levels normalized to β -Actin. n = 4. *p<0.05, **p<0.01. Two-way ANOVA followed by Sidak's multiple comparisons. D Orthogonal view of confocal images showing endothelial cells (CD31) colocalizing with TUNEL. E Quantification of CD31/TUNEL cells. F Representative confocal images of endothelial cells and endogenous fibrinogen. G Quantification of extravascular fibrinogen. n. 3-7. *p<0.05, ****p<0.0001. One-way ANOVA with Tukey's multiple comparisons. Scale bar 10 μ m and 20 μ m.

Paper IV | The SGLT2 Inhibitor Empagliflozin Promotes Post-Stroke Functional Recovery in Diabetic Mice

Stroke recovery is notably impaired by the comorbidity of T2D, yet no treatments currently address this critical clinical challenge. SGLT2i, such as Empagliflozin, have shown benefits beyond glycemic control, including weight reduction and anti-inflammatory effects. Expanding the focus beyond the acute phase of **Papers II** and **III**, this study investigated whether chronic Empagliflozin treatment could enhance post-stroke recovery in a T2D mouse model.

Empagliflozin improves stroke recovery in T2D mice, potentially through the regulation of pericyte density

Following the 8 months of HFD (diabetes model) and a transient occlusion of the MCA (stroke model), the potential efficacy of Empagliflozin on stroke recovery was assessed by the forepaw grip strength measurement. Within 5 weeks after stroke, Empagliflozin treatment completely normalized the T2D-induced worsening of stroke recovery.

To investigate if Empagliflozin treatment influenced the vasculature after stroke, we evaluated vessel density, pericyte density and coverage, vessel length and branching, pericyte activation and BBB leakage (Fig. 12A-E). We found a significant increase in pericyte density in the T2D-VH group compared to the non-T2D group, which was normalized by Empagliflozin treatment (Fig. 12A, C). The groups had comparable endothelial density and pericyte coverage (Fig. 12A-B, D), implicating that the increased overall pericyte density observed in the T2D-VH group was due to pericytes located in the parenchyma. Indeed, we observed a significant increase in parenchymal pericyte density in the T2D-VH group compared to the non-T2D group and we detected a strong trend towards a reduced parenchymal pericyte density in the T2D-E group compared to the T2D-VH group, and no difference was detected between non-T2D and T2D-E animals (Fig. 12A, E).

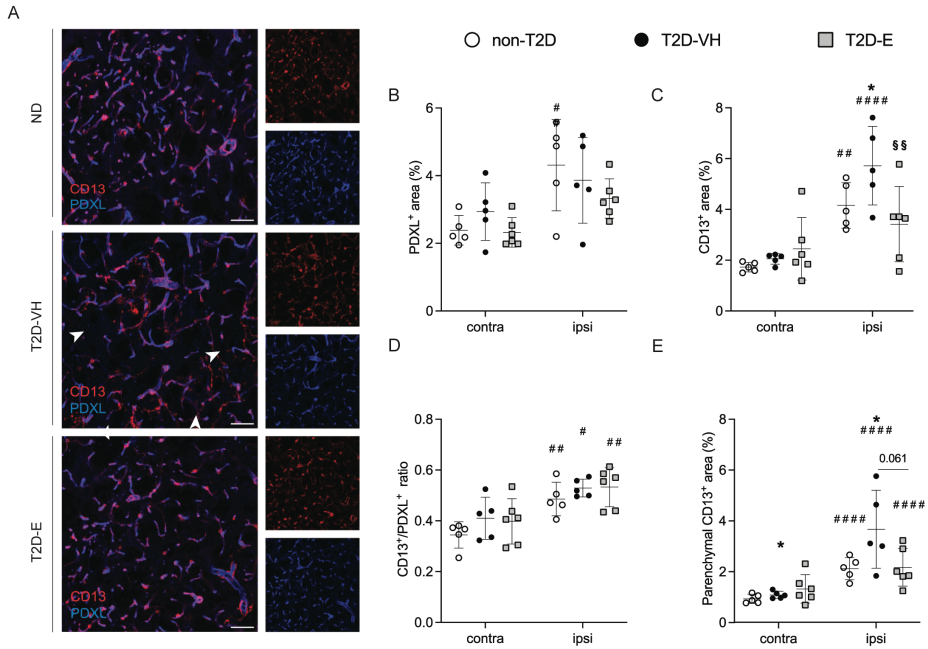


Figure 12. Effect of Empagliflozin on vascularization after stroke. A Confocal images showing pericytes (CD13, red) and endothelial cells (PDXL, blue) in the striatum of non-diabetic controls (non-T2D), diabetic mice (T2D-VH) and diabetic mice treated with Empagliflozin (T2D-E) after stroke. B assessment of vessel density, C pericyte density, D pericyte coverage and E parenchymal pericyte density calculated as % of area occupied by the staining in relation with the total area of the image. White arrows indicate the pericytes that are not associated with vessels. Data are presented as mean \pm SD. Statistical significance was calculated using two-way ANOVA followed by Benjamini, Krieger and Yekutieli multiple comparisons test. Results were considered statistically significant if $p < 0.05$. *denotes a difference between non-T2D and T2D-VH, ^denotes a difference between T2D-VH and T2D-E, #denotes a difference between contralateral and ipsilateral hemisphere within the same group. Scale bar = 50 μ m. non-T2D n = 5, T2D-VH n = 5, T2D-E n = 6

T2D and Empagliflozin do not affect BBB integrity, vascularization and pericyte activation

To assess BBB integrity, we examined the presence of plasma proteins in the brain parenchyma analyzing two different molecular sizes, albumin (~ 65 KDa) and fibrinogen (~ 340 KDa). We observed no significant differences in albumin or fibrinogen extravasation between the groups (Fig. 13A-B). We also assessed other vascular parameters, such as total vascular length, number of branches and branch average length, without finding any difference among hemispheres or groups, suggesting that at 5 weeks after stroke on a SD, the BBB integrity and vascular parameters were restored to the contralateral levels of non-diabetic mice.

We next evaluated pericytes activation by assessing CD13 and NG2 colocalization (Fig. 13 F-G). From our analysis we observed that ipsilateral pericytes were similarly activated in all the groups after stroke.

Taken together, in the study we demonstrate that Empagliflozin significantly improved functional recovery after stroke in T2D mice, and we propose that a possible mechanism is through the normalization of T2D-induced alterations in parenchymal pericyte density.

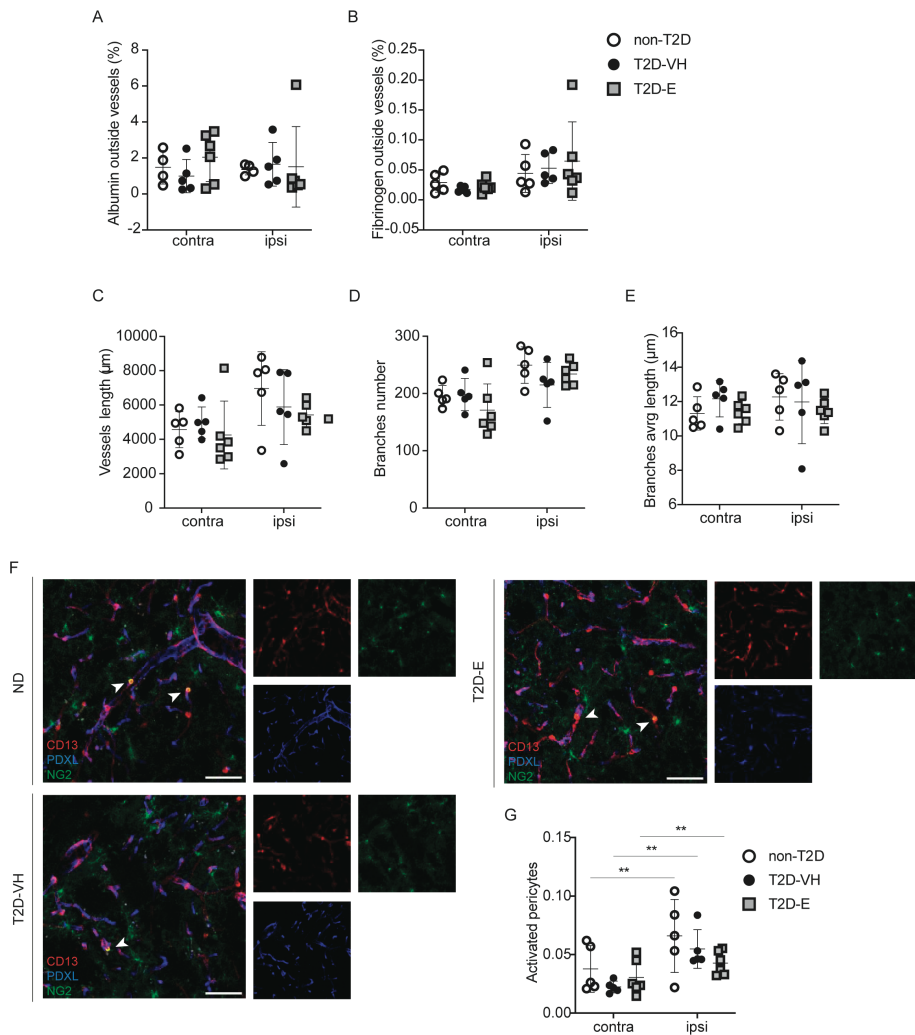


Figure 13: Effect of Empagliflozin on BBB leakage, vascularization and pericyte activation after stroke. Expression in the striatum of non-diabetic controls (non-T2D), diabetic mice (T2D-VH) and diabetic mice treated with Empagliflozin (T2D-E) after stroke of albumin (A) and fibrinogen (B) to evaluate BBB leakage; and other parameters related to vascularization such as vessel total length (C), branch number (D) and length (E). F Evaluation in the striatum of pericyte activation, calculated as density of colocalizing NG2 and CD13 positive signals normalized to total CD13 density. Scale bar = 50 μ m. Data are presented as mean \pm SD. Statistical significance was calculated using two-way ANOVA followed by Benjamini, Krieger and Yekutieli multiple comparisons test. Results were considered statistically significant if $p < 0.05$. p values are indicated between relevant. non-T2D n = 5, T2D-VH n = 5, T2D-E n = 6.

Paper V | Pericyte-Specific Secretome Profiling in Hypoxia Using TurboID in a Multicellular in Vitro Spheroid-Model

Pericytes are well-recognized for their extensive signaling capabilities, making the study of their secretome a valuable complement to transcriptomic and morphological analyses. In order to investigate the specific secretome of pericytes in a hypoxic environment, we utilized TID, a biotin ligase, to selectively label and isolate proteins secreted by pericytes in both mono- and co-culture systems under normoxic and hypoxic conditions, simulating stroke and GBM-like hypoxic environments.

TID specifically biotinylates pericyte proteins in mono- and spheroids-cultures

To achieve pericyte-specific labeling, we generated a stable pericyte cell line expressing TID anchored to the endoplasmic reticulum (ER). This localization facilitates the biotinylation of secreted proteins, which predominantly transit through the ER (Fig. 14A). Spheroids containing TID-expressing pericytes, endothelial cells, and astrocytes were established to simulate a multicellular environment (Fig. 14B).

To validate TID activity, we confirmed robust biotinylation of endogenous proteins in TID -pericytes. Co-localization of streptavidin with the ER marker calnexin and the TID V5-tag further corroborated the correct expression and ER localization of TID (Fig. 14C). Analysis of the cell culture supernatant by WB detected biotinylated secreted proteins under both normoxic and hypoxic conditions, but only in the presence of exogenous biotin. WT-pericytes and TID-pericytes without biotin exhibited undetectable levels of biotinylated proteins, confirming the specificity of our labeling system (Fig. D-E).

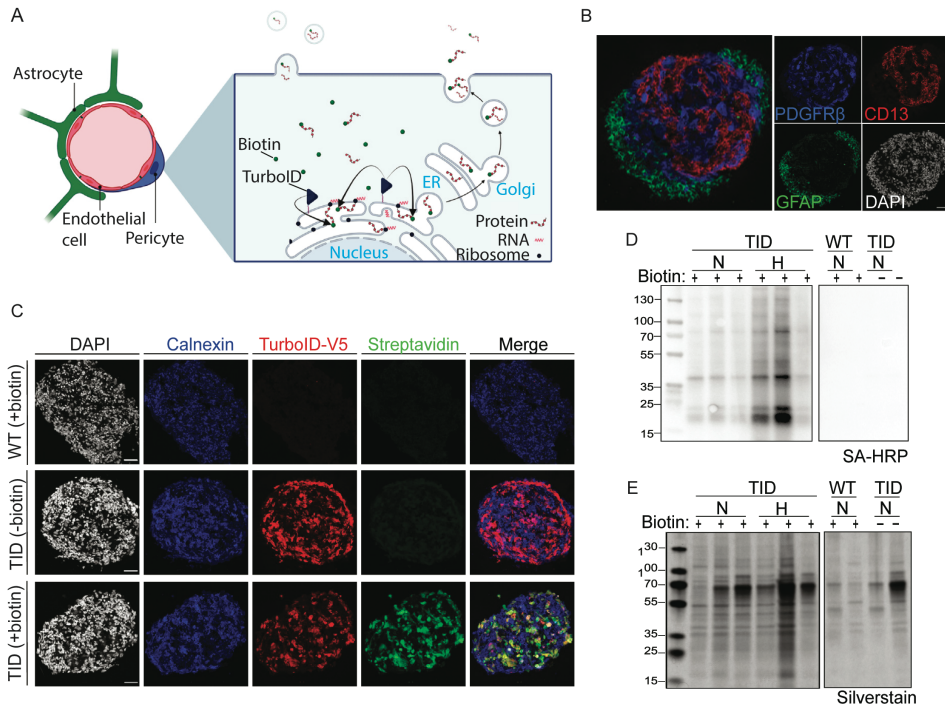


Figure 14. TID-mediated biotinylation of pericyte-secreted proteins in spheroid co-cultures. A Schematic representation of TID, anchored to the endoplasmic reticulum (ER) in pericytes, showing its biotin-labeling activity of nascent proteins in the ER. Proteins follow the conventional secretory pathway involving ER-Golgi trafficking and the release of extracellular vesicles. B Representative confocal image of a spheroid co-culture stained for pericytes (PDGFR β , blue), endothelial cells (CD31, red), astrocytes (GFAP, green), and cell nuclei (DAPI, white). C Confocal images of spheroids composed of either TID-expressing pericytes or WT-pericytes, treated with exogenous biotin. ER is labeled with calnexin (blue), TID with V5-tag (red), biotinylated proteins with streptavidin (green), and nuclei with DAPI (white). D Streptavidin blotting of supernatant samples from spheroids, harvested 24 hours post-biotin treatment, showing biotinylated secreted proteins. E Total protein content from the same samples analyzed via silver staining. N, normoxia; H, hypoxia; TID, TID-expressing pericytes. Scale bars, 50 μ m.

Pericyte alter their secretome depending on oxygen level and culture conditions

To investigate the pericyte secretome in hypoxia, we performed liquid chromatography-mass spectrometry proteomics on biotinylated proteins purified from cell culture supernatants. On average, over 2,000 proteins were detected, indicating extensive biotin labeling of the pericyte secretome. UpSet plot analysis of differentially expressed proteins (DEPs) displayed significant differences between experimental conditions (Fig. 15A-B). 33 proteins were significantly

altered in hypoxic monocultures, while 20 were altered in hypoxic spheroids compared to the normoxia counterpart. The most pronounced differences in protein secretion were observed between spheroid and monoculture conditions, irrespective of oxygen levels (Fig. 15 A-B). Specifically, we identified 73 secreted proteins significantly different between hypoxic spheroids (HS) and hypoxic monocultures (HM) and 87 proteins between normoxic spheroids (NS) to normoxic monocultures (NM).

In hypoxic monocultures (HM vs NM), proteins such as cellular nucleic acid binding protein, NAD(P)HX epimerase (NAXE), and angiopoietin-like 4 were upregulated, while others like protein S (PROS1) and insulin-like growth factor binding protein 2 were downregulated (Fig. 15C). Functional enrichment analysis highlighted the upregulation of pathways related to hypoxia, MTORC1 signaling, and cell cycle regulation in hypoxic monocultures, whereas pathways linked to apical junction formation, apoptosis, and protein secretion were downregulated (Fig. 15D).

The hypoxic spheroid (HS vs NS) comparison showed a distinct secretome profile. Proteins such as alanine aminopeptidase (NPEPPS), NAXE and others were enriched under hypoxia, while others like protein phosphatase 2A and tumor protein-translationally-controlled 1 were depleted (Fig. 15E). Enrichment analysis indicated that hypoxia in spheroids upregulated pathways associated with protein secretion, PI3K-AKT-MTOR signaling, and glycolysis, while pathways linked to epithelial-mesenchymal transition and DNA repair were downregulated (Fig. 15F).

Interestingly, although some proteins (e.g., NPEPPS and NAXE) were consistently differentially expressed under hypoxia in both culture systems, most changes were unique to each condition. Collectively, these findings suggest that pericytes exhibit a dynamic, hypoxia-responsive secretome that is highly influenced by cellular interactions within the BBB microenvironment.

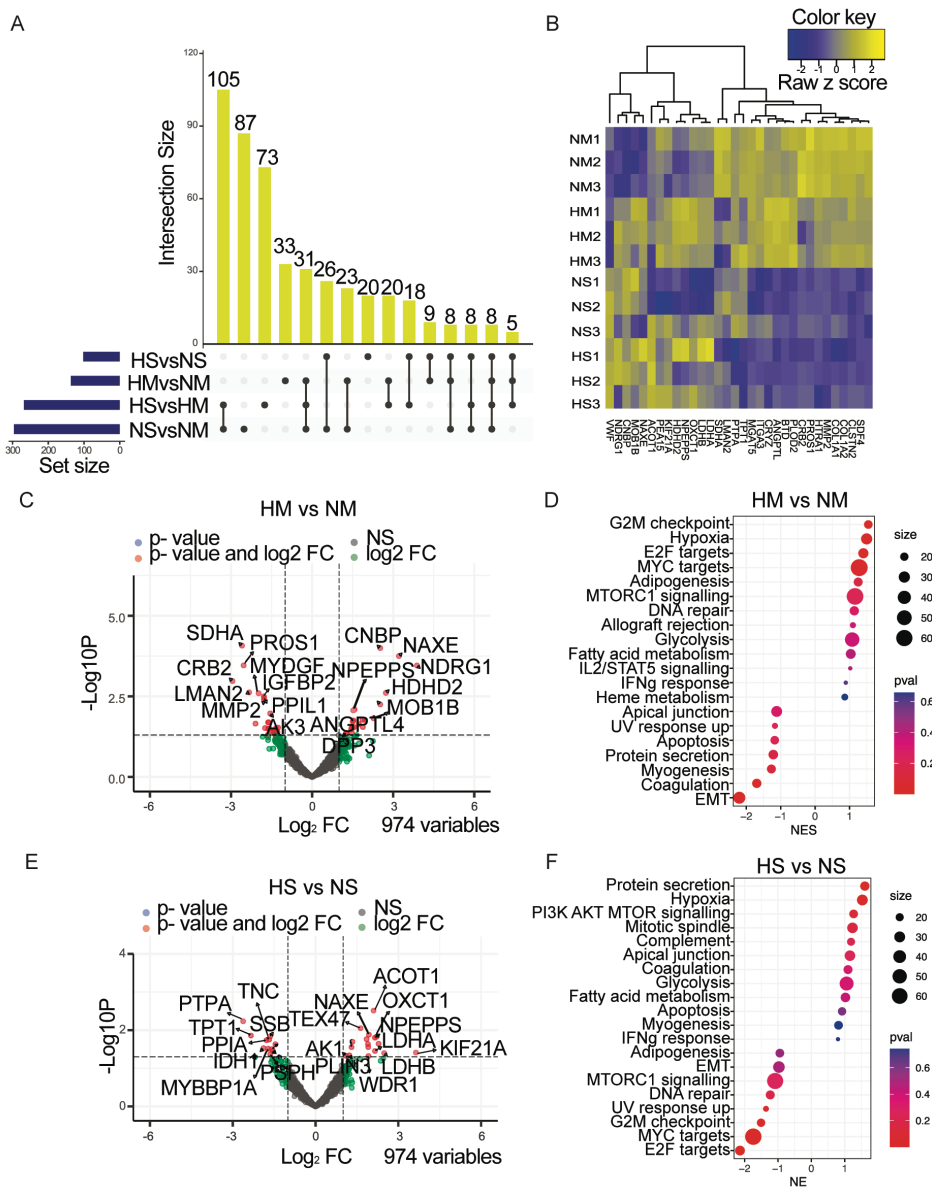
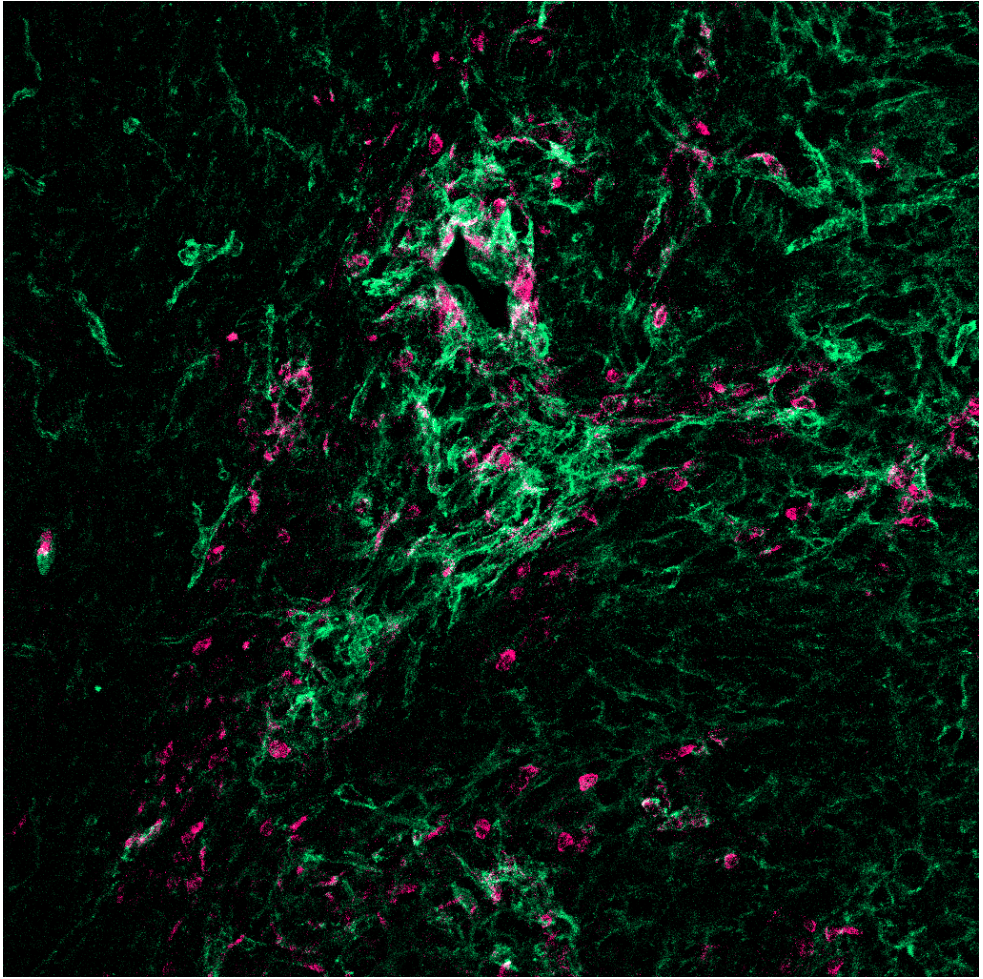


Figure 15. Proteomic differences of pericyte-secreted proteins in response to environmental cues. A Upset plot showing shared or specific differentially secreted proteins between the experimental conditions. Blue bars on the y-axis represent total number of proteins for comparison in each set size. Yellow bars on the x-axis represent the number of significantly differentially secreted proteins specific to a singular comparison or shared across comparisons illustrated by the black dots. B Heatmap of hierarchical clustering by z-score intensities to identify the top10 FC >2 with p<0.05 upregulated genes after 24 hours of hypoxia for mono- or spheroid-cultures. C Volcano plot showing the DEPs between HM compared to NM (left) D Hallmark signaling pathways associated with the DEPs (right) after 24 hours

hypoxia. E Volcano plot showing the DEPs between HS and NS (left) F Hallmark signaling pathways associated with the DEPs (right) after 24 hours hypoxia. EMT, epithelial mesenchymal transition; HM, hypoxia–monoculture; HS, hypoxia–spheroids; NM, normoxia–monoculture; NS, normoxia–spheroids. n = 3



Alternative Option

Discussion and Future Perspectives

In this thesis, we investigated the dynamic roles of pericytes in GBM and ischemic stroke. We analyzed the transcriptomic changes of pericytes in relation to spatial distribution (**Paper I**) and temporal progression (**Paper II**) of these pathologies, contextualizing these findings to their multiple roles in the brain. Morphological analyses in **Papers III** and **IV** further advanced our understanding of pericyte behavior in ischemic stroke, leading to an exploration of their cell-specific secretome under hypoxic conditions in **Paper V**.

Our findings reveal that pericytes undergo profound phenotypic and functional changes in both GBM and ischemic stroke, corroborating their classification as highly plastic cells. These results position pericytes as promising candidates for innovative therapeutic strategies aimed at addressing vascular dysfunction and promoting recovery in these brain pathologies.

In **Paper I**, we delineate transcriptional and communication changes in pericytes depending on their vicinity to the GBM mass. The increase in cellular adhesion and ECM communication pathways validates a similar result recently obtained by Xie *et al.* [73], who reported that a distinct pericyte cluster characterized by upregulated ECM-related genes emerged in GBM [189]. In GBM, excessive ECM production promotes malignant tumor phenotypes [190]. The normal brain ECM forms a complex network composed of glycoproteins, fibronectin, laminins, glycosaminoglycans, proteoglycans, and relatively low levels of collagens [191-193]. The ECM plays both a structural and a functional role, being the physical support of the microvasculature net, and influencing different signaling pathways among the cells [190]. For example, ECM physical, chemical, and biological signals influence the ability of the immune cells to infiltrate the TME during the development of cancer [194]. T cells typically migrate toward tumors following chemotactic signals, but alterations in the ECM create haptotactic signals that disrupt this process, causing T cells to migrate along ECM structures rather than infiltrating the tumor [195-199]. ECM proteins also directly regulate T cell activity; for example, collagen suppresses CD8⁺ T cells in murine models [200], while ECM stiffness enhances PD-L1 expression in lung cancer cells, suppressing anti-tumor CD8⁺ T cell responses [201]. Stiff ECM also hampers immune therapies by reducing immune cell infiltration and increasing tumor rigidity, which limits therapeutic penetration [202, 203]. ECM components influence macrophage polarization, with collagen and hyaluronic acid promoting M2 polarization [204, 205] while

fibronectin drives M1-like cytotoxic macrophage behavior [206]. Therefore, therapies aimed at ECM components may also enhance the effectiveness of immunotherapy.

Based on the above, it is plausible that pericytes secrete ECM components to regulate the adhesion and activation of immune cells. Alternatively, the overproduction of ECM by pericytes could represent an attempt (yet failure) to isolate GBM cells through a mechanism resembling scar formation. In this context, the scar functions to encapsulate the diseased tissue, potentially limiting its spread. Reflecting this, considerable efforts are focused on developing therapeutic strategies that target the ECM in GBM [207-213]. Recent studies have identified pericytes, along with SMCs, endothelial cells, and fibroblasts, as key contributors to ECM overproduction in GBM [213], further supporting our findings. Notably, the authors demonstrated that inhibiting collagen synthesis significantly improved chemotherapy efficacy in both murine and human patient-derived xenograft GBM models. Specifically, blocking the collagen crosslinking enzyme Lysyl oxidase homolog 2 enhanced treatment outcomes [213]. These findings underscore the potential of targeting ECM secreted by mural cells to mitigate GBM progression and reduce tumor invasiveness [194].

Recent studies highlighted the pericyte involvement in immune responses in GBM [22, 24, 101, 102]. Here, we corroborate those findings showing that an immune pericyte cluster was present in both mouse and human datasets. These pericyte clusters shared genes with previously reported mural cells immune cluster [73, 74]. Additionally, we found that pericytes engaged in distinct signaling pathways with specific immune cell types. These results confirm the immunosuppressive phenotype of tumor-residing pericytes found in previous studies [109, 214, 215].

The second key focus of this thesis was the temporal dynamics of pericyte responses after ischemic stroke, and particularly we predominantly focused on the pericyte response during the hyperacute and acute phases (**Papers II and III**). In **Paper II** we characterized the transcriptional changes of pericytes at 1, 12, and 24 hours after stroke onset, and in **Paper III** we described their detachment processes, death, and the resulting effects on BBB breakdown and endothelial cell viability at 1, 3-, 6-, 12-, and 24-hours post-stroke.

In **Paper II**, we found that pericytes express several transcripts that change across the first 24 hours after stroke and may constitute targets for the inhibition of early vascular dysfunctions associated with ischemic stroke. Pericyte responses already started as early as 1 hour after the ischemic insult in the stroke area. At this timepoint, pericytes ipsilateral to the stroke upregulated pathways related to TNF α signaling, P53, hypoxia, and apoptosis. At 12 and 24 hours post stroke, in **Paper II** we also found a stroke-specific subset of pericytes, not present at 1 hour. Our findings align with a previous scRNA-seq study using a transient MCAO model, which reported similar transcriptional changes in pericytes [216]. In the study, these

pericytes are associated with immune functions. Consistently, our FGSEA analysis revealed an increase in pathways related to inflammation, cytokine production, and vascular remodeling in the stroke-specific pericyte cluster. Despite differences in stroke models, our results confirm a comparable response in these pericyte subclusters at 24 hours post-stroke. IL11 was among the strongest upregulated genes, and it was also the only transcript uniquely expressed by the stroke-specific cluster of pericytes. IL11 is a cytokine with different functions depending on the context: it has been associated with a protective role in ischemic stroke [217], but it is also a critical promoter of fibrosis in multiple organs [218]. For this reason, future studies are needed to better understand the role of pericyte secreted IL11 in the acute phase of stroke. For example, knock-out studies would give valuable insights in determining the function of specific genes and whether their activation improves or exacerbates stroke outcome.

In **Paper III**, we establish a timeline of microvascular events during the first 24 hours following an ischemic injury. Results in this study further support the early response of pericytes to ischemic stroke. Here, we morphologically observe that pericytes are first responders to the ischemic injury, and that their response precedes BBB breakdown and endothelial cell death. 1 hour after stroke, approximately 30 % of pericytes exhibited the cell death marker TUNEL, aligning with the transcriptomic data in **Paper II** showing apoptosis. Early pericyte death also resonates with previous findings in rat brain slices cultured *ex vivo*, where the majority of pericytes constricted and died within 40 minutes following simulated ischemia [130]. However, at 1 hour nearly 50 % expressed NG2 and/or RGS5, underscoring their rapid activation and pivotal role in the acute phase of ischemic injury. RGS5 and NG2 have been associated with pericyte activation, particularly during processes such as angiogenesis and vascular remodeling [27, 219]. It is therefore plausible that activated pericytes contribute to these processes in the acute phase of ischemic stroke. Pericyte activation in pathology has been described in mouse models of Huntington's [220], Parkinson's diseases [221], pulmonary arterial hypertension [222] and diabetic retinopathy [117]. RGS5 expression is also linked to pericyte detachment from the vessels, causing subsequent BBB leakage [16, 94]. It is possible that the underlying mechanism of detachment involves the rapid stabilization of RGS5 in hypoxic conditions, leading to pericyte desensitization to the endothelial PDGF-BB chemotactic cues [94]. Indeed, within 3 hours post-stroke, pericytes displayed morphological changes and showed signs of detachment, consistent with previous studies [60, 93]. We and others have previously shown that pericytes migrating into the brain parenchyma change their phenotype and might play a role in inflammation and scar formation after ischemic stroke [16, 223]. In stroke, the activation and detachment of pericytes from blood vessels likely contribute to the reduced TJ levels [16, 66, 90], accompanied by increased BBB leakage, endothelial cell death, and a reduction in vascular length that we observed at 12 and 24 hours post-injury.

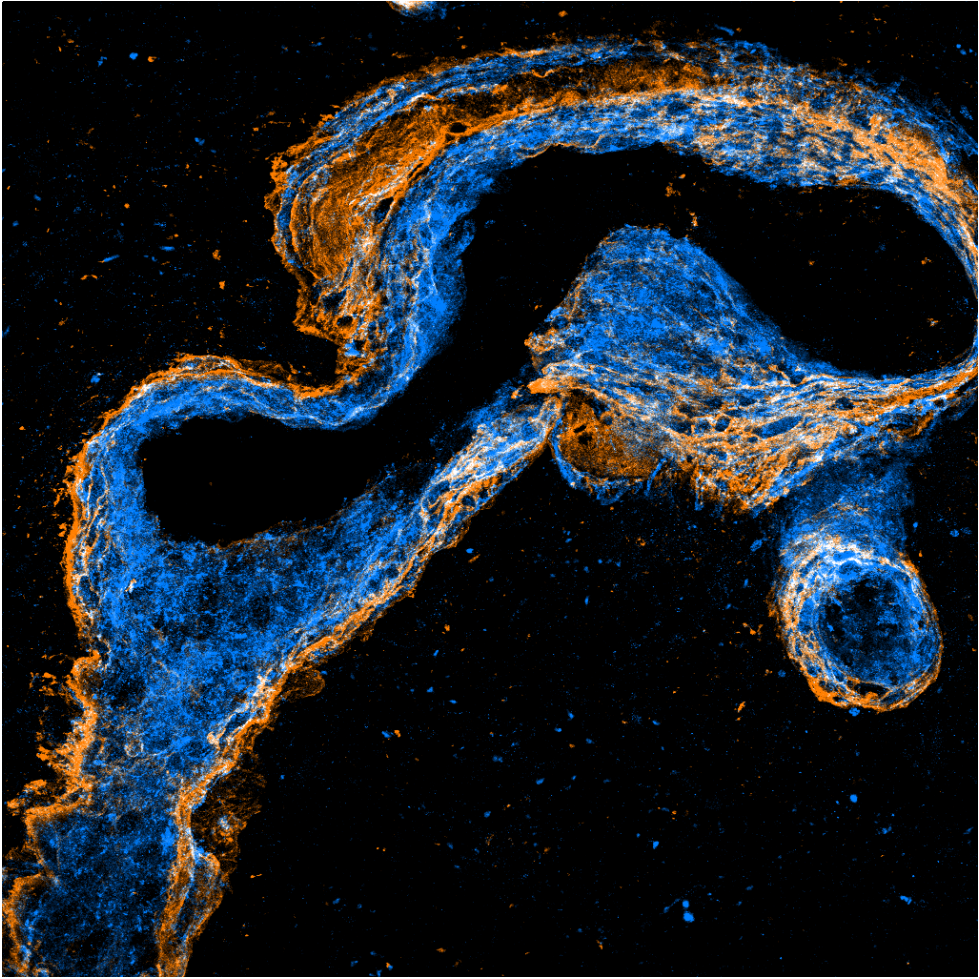
In **Paper IV**, even though the primary aim of the study was to evaluate the impact of Empagliflozin administration to diabetic mice after stroke, the study design allowed us to gain insights into the role of pericytes at 5 weeks post stroke, corresponding to the chronic phase. Our results, showing increased endothelial and pericyte densities, pericyte coverage, and pericyte activation in the stroke hemisphere, supported a previously published study from our group [138], and corroborates other results, showing that pericytes can replenish themselves and contribute to vascular repair mechanisms in the chronic phase after stroke [224]. In this study, 5 weeks after stroke pericyte numbers recovered 40 % more compared to the acute phase post-stroke. Our results revealed no differences in BBB leakage between stroke and non-stroke brain hemispheres, suggesting that at this timepoint BBB integrity was restored, in accordance with the normalized pericyte and endothelial coverage.

While we observed clear stroke-induced effects when comparing stroke and healthy hemispheres, diabetes did not mediate relevant effects on the vasculature, except for an increase in pericyte density. This result is surprising, considering that in diabetes, and particularly in the context of diabetic retinopathy, the number of pericytes is reduced [117, 225]. Since diabetes was associated with a higher pericyte density, which was not reflected in enhanced pericyte coverage of the vessels, we evaluated the density of parenchymal pericytes. Indeed, it has been reported that in diabetic retinopathy, pericytes migrate off vessels, and that if accounting for off- and on-vessel pericytes, there is no pericyte loss [226]. Reflecting this, we observed an increase in parenchymal pericytes in the diabetic mice, suggesting that pericytes migrate away from the vasculature. Pericyte detachment from the vessels might be a sign of initiating the process of angiogenesis, which is indeed pathological in diabetes, and considered to be among the causes of blindness [227]. These findings indicate a complex response of pericytes to hyperglycemic conditions, suggesting that while some pericytes are lost, others may adapt or change their functional roles.

GBM and ischemic stroke share a critical pathological feature: the presence of hypoxia in the brain. Hypoxia triggers a multitude of cellular responses aimed at maintaining homeostasis, including suppression of ATP-consuming reactions, metabolic reprogramming, and changes in gene expression. Given that pericytes act as early sensors of hypoxia in the brain, understanding their responses to hypoxic conditions is crucial. Pericytes have many functions, but their impact on disease progression is largely attributed to their secretory capacity [65, 66]. While advancements in sc-seq technologies have provided unprecedented resolution of cell-type-specific changes and population heterogeneity, these transcriptomic profiles offer limited predictive power for secreted signaling proteins. On another level, secretome analysis offers unique insights, especially in the context of cell-cell communication, which can be disrupted in pathologies. It also plays a critical role in identifying biomarkers within biofluids, providing direct translational relevance. To address this gap, **Paper V** focuses on characterizing the pericyte

secretome under hypoxic conditions. By utilizing TID expression in the pericyte ER we could detect all proteins destined for conventional secretion, since biotinylated. This approach enabled the isolation of pericyte-specific secreted proteins directly from brain homogenates. Our findings demonstrate that hypoxia induces significant shifts in the pericyte secretome. Using mass spectrometry, we identified nearly 15000 secreted peptides, with several proteins differentially expressed between normoxic and hypoxic conditions. Notably, conserved changes were found across monoculture and co-culture systems, including proteins such as NAXE and NPEPPS, highlighting their potential relevance in hypoxic brain pathologies.

Shedding light on the intricate dynamic cellular responses to GBM and ischemic stroke poses significant challenges, given the highly intricated and coordinated responses of diverse brain cell types to the pathologies. To unravel these complexities, an effective approach is to begin by dissecting the responses of a single cell type, gradually expanding the investigation to include the intricate crosstalk and interactions with other cells in the brain. This thesis has primarily focused on pericyte-specific responses, linking these to subsequent endothelial and immune cell dynamics. Our findings underscore the pivotal role of pericytes in mediating these interactions. The results presented in this thesis highlight the multifaceted and dynamic nature of pericytes in GBM and ischemic stroke, encompassing temporal and spatial transcriptomic shifts, phenotypic and signaling adaptations, and alterations in their secretome under hypoxic conditions. These insights underscore the potential of targeting pericytes as a clinically relevant strategy to address early vascular dysfunction and enhance recovery in brain diseases. Moving forward, a deeper understanding of pericyte plasticity and their integration within the cellular mosaic of the brain could pave the way for innovative therapeutic interventions to improve outcomes in GBM and ischemic stroke.



Tropical River

Acknowledgements

Panta rei: everything flows. And so here we are, at the end of this chapter. It feels like just yesterday when, on a sunny August morning, I was wandering lost trying to find the lab. And yet, as I write this, 1613 days have passed - almost four and a half years. Staying here all this time and making it through the PhD wouldn't have been possible without the amazing connections and friendships I've built along the way. For this, I want to take a moment to thank everyone who made this journey special.

First and foremost, a special thanks to my supervisor, **Gesine Paul**. You gave me the chance to grow both scientifically and personally, always valuing my ideas and opinions throughout this journey. Thanks for being audacious enough to choose a candidate who openly stated in the cover letter that she didn't know what pericytes were. **Robert Carlsson**, my co-supervisor: thank you for your patience, for teaching me so many different techniques, and for helping me to solve the technical problems, sometimes with a healthy dose of madness.

Thank you to my labmates.

Andreas, you have been my daily support for three long years: scientifically, morally, culinarily and even financially. Sure, we still disagree on the state of women's rights, but hey, no one's perfect. **Shub**, your energy, your powerful voice and your positive soul have brightened the office in my last few years. Every woman can only dream of being as independent and well-organized as you. My last PhD years would have not been the same without you! **Ellen** it was a pleasure to have you in the group. **Katharina**. Great last addition to our group. So, you are next; did you start writing your thesis? **Coralie, Abderahim, Osama**, thank you for teaching me so much when I first arrived. **Kavya**. I still remember teaching you qPCR. I wonder how much you'd have to teach me now! **Gayatri**. I hope I managed to pass on some knowledge and passion.

Thank you also to all the inhabitants of A10, past and present.

Caroline, thank you for a solid knowledge of confocal microscopy and the wine glasses you left me—they turned out to be essential for the rest of the journey. **Martino**. Mi hai iniziato alla pizza con le patate e la mortadella. Che altro serve per finire un dottorato? Grazie per tutti i consigli. **Edo**. Biondo! Si sente la tua mancanza, quando vieni a trovarci? **Alex**, a wise man once told me: "You should

study bioinformatics; it'll make your life easier." You'd be my favourite PI. **Laura**, from a ggplot to a grigri is but a moment. I can't wait for more outdoor adventures together! **Jana**, thank you for our conversations spanning from broccoli soups to life advice—preferably at 90 °C. **Alina**, between one moving and another, we still found time for gardening, mushroom picking and sauna. Thanks for making our office brighter. **Joaquin**, completing my PhD was easier than reading Power and Market. Thank you to the rest of **A10**, who made these years enjoyable: **Catarina**, **Susanne**, **Filip**, **Kajsa**, **Lautaro**, **Rana**, **Zahra**, **Marie**, **Maria**, and all the others.

Thanks to my friends, my family here.

Luis, you've been by my side through the highs and lows of the past two years, and this journey wouldn't have been the same without you. Take, for example, the heroic Gaviscon rescue in Porto that may have literally saved my life. Of course, you're also partly responsible for some sleep deprived nights—my rare ventures partying past 1 a.m. But I gladly take the fun and good company that come with it. **Julie**, where do I start? We've been through so much together. Thank you for the cozy evenings working together, for all the delicious dinners you cooked for me that were able to rescue my mood, for all our climbing sessions, and for the hours working under the sun – which never turned out enough. It was a privilege to have you in Lecco. Always keep being unapologetically yourself. **Georgios**, sometimes George, or better yet, Giorgos (?). The mystery surrounds you: is your apartment legend or real? Thank you for the serenades. **Artem**, you never fail to surprise me with a new opinion. Thank you for broadening my perspectives. **Liwa**, thank you for your contagious energy and hospitality. **Alrik**. Now I know I should have accepted to write that grant proposal with you, it would have been so much fun! I hope you'll manage to survive to the next extreme sport passion, I wanna taste your heat resistant coffee. **Alison**, la mia Anna dai capelli rossi. Continua a contagiare il mondo con la tua anima glitterata. **Simona**. Da corsi di svedese, a seratine, saunette, sessioni di pittura e naturreservat, mi hai deliziata con svariati piatti alternativi - il mio preferito rimane pane olio sale e origano. Grazie per esserci sempre stata. **Donna**, mystical creature. I can't wait for more deep conversations and fun adventures with you. **Frenki**. A casa mia succedono cose strane. Le piante, io le annaffio ma loro muoiono lo stesso. La frutta marcisce. I muri, sembra che avanzino... **Fabio**, thank you for our conversations on the balcony, among Cd11c, Cd11b and life problems. **Tori**, you give the orders, and I execute them. Thank you for letting me turn off my brain every now and then. **Shubham**. Thank you for introducing me to your creative world! **Sahra**, with your energy, you always bring blue skies. Thanks for all the digging we've done together. **Celine**, our conversations include stabbings or climbing gyms at the same level of enthusiasm. Thank you for listening. **Nienke**, I truly understood who I was dealing with when I saw you dancing to *Let It Go* on a table. You inspire me every day. **Tommaso**, ci vediamo presto alla gym o al seggio elettorale.

A huge thanks also to **Albert, Roberta, Evelyn, Eliška, Marta, Marija, Isak, Nadja, Matilde, Maria, Tiago, Giggi, Alex, Barbara, Juan, Ian** and everyone else who, in one way or another, filled these years with good moments.

Poi non posso che ringraziare tutti i miei amici che mi hanno supportata da Lecco in questi anni, e che non vedo mai abbastanza spesso. **Richi**, grazie per ricordarmi cosa significa essere vivi (essere vivi dopo aver visto la morte tra i monti). **Ebba**. La mia counterpart svedese. Grazie per aver reso le mie attività rischiose più accessibili. **Fedo**. Supporto psicologico (e medico) in falesia. Non sono ancora riuscita a convincerti a trasferirti in Svezia? **Cappi**. Per i nostri discorsi senza peli sulla lingua: diretti, onesti e sempre illuminanti. **Mary**. per le nostre videocchiamate e quelle colazioni deliziose che compensano la distanza. **Cora**. Tu sola saprai se l'incipit è corretto oppure no. Grazie per le nostre stupende chiacchierate.

E, ovviamente, le mie besties: **Vale, Eli, Jessi, Marti, Sere**, che mi conoscono dal lontano 2009 quando a malapena sapevo cosa fosse una proteina e quando il massimo dei problemi era capire se la Zuccoli avrebbe interrogato o meno. Adesso, tutte plurilaureate, le sfide di allora sembrano una passeggiata. Sono felice che, nonostante il tempo lontano e i vocali che ci scordiamo di ascoltare, siamo ancora qui a condividere i momenti più importanti.

Grazie alla mia famiglia. **Mamma e papà**: mi avete sempre incoraggiato e supportato nelle mie scelte, tra cui quella di vivere lontano, e mi avete sempre accolto a casa come se fossi partita soltanto ieri. Grazie anche per il servizio taxi da e per l'aeroporto. **Fratellino**, per il nostro rapporto fantastico che non cambia mai nonostante i chilometri e gli anni lontani. **Nonnino**: mi hai trasmesso l'interesse della scienza e medicina. Purtroppo, non sono riuscita né a curare l'Alzheimer né a vincere il Nobel per ora. Speriamo di riuscirci presto! Grazie anche a **zia Meme** e a tutti gli altri parenti che si sono interessati al mio PhD.

Thank you, **Tobi**, for being by my side these past two years, patiently listening to my dramas and celebrating every success alongside me. Let's not forget all the feedback you've given me - from sitting through my posters and figures to enduring my presentations rehearsals. Your discipline and resilience inspired me in this journey. I can't wait to see what other adventures lie ahead for us, hopefully ones that don't involve you pretending to enjoy my graphs and lines of code.

A special thanks to ChatGPT for being my code debugging ally, and to Copilot for giving my English the polish it needed.

References

1. Rolfe, D.F. and G.C. Brown, Cellular energy utilization and molecular origin of standard metabolic rate in mammals. *Physiol Rev*, 1997. 77(3): p. 731-58.
2. Mink, J.W., R.J. Blumenshine, and D.B. Adams, Ratio of central nervous system to body metabolism in vertebrates: its constancy and functional basis. *Am J Physiol*, 1981. 241(3): p. R203-12.
3. Zlokovic, B.V. and M.L. Apuzzo, Strategies to circumvent vascular barriers of the central nervous system. *Neurosurgery*, 1998. 43(4): p. 877-8.
4. Kumar, A., et al., Specification and Diversification of Pericytes and Smooth Muscle Cells from Mesenchymoangioblasts. *Cell Rep*, 2017. 19(9): p. 1902-1916.
5. Etchevers, H.C., et al., The cephalic neural crest provides pericytes and smooth muscle cells to all blood vessels of the face and forebrain. *Development*, 2001. 128(7): p. 1059-68.
6. Nortley, R., et al., Amyloid beta oligomers constrict human capillaries in Alzheimer's disease via signaling to pericytes. *Science*, 2019. 365(6450).
7. Ren, J., et al., Diabetic retinopathy: Involved cells, biomarkers, and treatments. *Front Pharmacol*, 2022. 13: p. 953691.
8. Winkler, E.A., et al., Reductions in brain pericytes are associated with arteriovenous malformation vascular instability. *J Neurosurg*, 2018. 129(6): p. 1464-1474.
9. Armulik, A., G. Genove, and C. Betsholtz, Pericytes: developmental, physiological, and pathological perspectives, problems, and promises. *Dev Cell*, 2011. 21(2): p. 193-215.
10. Mathiisen, T.M., et al., The perivascular astroglial sheath provides a complete covering of the brain microvessels: an electron microscopic 3D reconstruction. *Glia*, 2010. 58(9): p. 1094-103.

11. Sims, D.E., The pericyte--a review. *Tissue Cell*, 1986. 18(2): p. 153-74.
12. Gerhardt, H. and C. Betsholtz, Endothelial-pericyte interactions in angiogenesis. *Cell Tissue Res*, 2003. 314(1): p. 15-23.
13. Masuho, I., et al., A Global Map of G Protein Signaling Regulation by RGS Proteins. *Cell*, 2020. 183(2): p. 503-521 e19.
14. Bondjers, C., et al., Transcription profiling of platelet-derived growth factor-B-deficient mouse embryos identifies RGS5 as a novel marker for pericytes and vascular smooth muscle cells. *Am J Pathol*, 2003. 162(3): p. 721-9.
15. Cho, H., et al., Pericyte-specific expression of Rgs5: implications for PDGF and EDG receptor signaling during vascular maturation. *FASEB J*, 2003. 17(3): p. 440-2.
16. Ozen, I., et al., Brain pericytes acquire a microglial phenotype after stroke. *Acta Neuropathol*, 2014. 128(3): p. 381-96.
17. Hamzah, J., et al., Vascular normalization in Rgs5-deficient tumours promotes immune destruction. *Nature*, 2008. 453(7193): p. 410-4.
18. Guo, X., et al., Atp13a5 Marker Reveals Pericyte Specification in the Mouse Central Nervous System. *J Neurosci*, 2024. 44(43).
19. Bacakova, L., Travnickova, M., Filova, E., Matějka, R., Stepanovska, J., Musilkova, J., ... Molitor, M., The Role of Vascular Smooth Muscle Cells in the Physiology and Pathophysiology of Blood Vessels. InTech, 2018.
20. Miao, Y., et al., Different gene expression patterns between mouse and human brain pericytes revealed by single-cell/nucleus RNA sequencing. *Vascul Pharmacol*, 2024. 157: p. 107434.
21. El-Ghazawi, K., U.B. Eyo, and S.M. Peirce, Brain Microvascular Pericyte Pathology Linking Alzheimer's Disease to Diabetes. *Microcirculation*, 2024. 31(7): p. e12877.
22. Shih, Y.H., et al., Integrated molecular analysis identifies a conserved pericyte gene signature in zebrafish. *Development*, 2021. 148(23).
23. Lindahl, P., et al., Pericyte loss and microaneurysm formation in PDGF-B-deficient mice. *Science*, 1997. 277(5323): p. 242-5.
24. Wiens, K.M., et al., Platelet-derived growth factor receptor beta is critical for zebrafish intersegmental vessel formation. *PLoS One*, 2010. 5(6): p. e11324.

25. Winkler, E.A., R.D. Bell, and B.V. Zlokovic, Pericyte-specific expression of PDGF beta receptor in mouse models with normal and deficient PDGF beta receptor signaling. *Mol Neurodegener*, 2010. 5: p. 32.
26. Huang, F.J., et al., Pericyte deficiencies lead to aberrant tumor vascularization in the brain of the NG2 null mouse. *Dev Biol*, 2010. 344(2): p. 1035-46.
27. Ozerdem, U., et al., NG2 proteoglycan is expressed exclusively by mural cells during vascular morphogenesis. *Dev Dyn*, 2001. 222(2): p. 218-27.
28. Nehls, V., K. Denzer, and D. Drenckhahn, Pericyte involvement in capillary sprouting during angiogenesis in situ. *Cell Tissue Res*, 1992. 270(3): p. 469-74.
29. Kunz, J., et al., The 140-kDa protein of blood-brain barrier-associated pericytes is identical to aminopeptidase N. *J Neurochem*, 1994. 62(6): p. 2375-86.
30. Liu, H., S. Kennard, and B. Lilly, NOTCH3 expression is induced in mural cells through an autoregulatory loop that requires endothelial-expressed JAGGED1. *Circ Res*, 2009. 104(4): p. 466-75.
31. Kofler, N.M., et al., Combined deficiency of Notch1 and Notch3 causes pericyte dysfunction, models CADASIL, and results in arteriovenous malformations. *Sci Rep*, 2015. 5: p. 16449.
32. Gabbiani, G., et al., Vascular smooth muscle cells differ from other smooth muscle cells: predominance of vimentin filaments and a specific alpha-type actin. *Proc Natl Acad Sci U S A*, 1981. 78(1): p. 298-302.
33. Santoro, M.M., G. Pesce, and D.Y. Stainier, Characterization of vascular mural cells during zebrafish development. *Mech Dev*, 2009. 126(8-9): p. 638-49.
34. Solway, J., et al., Structure and expression of a smooth muscle cell-specific gene, SM22 alpha. *J Biol Chem*, 1995. 270(22): p. 13460-9.
35. Wang, D., et al., Activation of cardiac gene expression by myocardin, a transcriptional cofactor for serum response factor. *Cell*, 2001. 105(7): p. 851-62.
36. Miano, J.M. and E.N. Olson, Expression of the smooth muscle cell calponin gene marks the early cardiac and smooth muscle cell lineages during mouse embryogenesis. *J Biol Chem*, 1996. 271(12): p. 7095-103.

37. Babij, P., et al., Differential expression of SM1 and SM2 myosin isoforms in cultured vascular smooth muscle. *Am J Physiol*, 1992. 262(3 Pt 1): p. C607-13.
38. Birbrair, A., et al., Type-1 pericytes accumulate after tissue injury and produce collagen in an organ-dependent manner. *Stem Cell Res Ther*, 2014. 5(6): p. 122.
39. Birbrair, A., et al., Skeletal muscle pericyte subtypes differ in their differentiation potential. *Stem Cell Res*, 2013. 10(1): p. 67-84.
40. Birbrair, A., et al., Role of pericytes in skeletal muscle regeneration and fat accumulation. *Stem Cells Dev*, 2013. 22(16): p. 2298-314.
41. Goritz, C., et al., A pericyte origin of spinal cord scar tissue. *Science*, 2011. 333(6039): p. 238-42.
42. Park, T.I., et al., Cultured pericytes from human brain show phenotypic and functional differences associated with differential CD90 expression. *Sci Rep*, 2016. 6: p. 26587.
43. Bohannon, D.G., et al., A subtype of cerebrovascular pericytes is associated with blood-brain barrier disruption that develops during normal aging and simian immunodeficiency virus infection. *Neurobiol Aging*, 2020. 96: p. 128-136.
44. Bohannon, D.G., et al., Type-1-to-type-2 transition of brain microvascular pericytes induced by cytokines and disease-associated proteins: Role in neuroinflammation and blood-brain barrier disruption. *J Cereb Blood Flow Metab*, 2024: p. 271678X241296270.
45. Grant, R.I., et al., Organizational hierarchy and structural diversity of microvascular pericytes in adult mouse cortex. *J Cereb Blood Flow Metab*, 2019. 39(3): p. 411-425.
46. Hill, R.A., et al., Regional Blood Flow in the Normal and Ischemic Brain Is Controlled by Arteriolar Smooth Muscle Cell Contractility and Not by Capillary Pericytes. *Neuron*, 2015. 87(1): p. 95-110.
47. Vanlandewijck, M., et al., A molecular atlas of cell types and zonation in the brain vasculature. *Nature*, 2018. 554(7693): p. 475-480.
48. Dias, D.O., et al., Pericyte-derived fibrotic scarring is conserved across diverse central nervous system lesions. *Nat Commun*, 2021. 12(1): p. 5501.

49. Yang, A.C., et al., A human brain vascular atlas reveals diverse mediators of Alzheimer's risk. *Nature*, 2022. 603(7903): p. 885-892.
50. Oudenaarden, C., J. Sjolund, and K. Pietras, Upregulated functional gene expression programmes in tumour pericytes mark progression in patients with low-grade glioma. *Mol Oncol*, 2022. 16(2): p. 405-421.
51. Ruiz-Moreno, C.S., S.M. Samuelsson, E. Brandner, S. Kranendonk, M.E.G. Nilsson, M. & Stunnenberg, H.G., Harmonized single-cell landscape, intercellular crosstalk and tumor architecture of glioblastoma. *bioRxiv*, 2022.
52. Sa-Pereira, I., D. Brites, and M.A. Brito, Neurovascular unit: a focus on pericytes. *Mol Neurobiol*, 2012. 45(2): p. 327-47.
53. McConnell, H.L. and A. Mishra, Cells of the Blood-Brain Barrier: An Overview of the Neurovascular Unit in Health and Disease. *Methods Mol Biol*, 2022. 2492: p. 3-24.
54. Keaney, J. and M. Campbell, The dynamic blood-brain barrier. *FEBS J*, 2015. 282(21): p. 4067-79.
55. Daneman, R., et al., Pericytes are required for blood-brain barrier integrity during embryogenesis. *Nature*, 2010. 468(7323): p. 562-6.
56. Armulik, A., et al., Pericytes regulate the blood-brain barrier. *Nature*, 2010. 468(7323): p. 557-61.
57. Bell, R.D., et al., Pericytes control key neurovascular functions and neuronal phenotype in the adult brain and during brain aging. *Neuron*, 2010. 68(3): p. 409-27.
58. Schaffenrath, J., et al., Characterization of the blood-brain barrier in genetically diverse laboratory mouse strains. *Fluids Barriers CNS*, 2021. 18(1): p. 34.
59. Sweeney, M.D., S. Ayyadurai, and B.V. Zlokovic, Pericytes of the neurovascular unit: key functions and signaling pathways. *Nat Neurosci*, 2016. 19(6): p. 771-83.
60. Gonul, E., et al., Early pericyte response to brain hypoxia in cats: an ultrastructural study. *Microvasc Res*, 2002. 64(1): p. 116-9.
61. Patan, S., Vasculogenesis and angiogenesis. *Cancer Treat Res*, 2004. 117: p. 3-32.
62. Folkman, J., Angiogenesis. *Annu Rev Med*, 2006. 57: p. 1-18.

63. Burri, P.H. and M.R. Tarek, A novel mechanism of capillary growth in the rat pulmonary microcirculation. *Anat Rec*, 1990. 228(1): p. 35-45.
64. Diaz-Flores, L., et al., Comparison of the Behavior of Perivascular Cells (Pericytes and CD34+ Stromal Cell/Telocytes) in Sprouting and Intussusceptive Angiogenesis. *Int J Mol Sci*, 2022. 23(16).
65. Gaceb, A. and G. Paul, Pericyte Secretome. *Adv Exp Med Biol*, 2018. 1109: p. 139-163.
66. Gaceb, A., et al., The pericyte secretome: Potential impact on regeneration. *Biochimie*, 2018. 155: p. 16-25.
67. Kovac, A., M.A. Erickson, and W.A. Banks, Brain microvascular pericytes are immunoactive in culture: cytokine, chemokine, nitric oxide, and LRP-1 expression in response to lipopolysaccharide. *J Neuroinflammation*, 2011. 8: p. 139.
68. Gaceb, A., et al., Pericytes secrete pro-regenerative molecules in response to platelet-derived growth factor-BB. *J Cereb Blood Flow Metab*, 2018. 38(1): p. 45-57.
69. Dabravolski, S.A., et al., The Role of Pericytes in Regulation of Innate and Adaptive Immunity. *Biomedicines*, 2023. 11(2).
70. Navarro, R., et al., Immune Regulation by Pericytes: Modulating Innate and Adaptive Immunity. *Front Immunol*, 2016. 7: p. 480.
71. Caspani, E.M., et al., Glioblastoma: a pathogenic crosstalk between tumor cells and pericytes. *PLoS One*, 2014. 9(7): p. e101402.
72. Balabanov, R., T. Beaumont, and P. Dore-Duffy, Role of central nervous system microvascular pericytes in activation of antigen-primed splenic T-lymphocytes. *J Neurosci Res*, 1999. 55(5): p. 578-87.
73. Stark, K., et al., Capillary and arteriolar pericytes attract innate leukocytes exiting through venules and 'instruct' them with pattern-recognition and motility programs. *Nat Immunol*, 2013. 14(1): p. 41-51.
74. Tu, Z., et al., Retinal pericytes inhibit activated T cell proliferation. *Invest Ophthalmol Vis Sci*, 2011. 52(12): p. 9005-10.
75. Proebstl, D., et al., Pericytes support neutrophil subendothelial cell crawling and breaching of venular walls in vivo. *J Exp Med*, 2012. 209(6): p. 1219-34.

76. Gil, E., et al., Pericyte derived chemokines amplify neutrophil recruitment across the cerebrovascular endothelial barrier. *Front Immunol*, 2022. 13: p. 935798.
77. Torok, O., et al., Pericytes regulate vascular immune homeostasis in the CNS. *Proc Natl Acad Sci U S A*, 2021. 118(10).
78. Nyland, H. and R. Nilsen, Localization of Fc gamma receptors in the human central nervous system. *Acta Pathol Microbiol Immunol Scand C*, 1982. 90(4): p. 217-21.
79. Graeber, M.B., W.J. Streit, and G.W. Kreutzberg, Identity of ED2-positive perivascular cells in rat brain. *J Neurosci Res*, 1989. 22(1): p. 103-6.
80. Balabanov, R., et al., CNS microvascular pericytes express macrophage-like function, cell surface integrin alpha M, and macrophage marker ED-2. *Microvasc Res*, 1996. 52(2): p. 127-42.
81. Sasaki, A., et al., The immunophenotype of perivascular cells in the human brain. *Pathol Int*, 1996. 46(1): p. 15-23.
82. Pieper, C., et al., Brain capillary pericytes contribute to the immune defense in response to cytokines or LPS in vitro. *Brain Res*, 2014. 1550: p. 1-8.
83. Smith, A.M., et al., Adult human glia, pericytes and meningeal fibroblasts respond similarly to IFN γ but not to TGF β 1 or M-CSF. *PLoS One*, 2013. 8(12): p. e80463.
84. Olson, L.E. and P. Soriano, PDGFR β signaling regulates mural cell plasticity and inhibits fat development. *Dev Cell*, 2011. 20(6): p. 815-26.
85. Weninger, W., M. Biro, and R. Jain, Leukocyte migration in the interstitial space of non-lymphoid organs. *Nat Rev Immunol*, 2014. 14(4): p. 232-46.
86. Zachariah, M.A. and J.G. Cyster, Neural crest-derived pericytes promote egress of mature thymocytes at the corticomedullary junction. *Science*, 2010. 328(5982): p. 1129-35.
87. Domev, H., et al., Immuno-evasive pericytes from human pluripotent stem cells preferentially modulate induction of allogeneic regulatory T cells. *Stem Cells Transl Med*, 2014. 3(10): p. 1169-81.
88. Maier, C.L. and J.S. Pober, Human Placental Pericytes Poorly Stimulate and Actively Regulate Allogeneic CD4 T Cell Responses.

- Arteriosclerosis Thrombosis and Vascular Biology, 2011. 31(1): p. 183-+.
89. Enstrom, A., et al., Pericyte-Specific Secretome Profiling in Hypoxia Using TurboID in a Multicellular in Vitro Spheroid Model. *Mol Cell Proteomics*, 2024. 23(6): p. 100782.
 90. Carlsson, R., A. Enstrom, and G. Paul, Molecular Regulation of the Response of Brain Pericytes to Hypoxia. *Int J Mol Sci*, 2023. 24(6).
 91. Schodel, J. and P.J. Ratcliffe, Mechanisms of hypoxia signalling: new implications for nephrology. *Nat Rev Nephrol*, 2019. 15(10): p. 641-659.
 92. Markolovic, S., S.E. Wilkins, and C.J. Schofield, Protein Hydroxylation Catalyzed by 2-Oxoglutarate-dependent Oxygenases. *J Biol Chem*, 2015. 290(34): p. 20712-20722.
 93. Duz, B., et al., The effect of moderate hypothermia in acute ischemic stroke on pericyte migration: an ultrastructural study. *Cryobiology*, 2007. 55(3): p. 279-84.
 94. Enstrom, A., et al., RGS5: a novel role as a hypoxia-responsive protein that suppresses chemokinetic and chemotactic migration in brain pericytes. *Biol Open*, 2022. 11(10).
 95. Lee, M.J., et al., Characterization of arginylation branch of N-end rule pathway in G-protein-mediated proliferation and signaling of cardiomyocytes. *J Biol Chem*, 2012. 287(28): p. 24043-52.
 96. Lee, M.J., et al., RGS4 and RGS5 are in vivo substrates of the N-end rule pathway. *Proc Natl Acad Sci U S A*, 2005. 102(42): p. 15030-5.
 97. Masson, N., et al., Conserved N-terminal cysteine dioxygenases transduce responses to hypoxia in animals and plants. *Science*, 2019. 365(6448): p. 65-69.
 98. Ozen, I., et al., Loss of Regulator of G-Protein Signaling 5 Leads to Neurovascular Protection in Stroke. *Stroke*, 2018. 49(9): p. 2182-2190.
 99. Roth, M., et al., Regulator of G-protein signaling 5 regulates the shift from perivascular to parenchymal pericytes in the chronic phase after stroke. *FASEB J*, 2019: p. fj201900153R.
 100. Hanif, F., et al., Glioblastoma Multiforme: A Review of its Epidemiology and Pathogenesis through Clinical Presentation and Treatment. *Asian Pac J Cancer Prev*, 2017. 18(1): p. 3-9.

101. Rong, L., N. Li, and Z. Zhang, Emerging therapies for glioblastoma: current state and future directions. *J Exp Clin Cancer Res*, 2022. 41(1): p. 142.
102. Rick, J., A. Chandra, and M.K. Aghi, Tumor treating fields: a new approach to glioblastoma therapy. *J Neurooncol*, 2018. 137(3): p. 447-453.
103. Delgado-Lopez, P.D. and E.M. Corrales-Garcia, Survival in glioblastoma: a review on the impact of treatment modalities. *Clin Transl Oncol*, 2016. 18(11): p. 1062-1071.
104. Kuczynski, E.A., et al., Vessel co-option in cancer. *Nat Rev Clin Oncol*, 2019. 16(8): p. 469-493.
105. Lugassy, C., et al., Angiotropism, pericytic mimicry and extravascular migratory metastasis in melanoma: an alternative to intravascular cancer dissemination. *Cancer Microenviron*, 2014. 7(3): p. 139-52.
106. Hendrix, M.J., et al., Tumor cell vascular mimicry: Novel targeting opportunity in melanoma. *Pharmacol Ther*, 2016. 159: p. 83-92.
107. Wechman, S.L., et al., Vascular mimicry: Triggers, molecular interactions and in vivo models. *Adv Cancer Res*, 2020. 148: p. 27-67.
108. Ribatti, D. and F. Pezzella, Vascular Co-Option and Other Alternative Modalities of Growth of Tumor Vasculature in Glioblastoma. *Front Oncol*, 2022. 12: p. 874554.
109. Valdor, R., et al., Glioblastoma progression is assisted by induction of immunosuppressive function of pericytes through interaction with tumor cells. *Oncotarget*, 2017. 8(40): p. 68614-68626.
110. Cuddapah, V.A., et al., A neurocentric perspective on glioma invasion. *Nat Rev Neurosci*, 2014. 15(7): p. 455-65.
111. Fabian, C., et al., Novel facets of glioma invasion. *Int Rev Cell Mol Biol*, 2021. 360: p. 33-64.
112. Morikawa, S., et al., Abnormalities in pericytes on blood vessels and endothelial sprouts in tumors. *Am J Pathol*, 2002. 160(3): p. 985-1000.
113. Sun, H., et al., Hyperplasia of pericytes is one of the main characteristics of microvascular architecture in malignant glioma. *PLoS One*, 2014. 9(12): p. e114246.

114. Svensson, A., et al., Endogenous brain pericytes are widely activated and contribute to mouse glioma microvasculature. *PLoS One*, 2015. 10(4): p. e0123553.
115. Quaegebeur, A., I. Segura, and P. Carmeliet, Pericytes: blood-brain barrier safeguards against neurodegeneration? *Neuron*, 2010. 68(3): p. 321-3.
116. Ochs, K., et al., Immature mesenchymal stem cell-like pericytes as mediators of immunosuppression in human malignant glioma. *J Neuroimmunol*, 2013. 265(1-2): p. 106-16.
117. Ferland-McCollough, D., et al., Pericytes, an overlooked player in vascular pathobiology. *Pharmacol Ther*, 2017. 171: p. 30-42.
118. Warlow, C.P., Epidemiology of stroke. *Lancet*, 1998. 352 Suppl 3: p. SIII1-4.
119. Collaborators, G.B.D.S.R.F., Global, regional, and national burden of stroke and its risk factors, 1990-2021: a systematic analysis for the Global Burden of Disease Study 2021. *Lancet Neurol*, 2024. 23(10): p. 973-1003.
120. Feigin, V.L., M.O. Owolabi, and G. World Stroke Organization-Lancet Neurology Commission Stroke Collaboration, Pragmatic solutions to reduce the global burden of stroke: a World Stroke Organization-Lancet Neurology Commission. *Lancet Neurol*, 2023. 22(12): p. 1160-1206.
121. Bamford, J., et al., Classification and natural history of clinically identifiable subtypes of cerebral infarction. *Lancet*, 1991. 337(8756): p. 1521-6.
122. Candelario-Jalil, E., Injury and repair mechanisms in ischemic stroke: considerations for the development of novel neurotherapeutics. *Curr Opin Investig Drugs*, 2009. 10(7): p. 644-54.
123. Yang, Y. and G.A. Rosenberg, Blood-brain barrier breakdown in acute and chronic cerebrovascular disease. *Stroke*, 2011. 42(11): p. 3323-8.
124. Bader, M.K. and S. Palmer, What's the "hyper" in hyperacute stroke? Strategies to improve outcomes in ischemic stroke patients presenting within 6 hours. *AACN Adv Crit Care*, 2006. 17(2): p. 194-214.
125. Cai, W., et al., Pericytes in Brain Injury and Repair After Ischemic Stroke. *Transl Stroke Res*, 2017. 8(2): p. 107-121.

126. Liu, J., et al., Vascular remodeling after ischemic stroke: mechanisms and therapeutic potentials. *Prog Neurobiol*, 2014. 115: p. 138-56.
127. Pekna, M., M. Pekny, and M. Nilsson, Modulation of neural plasticity as a basis for stroke rehabilitation. *Stroke*, 2012. 43(10): p. 2819-28.
128. Herpich, F. and F. Rincon, Management of Acute Ischemic Stroke. *Crit Care Med*, 2020. 48(11): p. 1654-1663.
129. Zhang, B., X.J. Sun, and C.H. Ju, Thrombolysis with alteplase 4.5-6 hours after acute ischemic stroke. *Eur Neurol*, 2011. 65(3): p. 170-4.
130. Hall, C.N., et al., Capillary pericytes regulate cerebral blood flow in health and disease. *Nature*, 2014. 508(7494): p. 55-60.
131. Yang, S., et al., Diverse Functions and Mechanisms of Pericytes in Ischemic Stroke. *Curr Neuropharmacol*, 2017. 15(6): p. 892-905.
132. Roth, M., et al., Parenchymal pericytes are not the major contributor of extracellular matrix in the fibrotic scar after stroke in male mice. *J Neurosci Res*, 2020. 98(5): p. 826-842.
133. Fernandez-Klett, F. and J. Priller, The fibrotic scar in neurological disorders. *Brain Pathol*, 2014. 24(4): p. 404-13.
134. Goyal, R., M. Singhal, and I. Jialal, Type 2 Diabetes, in *StatPearls*. 2024: Treasure Island (FL).
135. Mizukami, H. and K. Kudoh, Diversity of pathophysiology in type 2 diabetes shown by islet pathology. *J Diabetes Investig*, 2022. 13(1): p. 6-13.
136. Hayes, K.L., Pericytes in Type 2 Diabetes. *Adv Exp Med Biol*, 2019. 1147: p. 265-278.
137. Elabi, O.F., et al., DPP-4 Inhibitor and Sulfonylurea Differentially Reverse Type 2 Diabetes-Induced Blood-Brain Barrier Leakage and Normalize Capillary Pericyte Coverage. *Diabetes*, 2023. 72(3): p. 405-414.
138. Augustad, I.L., et al., Normalisation of glucose metabolism by exendin-4 in the chronic phase after stroke promotes functional recovery in male diabetic mice. *Br J Pharmacol*, 2022. 179(4): p. 677-694.
139. Storgaard, H., et al., Benefits and Harms of Sodium-Glucose Co-Transporter 2 Inhibitors in Patients with Type 2 Diabetes: A Systematic Review and Meta-Analysis. *PLoS One*, 2016. 11(11): p. e0166125.

140. Ott, C., et al., A randomised study of the impact of the SGLT2 inhibitor dapagliflozin on microvascular and macrovascular circulation. *Cardiovasc Diabetol*, 2017. 16(1): p. 26.
141. Striepe, K., et al., Effects of the Selective Sodium-Glucose Cotransporter 2 Inhibitor Empagliflozin on Vascular Function and Central Hemodynamics in Patients With Type 2 Diabetes Mellitus. *Circulation*, 2017. 136(12): p. 1167-1169.
142. Xu, L., et al., SGLT2 Inhibition by Empagliflozin Promotes Fat Utilization and Browning and Attenuates Inflammation and Insulin Resistance by Polarizing M2 Macrophages in Diet-induced Obese Mice. *EBioMedicine*, 2017. 20: p. 137-149.
143. Bonnet, F. and A.J. Scheen, Effects of SGLT2 inhibitors on systemic and tissue low-grade inflammation: The potential contribution to diabetes complications and cardiovascular disease. *Diabetes Metab*, 2018. 44(6): p. 457-464.
144. He, L., et al., Analysis of the brain mural cell transcriptome. *Sci Rep*, 2016. 6: p. 35108.
145. Romanoski, C.E., et al., Transcriptomic profiles in pulmonary arterial hypertension associate with disease severity and identify novel candidate genes. *Pulm Circ*, 2020. 10(4): p. 2045894020968531.
146. Rangasamy, S., et al., Transcriptomics analysis of pericytes from retinas of diabetic animals reveals novel genes and molecular pathways relevant to blood-retinal barrier alterations in diabetic retinopathy. *Exp Eye Res*, 2020. 195: p. 108043.
147. Zhang, Y., et al., Pericytes in Alzheimer's disease: Key players and therapeutic targets. *Exp Neurol*, 2024. 379: p. 114825.
148. Reimegard, J., et al., A combined approach for single-cell mRNA and intracellular protein expression analysis. *Commun Biol*, 2021. 4(1): p. 624.
149. Bauernfeind, A.L. and C.C. Babbitt, The predictive nature of transcript expression levels on protein expression in adult human brain. *BMC Genomics*, 2017. 18(1): p. 322.
150. Nwadozi, E., M. Rudnicki, and T.L. Haas, Metabolic Coordination of Pericyte Phenotypes: Therapeutic Implications. *Front Cell Dev Biol*, 2020. 8: p. 77.

151. Moriggi, M., et al., Characterization of Proteome Changes in Aged and Collagen VI-Deficient Human Pericyte Cultures. *Int J Mol Sci*, 2024. 25(13).
152. Nisancioglu, M.H., et al., Generation and characterization of rgs5 mutant mice. *Mol Cell Biol*, 2008. 28(7): p. 2324-31.
153. Abdelwahab, M.G., et al., Intracranial implantation with subsequent 3D in vivo bioluminescent imaging of murine gliomas. *J Vis Exp*, 2011(57): p. e3403.
154. Candolfi, M., et al., Intracranial glioblastoma models in preclinical neuro-oncology: neuropathological characterization and tumor progression. *J Neurooncol*, 2007. 85(2): p. 133-48.
155. Llovera, G., et al., Modeling stroke in mice: permanent coagulation of the distal middle cerebral artery. *J Vis Exp*, 2014(89): p. e51729.
156. Hara, H., et al., Reduced brain edema and infarction volume in mice lacking the neuronal isoform of nitric oxide synthase after transient MCA occlusion. *J Cereb Blood Flow Metab*, 1996. 16(4): p. 605-11.
157. Lockowandt, M., et al., Optimization of production and transgene expression of a retrogradely transported pseudotyped lentiviral vector. *J Neurosci Methods*, 2020. 336: p. 108542.
158. Branon, T.C., et al., Efficient proximity labeling in living cells and organisms with TurboID. *Nat Biotechnol*, 2018. 36(9): p. 880-887.
159. Chang, J., et al., Gpr124 is essential for blood-brain barrier integrity in central nervous system disease. *Nat Med*, 2017. 23(4): p. 450-460.
160. McCall, M.N., et al., On non-detects in qPCR data. *Bioinformatics*, 2014. 30(16): p. 2310-6.
161. Schindelin, J., et al., Fiji: an open-source platform for biological-image analysis. *Nat Methods*, 2012. 9(7): p. 676-82.
162. Arganda-Carreras, I., et al., 3D reconstruction of histological sections: Application to mammary gland tissue. *Microsc Res Tech*, 2010. 73(11): p. 1019-29.
163. Heath, V.L., R. Bicknell, and V.A. Simms, Development of an ImageJ-based method for analysing the developing zebrafish vasculature. *Vascular Cell*, 2017. 9(1).
164. de Saint Basile, G., et al., Severe combined immunodeficiency caused by deficiency in either the delta or the epsilon subunit of CD3. *J Clin Invest*, 2004. 114(10): p. 1512-7.

165. Dorrier, C.E., et al., CNS fibroblasts form a fibrotic scar in response to immune cell infiltration. *Nat Neurosci*, 2021. 24(2): p. 234-244.
166. Jablonski, K.A., et al., Novel Markers to Delineate Murine M1 and M2 Macrophages. *PLoS One*, 2015. 10(12): p. e0145342.
167. Leslie, J., et al., FPR-1 is an important regulator of neutrophil recruitment and a tissue-specific driver of pulmonary fibrosis. *JCI Insight*, 2020. 5(4).
168. Liu, X.S., et al., Gene profiles and electrophysiology of doublecortin-expressing cells in the subventricular zone after ischemic stroke. *J Cereb Blood Flow Metab*, 2009. 29(2): p. 297-307.
169. Sharma, A., et al., Divergent roles of astrocytic versus neuronal EAAT2 deficiency on cognition and overlap with aging and Alzheimer's molecular signatures. *Proc Natl Acad Sci U S A*, 2019. 116(43): p. 21800-21811.
170. Wang, K., G. Wei, and D. Liu, CD19: a biomarker for B cell development, lymphoma diagnosis and therapy. *Exp Hematol Oncol*, 2012. 1(1): p. 36.
171. Jin, S., et al., Inference and analysis of cell-cell communication using CellChat. *Nat Commun*, 2021. 12(1): p. 1088.
172. Xie, Y., et al., Key molecular alterations in endothelial cells in human glioblastoma uncovered through single-cell RNA sequencing. *JCI Insight*, 2021. 6(15).
173. Li, Q. and I.M. Verma, NF-kappaB regulation in the immune system. *Nat Rev Immunol*, 2002. 2(10): p. 725-34.
174. Dunn, G.P., C.M. Koebel, and R.D. Schreiber, Interferons, immunity and cancer immunoediting. *Nat Rev Immunol*, 2006. 6(11): p. 836-48.
175. Arlt, A. and H. Schafer, Role of the immediate early response 3 (IER3) gene in cellular stress response, inflammation and tumorigenesis. *Eur J Cell Biol*, 2011. 90(6-7): p. 545-52.
176. Zou, J., et al., Lipopolysaccharide-induced tumor necrosis factor-alpha factor enhances inflammation and is associated with cancer (Review). *Mol Med Rep*, 2015. 12(5): p. 6399-404.
177. McFarland, B.C., et al., Loss of SOCS3 in myeloid cells prolongs survival in a syngeneic model of glioma. *Oncotarget*, 2016. 7(15): p. 20621-35.

178. Wang, F., et al., USP14: Structure, Function, and Target Inhibition. *Front Pharmacol*, 2021. 12: p. 801328.
179. Chen, Y., et al., Tumor-associated monocytes promote mesenchymal transformation through EGFR signaling in glioma. *Cell Rep Med*, 2023. 4(9): p. 101177.
180. Du, H., et al., FOSL2-mediated transcription of ISG20 induces M2 polarization of macrophages and enhances tumorigenic ability of glioblastoma cells. *J Neurooncol*, 2024. 169(3): p. 659-670.
181. Valdor, R. and M. Martinez-Vicente, The Role of Chaperone-Mediated Autophagy in Tissue Homeostasis and Disease Pathogenesis. *Biomedicines*, 2024. 12(2).
182. Yang, Y., et al., The ER-localized Ca(2+)-binding protein calreticulin couples ER stress to autophagy by associating with microtubule-associated protein 1A/1B light chain 3. *J Biol Chem*, 2019. 294(3): p. 772-782.
183. Ho, K.H., et al., A Key Role of DNA Damage-Inducible Transcript 4 (DDIT4) Connects Autophagy and GLUT3-Mediated Stemness To Desensitize Temozolomide Efficacy in Glioblastomas. *Neurotherapeutics*, 2020. 17(3): p. 1212-1227.
184. Sun, Y. and G.A. Grabowski, Altered autophagy in the mice with a deficiency of saposin A and saposin B. *Autophagy*, 2013. 9(7): p. 1115-6.
185. Wang, P., D. Kou, and W. Le, Roles of VMP1 in Autophagy and ER-Membrane Contact: Potential Implications in Neurodegenerative Disorders. *Front Mol Neurosci*, 2020. 13: p. 42.
186. Sandoval, K.E. and K.A. Witt, Blood-brain barrier tight junction permeability and ischemic stroke. *Neurobiol Dis*, 2008. 32(2): p. 200-19.
187. Nahirney, P.C., P. Reeson, and C.E. Brown, Ultrastructural analysis of blood-brain barrier breakdown in the peri-infarct zone in young adult and aged mice. *J Cereb Blood Flow Metab*, 2016. 36(2): p. 413-25.
188. Yu, Q.J., et al., Targeting brain microvascular endothelial cells: a therapeutic approach to neuroprotection against stroke. *Neural Regen Res*, 2015. 10(11): p. 1882-91.
189. Hoogstrate, Y., et al., Transcriptome analysis reveals tumor microenvironment changes in glioblastoma. *Cancer Cell*, 2023. 41(4): p. 678-692 e7.

190. Qian, C., et al., A Novel Extracellular Matrix Gene-Based Prognostic Model to Predict Overall Survive in Patients With Glioblastoma. *Front Genet*, 2022. 13: p. 851427.
191. Lau, L.W., et al., Pathophysiology of the brain extracellular matrix: a new target for remyelination. *Nat Rev Neurosci*, 2013. 14(10): p. 722-9.
192. Theocharis, A.D., et al., Cell-matrix interactions: focus on proteoglycan-proteinase interplay and pharmacological targeting in cancer. *FEBS J*, 2014. 281(22): p. 5023-42.
193. Theocharis, A.D., et al., Extracellular matrix structure. *Adv Drug Deliv Rev*, 2016. 97: p. 4-27.
194. Huang, J., et al., Extracellular matrix and its therapeutic potential for cancer treatment. *Signal Transduct Target Ther*, 2021. 6(1): p. 153.
195. Luo, X., et al., Lymphocytes perform reverse adhesive haptotaxis mediated by LFA-1 integrins. *J Cell Sci*, 2020. 133(16).
196. Ferrero, E., et al., Tumor-driven matrix invasion by infiltrating lymphocytes: involvement of the alpha1 integrin I-domain. *Eur J Immunol*, 1998. 28(8): p. 2530-6.
197. Hauzenberger, D., J. Klominek, and K.G. Sundqvist, Functional specialization of fibronectin-binding beta 1-integrins in T lymphocyte migration. *J Immunol*, 1994. 153(3): p. 960-71.
198. Pruitt, H.C., et al., Collagen fiber structure guides 3D motility of cytotoxic T lymphocytes. *Matrix Biol*, 2020. 85-86: p. 147-159.
199. Bougherara, H., et al., Real-Time Imaging of Resident T Cells in Human Lung and Ovarian Carcinomas Reveals How Different Tumor Microenvironments Control T Lymphocyte Migration. *Front Immunol*, 2015. 6: p. 500.
200. Peng, D.H., et al., Collagen promotes anti-PD-1/PD-L1 resistance in cancer through LAIR1-dependent CD8(+) T cell exhaustion. *Nat Commun*, 2020. 11(1): p. 4520.
201. Miyazawa, A., et al., Regulation of PD-L1 expression by matrix stiffness in lung cancer cells. *Biochem Biophys Res Commun*, 2018. 495(3): p. 2344-2349.
202. Long, K.B., et al., CAR T Cell Therapy of Non-hematopoietic Malignancies: Detours on the Road to Clinical Success. *Front Immunol*, 2018. 9: p. 2740.

203. Jain, R.K., Vascular and interstitial barriers to delivery of therapeutic agents in tumors. *Cancer Metastasis Rev*, 1990. 9(3): p. 253-66.
204. Kim, H., et al., Hyaluronic acid-based extracellular matrix triggers spontaneous M2-like polarity of monocyte/macrophage. *Biomater Sci*, 2019. 7(6): p. 2264-2271.
205. Kaplan, G., In vitro differentiation of human monocytes. Monocytes cultured on glass are cytotoxic to tumor cells but monocytes cultured on collagen are not. *J Exp Med*, 1983. 157(6): p. 2061-72.
206. Perri, R.T., et al., Fibronectin enhances in vitro monocyte-macrophage-mediated tumoricidal activity. *Blood*, 1982. 60(2): p. 430-5.
207. Eisele, G., et al., Cilengitide treatment of newly diagnosed glioblastoma patients does not alter patterns of progression. *J Neurooncol*, 2014. 117(1): p. 141-5.
208. Friedlander, D.R., et al., Migration of brain tumor cells on extracellular matrix proteins in vitro correlates with tumor type and grade and involves alphaV and beta1 integrins. *Cancer Res*, 1996. 56(8): p. 1939-47.
209. Ishida, J., et al., Integrin inhibitor suppresses bevacizumab-induced glioma invasion. *Transl Oncol*, 2014. 7(2): p. 292-302 e1.
210. Koh, I., et al., The mode and dynamics of glioblastoma cell invasion into a decellularized tissue-derived extracellular matrix-based three-dimensional tumor model. *Sci Rep*, 2018. 8(1): p. 4608.
211. Koutroulis, I., A. Zarros, and S. Theocharis, The role of matrix metalloproteinases in the pathophysiology and progression of human nervous system malignancies: a chance for the development of targeted therapeutic approaches? *Expert Opin Ther Targets*, 2008. 12(12): p. 1577-86.
212. Razinia, Z., et al., Stiffness-dependent motility and proliferation uncoupled by deletion of CD44. *Sci Rep*, 2017. 7(1): p. 16499.
213. Xie, Y., et al., Single-cell dissection of the human blood-brain barrier and glioma blood-tumor barrier. *Neuron*, 2024. 112(18): p. 3089-3105 e7.
214. Valdor, R., et al., Glioblastoma ablates pericytes antitumor immune function through aberrant up-regulation of chaperone-mediated autophagy. *Proc Natl Acad Sci U S A*, 2019. 116(41): p. 20655-20665.

215. Molina, M.L., et al., Chaperone-Mediated Autophagy Ablation in Pericytes Reveals New Glioblastoma Prognostic Markers and Efficient Treatment Against Tumor Progression. *Front Cell Dev Biol*, 2022. 10: p. 797945.
216. Zheng, K., et al., Single-cell RNA-seq reveals the transcriptional landscape in ischemic stroke. *J Cereb Blood Flow Metab*, 2022. 42(1): p. 56-73.
217. Zhang, B., et al., Interleukin-11 treatment protected against cerebral ischemia/reperfusion injury. *Biomed Pharmacother*, 2019. 115: p. 108816.
218. O'Reilly, S., Interleukin-11 and its eminent role in tissue fibrosis: a possible therapeutic target. *Clin Exp Immunol*, 2023. 214(2): p. 154-161.
219. Berger, M., et al., Regulator of G-protein signaling-5 induction in pericytes coincides with active vessel remodeling during neovascularization. *Blood*, 2005. 105(3): p. 1094-101.
220. Padel, T., et al., Brain pericyte activation occurs early in Huntington's disease. *Exp Neurol*, 2018. 305: p. 139-150.
221. Padel, T., et al., Platelet-derived growth factor-BB has neurorestorative effects and modulates the pericyte response in a partial 6-hydroxydopamine lesion mouse model of Parkinson's disease. *Neurobiol Dis*, 2016. 94: p. 95-105.
222. Yuan, K., et al., Activation of the Wnt/planar cell polarity pathway is required for pericyte recruitment during pulmonary angiogenesis. *Am J Pathol*, 2015. 185(1): p. 69-84.
223. Fernandez-Klett, F., et al., Early loss of pericytes and perivascular stromal cell-induced scar formation after stroke. *J Cereb Blood Flow Metab*, 2013. 33(3): p. 428-39.
224. Tingbo Li, L.Y., Jiaqi Tu, Yufan Hao, Zhu Zhu, Yingjie Xiong, Qingzhu Gao, Lili Zhou, Guanglei Xie, Dongdong Zhang, Xuzhao Li, Yuxiao Jin, Yiyi Zhang, Bingrui Zhao, Nan Li, Xi Wang, Jie-Min Jia, The myeloid cell-driven transdifferentiation of endothelial cells into pericytes promotes the restoration of BBB function and brain self-repair after stroke. *bioRxiv*, 2024. 2023.12.07.570712.
225. Beltramo, E. and M. Porta, Pericyte loss in diabetic retinopathy: mechanisms and consequences. *Curr Med Chem*, 2013. 20(26): p. 3218-25.

226. Corliss, B.A., et al., Pericyte Bridges in Homeostasis and Hyperglycemia. *Diabetes*, 2020. 69(7): p. 1503-1517.
227. Tan, G.S., et al., Diabetic macular oedema. *Lancet Diabetes Endocrinol*, 2017. 5(2): p. 143-155.

Appendix (Papers I-V)

